c.2

TECHNICAL REPORT
NATICK/TR-89/040

AD A 212 525

FEASIBILITY OF INSPECTION OF FUNGICIDAL FINISHES ON TEXTILES BY X-RAY, INFRARED AND ULTRASONIC METHODS

BY

PAUL BURSTEIN
SKIAMETRICS, INC.
WINCHESTER, MA 01890

AUGUST 1989

FINAL REPORT

JUNE 1987 - MARCH 1988

APPROVED FOR PUBLIC RELEASE;
DISTRIBUTION UNLIMITED

Prepared for

UNITED STATES ARMY NATICK
RESEARCH, DEVELOPMENT AND ENGINEERING CENTER
NATICK, MASSACHUSETTS 01760-5000

SCIENCE AND ADVANCED TECHNOLOGY
DIRECTORATE

DISCLAIMERS

The findings contained in this report are not to be construed as an official Department of the Army position unless so designated by other authorized documents.

Citation of trade names in this report does not constitute an official endorsement or approval of the use of such items.

DESTRUCTION NOTICE

For Clsssified Documents:

Follow the procedures in DoD 5200.22-M, Industrial Security Msnual, Section II-19 or DoD 5200.1-R, Information Security Program Regulation, Chapter IX.

For Unclassified/Limited Distribution Documents:

Deatroy by any method that prevents disclosure of contents or reconstruction of the document.

UNCLASSIFIED

SECURITY CLASSIFICATION OF THIS PAGE

REPORT DOCUMENTATION PAGE

Form Approved OMB No. 0704-0188

1a. REPORT SECURITY CLASSIFICATION: UNCLASSIFIED	1b. RESTRICTIVE MARKINGS
2a. SECURITY CLASSIFICATION AUTHORITY	3. DISTRIBUTION / AVAILABILITY OF REPORT: Approved for public release; distribution unlimited
2b. DECLASSIFICATION / DOWNGRADING SCHEDULE	
4. PERFORMING ORGANIZATION REPORT NUMBER(S)	5. MONITORING ORGANIZATION REPORT NUMBER(S): NATICK/TR-89/040
6a. NAME OF PERFORMING ORGANIZATION: Skiametrics, Inc. / 6b. OFFICE SYMBOL (If applicable)	7a. NAME OF MONITORING ORGANIZATION: U.S. Army Natick RD&E Center
6c. ADDRESS (City, State, and ZIP Code): 19 Gilgarry Road, Winchester, MA 01890	7b. ADDRESS (City, State, and ZIP Code): Natick, MA 01760-5020
8a. NAME OF FUNDING / SPONSORING ORGANIZATION / 8b. OFFICE SYMBOL (If applicable)	9. PROCUREMENT INSTRUMENT IDENTIFICATION NUMBER: Contract No. DAAK60-87-C-0045
8c. ADDRESS (City, State, and ZIP Code)	10. SOURCE OF FUNDING NUMBERS

PROGRAM ELEMENT NO.	PROJECT NO.	TASK NO.	WORK UNIT ACCESSION NO.
65502	1L665502 MM40	25	DA313129

11. TITLE (Include Security Classification)
(U) Feasibility of Inspection of Fungicidal Finishes on Textiles by X-ray, Infrared and Ultrasonic Methods

12. PERSONAL AUTHOR(S)
Paul Burstein

13a. TYPE OF REPORT	13b. TIME COVERED	14. DATE OF REPORT (Year, Month, Day)	15. PAGE COUNT
Final	FROM 6/87 TO 3/88	1989 August	135

16. SUPPLEMENTARY NOTATION

17. COSATI CODES		
FIELD	GROUP	SUB-GROUP

18. SUBJECT TERMS (Continue on reverse if necessary and identify by block number)
X-ray fluorescence, X-ray scattering, ultrasonic tests, fungicides, copper compounds, cotton textiles, infrared tests, quality control

19. ABSTRACT (Continue on reverse if necessary and identify by block number)

A series of methods for determining the amount of copper-8-quinolinolate on a cellulose textile have been investigated. Several methods were selected for detailed calculations and experimental confirmation. These included x-ray fluorescence, dual energy x-ray transmission, Fourier transform infrared (FTIR) spectroscopy, and ultrasonic pulse (transmission mode). The results of these experiments prove feasibility for continuous and large-scale inspection coverage of copper-8-quinolinolate-treated cotton duck. Moreover, these inspection techniques can provide inspection for the entire variety of circumstances to be encountered. These methods are extensible to other treatments and textiles. System designs for x-ray, FTIR, and UT systems are presented. These system designs utilize existing technology and require only small changes to commercial instrumentation. A Phase II program that provides delivered prototypes of all instruments is proposed.

20. DISTRIBUTION / AVAILABILITY OF ABSTRACT	21. ABSTRACT SECURITY CLASSIFICATION
☐ UNCLASSIFIED/UNLIMITED ☒ SAME AS RPT ☐ DTIC USERS	UNCLASSIFIED

22a. NAME OF RESPONSIBLE INDIVIDUAL	22b. TELEPHONE (Include Area Code)	22c. OFFICE SYMBOL
David L. Kaplan	(508) 651-5525	STRNC-YMI

DD Form 1473, JUN 86 — Previous editions are obsolete. — SECURITY CLASSIFICATION OF THIS PAGE

UNCLASSIFIED

PREFACE

This report on inspection of fungicidal finishes on textiles by x-ray, infrared and ultrasonic methods was prepared by Paul Burstein of Skiametrics, Inc., Winchester, MA 01890 during the period June 1987 to April 1988, under Contract Number DAAK60-87-C-0045.

The project officers at U.S. Army Natick RD&E Center were David Kaplan and Marvin Greenberger.

TABLE OF CONTENTS

TABLE OF CONTENTS (Continued)

LIST OF FIGURES

LIST OF FIGURES (Continued)

LIST OF FIGURES (Continued)

LIST OF TABLES

FEASIBILITY OF INSPECTION OF FUNGICIDAL FINISHES ON TEXTILES BY X-RAY, INFRARED AND ULTRASONIC METHODS

1.0 INTRODUCTION AND SUMMARY

The aim of this Phase I program was to find a way to measure the amount of fungicide deposited on an underlying base textile.

The main result of the Phase I program is that a combination of inspection modes can provide rapid and unambiguous inspection of large-scale production runs of fungicide-treated textiles. Each of the separate inspection techniques can supply a critical amount of information, which (under reasonable assumptions) would yield adequate inspection data. Applied together, these techniques isolate the amount of fungicide, the penetration depth, and the presence of doped samples. Quantitative information can be obtained on spatial scales as fine as 0.010 inches (0.25 mm) if required. These techniques have time-scale responses ranging from milliseconds to seconds for on-line production inspections. The techniques will work under modern textile run speeds of 30-120 yards/minute (0.46 - 1.8 m/second). The trade-off for speed is in a reduced spatial resolution.

Samples of copper 8-quinolinolate fungicide on 10 oz (283g) cotton duck (cellulose) and untreated cotton duck were provided by the Army technical monitor. Eventually, confirming tests were run in x-ray fluorescence, dual energy x-ray, Fourier transform infrared spectrometry (FTIR), and in ultrasonic transmission.

After detailed study of the problem, which included simulations, calculations and much library work, we decided on experimental verifications for three general approaches. The first two are based on x-rays, and the third is based on Fourier transform infrared spectroscopy. Only after the initial set of data was obtained and analyzed was the decision to utilize ultrasonics taken. The x-ray and FTIR approaches were utilized because they yielded direct quantitative data on the amount of copper and the organic component (i.e., the quinolinolate) respectively. The ultrasonic approach measures a materials property that is an indicator of degree of penetration of the fungicide into the textile. This last measure guarantees that an application where the manufacturer has purposely doped the fungicide with extra copper (in order to pass the current mandated inspection test) will be discovered.

The first of the two x-ray approaches is a fluorescent x-ray determination using a conventional x-ray fluorescence arrangement. The second is an adaptation of a dual-energy x-ray technique that has recently been implemented in a medical context. The conventional x-ray fluorescence technique is sensitive to the higher atomic number (Z) components of the test specimen. The dual energy technique is applicable over a much wider range of materials and effective atomic numbers, although it may be fooled by high-Z contaminants. Both of these x-ray techniques present viable inspection means for copper-8-quinolinolate on fabric, the first test case for the system.

The FTIR approach uses either diffuse-reflectance or reflectance-absorbance techniques that are sensitive to the presence of the quinolinolate portion of the copper-8-quinolinolate, rather than to the

copper portion. The advantage in the FTIR approach is that it' s easier, cheaper, and less environmentally troublesome (from a radiation safety perspective) to operate. The disadvantage is that the method yields information only on or near the outside surface of the material, and that the area over which the measurement is taken is relatively large, typically 30 mm^2, although this can be reduced, perhaps to a size as much as 10 times smaller.

Confirming experiments were run for all sets of approaches, and the results were as expected. The x-ray experiments were sensitive to the copper portion of the copper-8-quinolinolate, and to precisely the right degree. The IR experiments dictated searching for a characteristic quinolinolate line or band. This was discovered at 1573 cm^{-1}. An unexpected, but welcome, surprise was found in the examination of government-supplied samples of copper-8-quinolinolate treated cotton duck: The characteristic line at wavenumber 1573 cm^{-1} was significantly broadened over its appearance as seen in a neat sample analysis. This broadening probably indicates a degree of cross-linking to the underlying textile. The IR experiments in transmission through the cloth were not of sufficient intensity to yield the total amount of quinolinolate along the line-of-sight.

The ultrasonic measurements are through-body transmission attenuations where the signal levels and delay times were measured for a variety of different copper-8-quinolinolate kinds of applications. The results consistently showed a very small statistical spread between members of the same group, and a very wide difference between members of different groups, the best of all results. These experiments showed that ultrasonics would be a powerful indicator of fungicide penetration depth.

Several system designs are presented: x-ray, FTIR, and ultrasonics based. By itself, each technology could satisfy almost all of the inspection requirements under reasonable assumptions. In a production system meant to detect and measure not only misfeasance, but clever and technically astute malfeasance, the combination of technologies is virtually impossible to defeat. In this latter scheme, each of these separate inspection technologies can be a station along a production line. These system designs are based on existing hardware systems available commercially. The modifications that we propose are minor relative to the cost of complete system development. This approach, detailed in the Phase II program plan, will deliver to the government prototype systems for detection and measurement of fungicides, fungicide distribution, and presence of any nonconforming copper (or similar element) in textiles. These techniques will also prove useful in examination of other types of penetration processes, e.g., copper-based preservatives in wood.

2.0 INSPECTION SYSTEM REQUIREMENTS

In this section we address the ideal requirements that the fungicide inspection system should fulfill, and practical limitations on those requirements. Thus, a machine that could in theory provide very fine spatial resolution would be impractical in a production environment because the reams of data to be processed on each bolt of material would be overwhelming. (For instance, a bolt of cloth 150 feet (46m) long and 10 feet (3m) wide with spatial resolution elements 0.010 inches (0.25mm) square would yield over two billion measurements, clearly a monumental data acquisition and analysis effort.)

2.1 Variety of materials

The variety of textiles and their configurations, e.g., warp, weave, numbers of lines per inch, etc. is large. For any inspection technique to be practical beyond a single fabric base, the range of materials and thicknesses must be taken into account. Ideally, thick materials, such as leather, should also be considered.

2.2 Low atomic number based textiles

All of the textiles are based on cellulose or nylon or some other carbon, nitrogen, oxygen, and hydrogen based compounds. The underlying textile should contain no high-Z (high atomic number) materials insofar as contamination is concerned. The expected degree of contamination by any high-Z materials was expected to be very small, probably less than 1 part in 10,000, unless some unaccounted process was at work. As is discussed in the x-ray experimental verification section, this turned out not to be true. Nickel-based salts are used as a dissolving medium for the copper-8-quinolinolate, a fact which was uncovered only when the x-ray tests yielded discrepant figures.

2.3 Spatial resolution

The spatial scale that is preferred for these investigations is, "as fine as possible". Ideally, information on a scale smaller than the individual thread scale is desired. Present techniques, however, are limited to average material properties over several square inches of sample. Previous micro-techniques that have been tried include scanning electron microscopy and coarse x-ray fluorescence measurements. These, however, were incredibly slow, and they involved significant destructive testing.

2.4 Penetration and evenness of the fungicide

Information on the evenness of the application of the fungicide (and any other finish coating that may be applied simultaneously) is necessary. Knowledge of the degree of penetration of the fungicide into the threads is also required.

2.5 Holes in the fungicide application

Ideally, the inspection technique should be able to find holes where there is no fungicide. Fungal spores with characteristic sizes of 1-2 microns can penetrate through holes that are larger than this size and begin the rotting process in the textiles.

2.6 Chemical cross-linking

There may be, at least in some fungicides, chemical cross-linking with the materials in the textiles. This cross-linking may inhibit growth of fungi. The main issue in retarding fungal growth is whether the inhibitor mechanism is due to the physical blocking of access to the underlying textile or to the chemical cross-linking. X-ray techniques are not able to discriminate cross-linking from mere physical presence. The reason is that all x-ray-based measurement schemes are sensitive only to the elemental presence. The change in separation of the energy levels is too small to be measured with current technology. The infrared results, however, yield some evidence for presence of cross-linking, as discussed in Section 5.

2.7 Samples

The initial test sample is 10 oz. cotton duck, coated with copper 8-quinolinolate. According to the specification for treating (CCC-D-950E), the percentages of copper (not copper-8-quinolinolate compound) that is within tolerance varies from 0.18% to 0.27%, a relatively small fraction by most x-ray inspection standards.

2.8 Interface

There is no specific requirement on interfaces, except insofar as the technique must ultimately allow for installation at the factory or depot level.

2.9 Time for inspection/inspection coverage

Ideally, the inspection could be accomplished in real-time, and the inspection coverage would be 100%. As it turns out, for spatial resolutions compatible with individual thread isolation, the inspection times for all technologies almost certainly prohibit 100% inspection. Some type of sampling is necessary. The question is what type of sampling.

In general, there are three choices: (1) Fine spatial sampling at a very limited number of positions in real-time. (2) Coarse sampling (over many threads) over a very large number of positions in real-time. (3) Fine spatial sampling over a very large number of positions in nonreal-time (much time spent in data acquisition). Subsequent discussion with the technical monitor revealed that a compromise between the first and second positions would be the most preferable of the approaches for production machinery, while a more research-oriented approach (e.g., for eventual process control) favored the third.

3.0 THEORETICAL INVESTIGATIONS

Within the total electromagnetic spectrum, photons in two wavelength bands make good sense as inspection probes for the base textile material and the copper-8-quinolinolate fungicide. These are the soft x-ray band, extending from 5-50 keV or so, and the mid-infrared to far-infrared band, 50-5000 cm^{-1}.

The x-ray band provides good probability for excitation and fluorescence of the K-alpha lines of copper in the copper-8-quinolinolate. As the time of original submission of the proposal, our understanding of the problem was that the material to be analyzed was a low-Z base textile coated with a thin layer of the fungicide. This model was wrong, as the first meeting with the technical monitor showed, and various configurations for making workable the originally proposed fluorescence-based detection were tried.

This original scheme, shown in Figure 1, utilized a radioactive source, and featured pulse height discrimination of a fast single-photon x-ray detector. Unfortunately, the count rates in x-ray fluorescence were simply too low to accommodate a radioactive source, no matter what kinds of filters or multiple source and detector combinations were used. Data acquisition times as calculated for a single copper-8-quinolinolate measurement, which was averaged over a 6 mm diameter circle, were at least several minutes for the most favorable of configurations. This fact led to inordinately long data acquisition times for even the sparsest of sampling approaches.

Replacing the radioactive source with an x-ray generator provided significantly better results, and these are discussed below. However, the fluorescence technique has some definite drawbacks, which are also discussed below.

Dual x-ray energy techniques were approached, and number of different experiments conducted. This approach provides more satisfactory results, again, with some drawbacks.

Finally, investigations of inspection possibilities in the infrared were initiated as an alternative to the x-ray methods. Infrared approaches

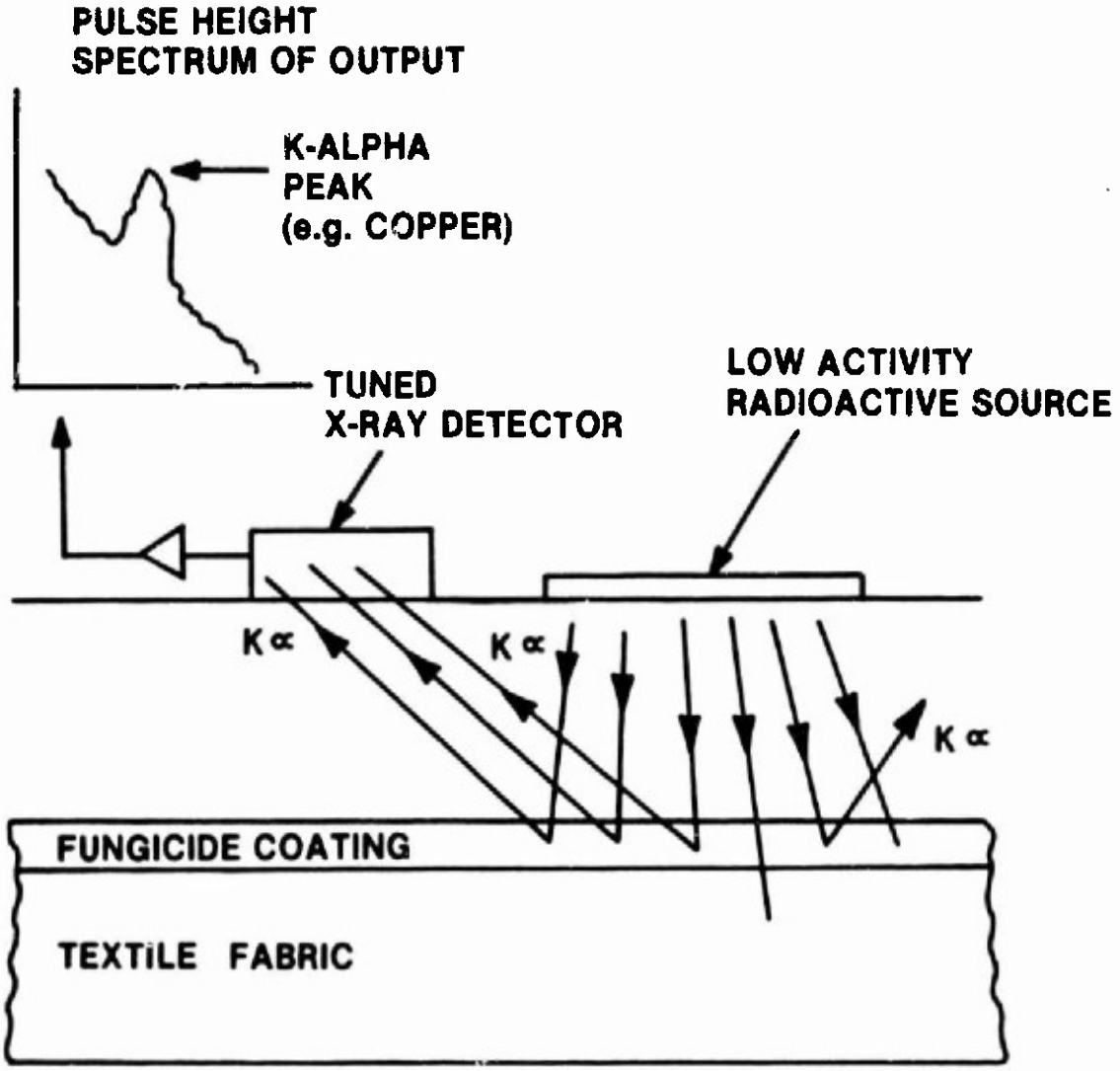

Figure 1. Original concept for tuned x-ray analysis of a thin fungicide coating.

differ from the x-ray approaches in that the sensitivity is to the organic molecule part of the compound, rather than to the heavy element part, as the x-ray techniques are.

This section of the report chronicles these pre-experiment calculations and analyses.

3.1 Model for textile and fungicide

Our initial model for the fungicide application to the textile was as a coating on a relatively impervious substrate. We quickly discarded this model and adopted one of a series of threads into which the copper-8-quinolinolate solution was absorbed, a penetrating fungicide model.

If the fungicide were relatively uniformly absorbed throughout the fabric, then the fungicide fraction of the whole (i.e., textile base + fungicide penetrant) would be constant, no matter what method of analysis was tried. If, on the other hand, the fungicide was not uniformly distributed, but rather stuck closer to the surface of the fabric, then the combination of through-body (i.e., transmission) measurements and surface- and near-surface-measurements together would yield a quantitative index of how far the fungicide had penetrated.

We have chosen this type of model and approach because any further localization of fungicide concentration within the body of the textile (and hence, within individual threads) requires localization of entering and exit beams of radiation to minuscule scale. While this is theoretically possible (and to a certain extent useful via computed reconstructions, e.g., microlaminography approach by ARACOR of Sunnyvale, California) data acquisition times, intrinsic variations of the textile, and the need for precise mechanical fixturing and positioning make this choice less than

desirable. Development of such a machine is currently being undertaken by ARACOR at a cost of upwards of $1.5 million; data acquisition on a single square sample 15 cm on a side is expected to take tens of minutes.

3.2 X-ray scattering solutions

The basic approach is to utilize a needle-beam of radiation that impinges on the treated fabric as shown in Figure 2. The x-ray beam then interacts with the elements in the treated fabric. The two main interaction processes are scatter and photoelectric interactions. It is the resulting outcome of the photoelectric process that we seek to exploit.

The photoelectric interactions can produce fluorescence radiation as one of the products. This fluorescence radiation is characteristic K-line radiation of the element involved. Thus, the characteristic K-line of copper at 8 keV is a good signature for the presence of the copper-8-quinolinolate as long as two conditions are fulfilled. First, there must not be significant absorption of the entrance or exit beam, and second, that the x-ray detection system be able to resolve the copper K-line energy from other extraneous signals.

The samples of cotton duck provided by the Army were sufficiently transparent to the x-rays so that the first condition of little absorption was fulfilled. The second condition of not confusing the copper K-line with other signals can be attained for detectors that have only moderate energy resolution, as long as there are no other elements with atomic numbers near copper. (This latter condition, however, turned out not be true. An x-ray fluorescence analysis at very high energy resolution revealed the presence of not only copper, but nickel and manganese at concentrations sufficiently high so as to swamp or spoil the signal

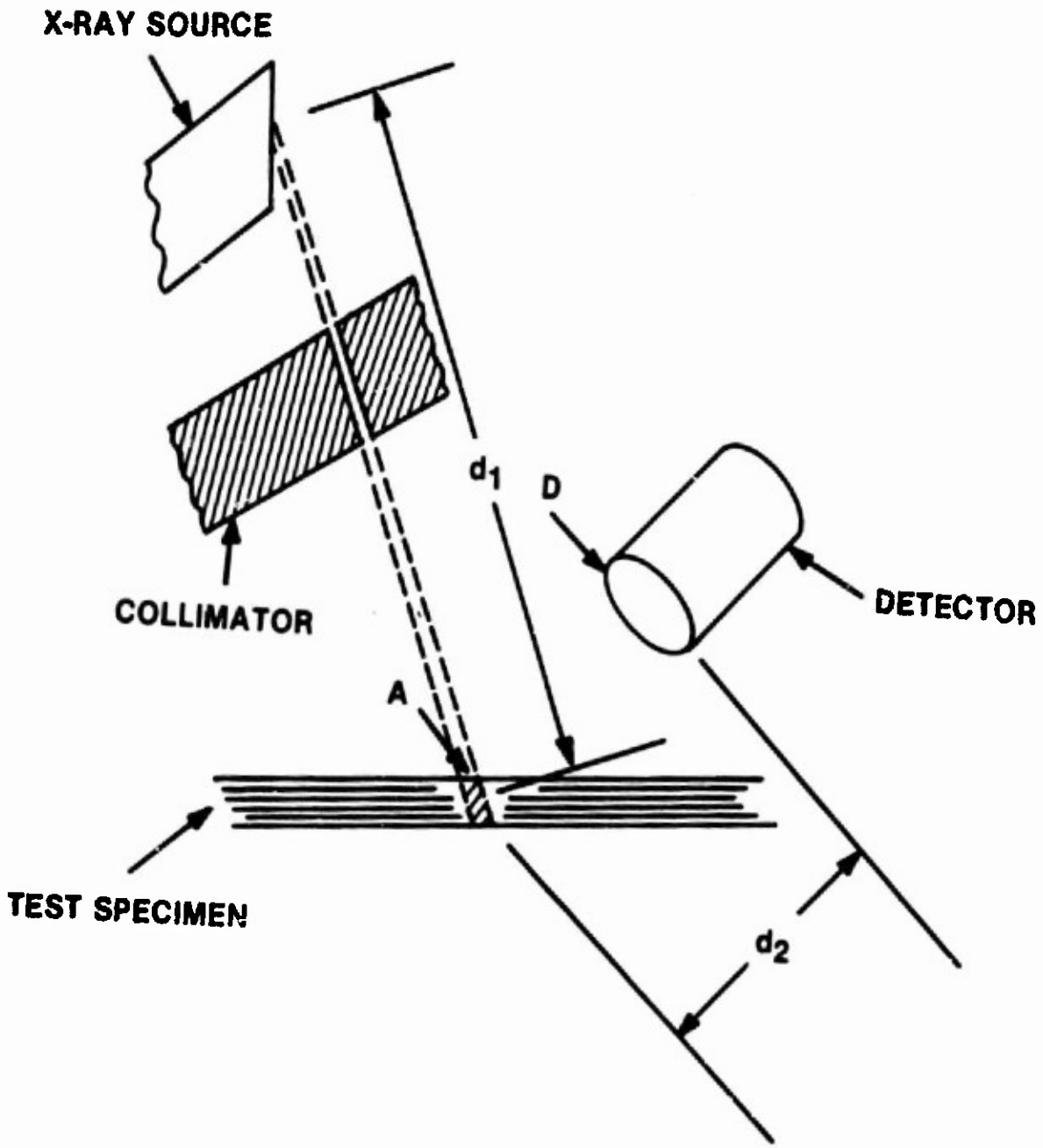

Figure 2. Basic layout of needle-beam geometries. An x-ray source, a distance d_1 from the test specimen illuminates an area A on the test specimen. This is defined by a collimator, also shown. A detector of area D, a distance d_2 from the test specimen, collects the scattered and emitted radiation.

provided by the copper in a detector of coarser energy resolution. The presence of the nickel and manganese was not discovered until after all other x-ray measurements were made and analyzed. These high-resolution measurements were made to verify the results obtained under the coarser resolution conditions; they will be discussed in more detail later.

3.2.1 Scattering interaction mechanism

The scattering interaction is shown in Figure 3. An incoming beam of x-rays is shown impinging on the test specimen. Noninteracting x-ray photons simply pass through the sample. Interacting photons do so in one of two major ways: The photoelectric effect (as described above) or by Compton scattering.

The photoelectric effect process involves interaction of the x-ray with the atom as a whole. The photoelectric effect is applicable only to the absorption of the incoming x-ray beam. The particular class of atomic rearrangement to be exploited is the rearrangement and emission of characteristic K-alpha radiation from the copper.

The process consists of: the absorption of the interacting x-ray, the ejection of a K-shell electron from the atom, rearrangement of the atom by the simultaneous drop of an L-shell electron to the K-shell and the emission of an x-ray photon with a definite energy (corresponding to the difference between the K- and L-shell energy levels), and similar M- to L-shell drops, etc.

The emission of the characteristic K-line radiation is isotropic. Thus, a detector whose field-of-view encompasses the impinging x-ray needle beam on the test specimen but is not in line with the beam will see a fraction of this fluorescent copper K-line radiation. As long as copper-

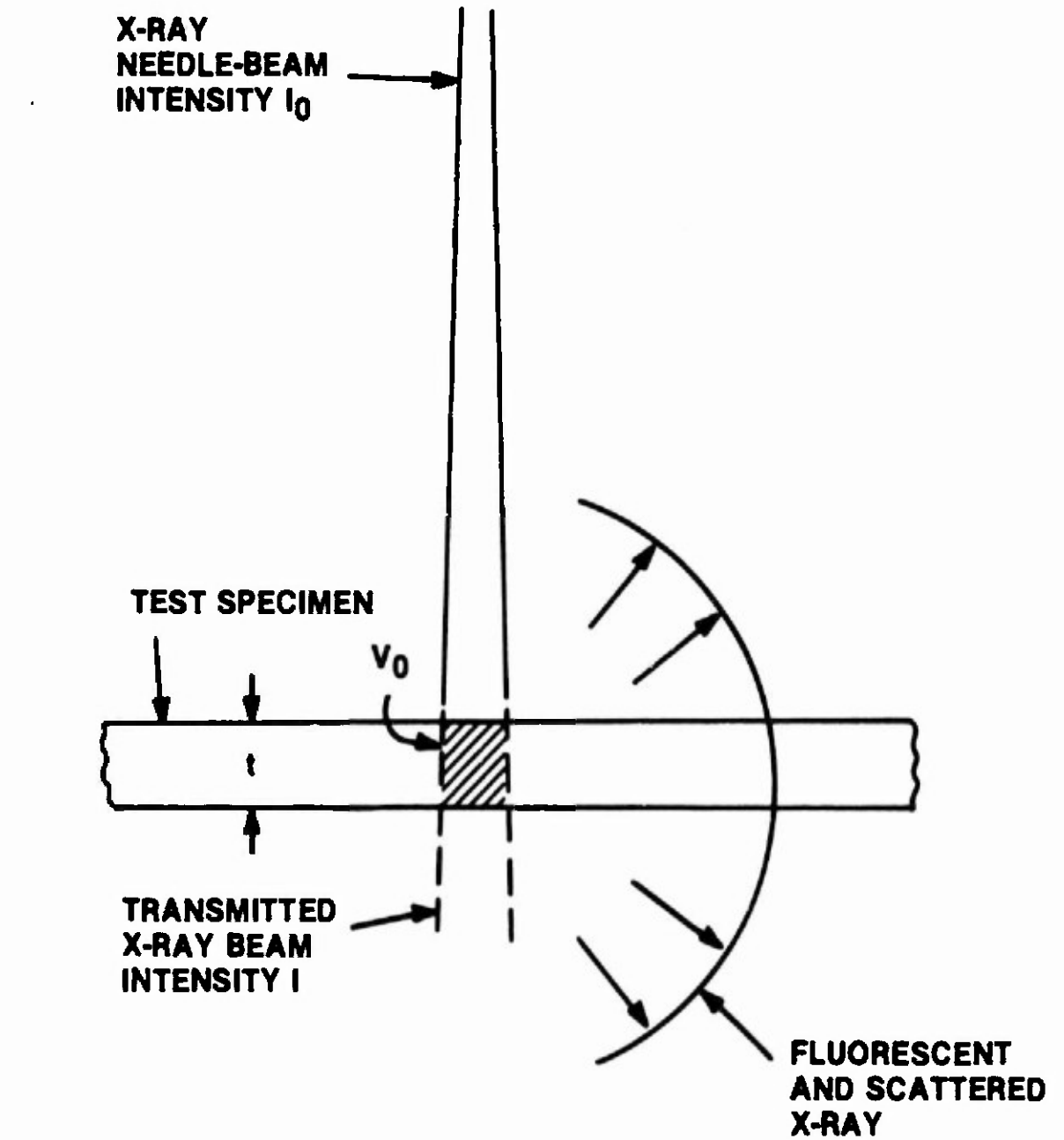

$I = I_0 e^{-(\mu/\rho)(\rho t)}$

V_0 = INTERACTION VOLUME
ρ = DENSITY OF TEST SPECIMEN

Figure 3. Interaction diagram for scattered and fluoresced x-rays.

is the only high atomic number element present, copper K is the only x-ray fluorescence signal in the x-rays that emanate from the test specimen.

The second component of x-rays from the illuminated region of the test specimen is Compton-scattered x-rays. At low x-ray energies, i.e., those below 20 keV, the probability for Compton interaction in this test specimen is quite low. While the probability for Compton interaction grows with increasing incident x-ray energy, the only component that truly matters is that which is in the detector's effective energy resolution band covering the 8 keV copper K-line. This is the reason for a certain amount of spectral resolution in the detector. With this spectral discrimination, permissible voltages for the x-ray source are substantially higher than those required for a simple broadband detector with no energy discrimination.

Ideally, there would be a substantial flux from the K-line that could be utilized in a "current-mode" detector — one that would not have to sort through individual photons. This mode would allow substantially greater signal throughput, if the flux were present. The next section presents some of the results of these calculations, and points the way for system design, including the choice of detector.

3.2.2 Estimating the flux

The aim of the estimate is to establish the relationship between sample size, the x-ray generator characteristics, the detector characteristics, the overall configuration, the sensitivity, and the time required to measure the amount of copper present.

The equation looks like this:

$$N = \left(\frac{1.1\times10^{-9} Z V^2 I}{E}\right)\left(\frac{A}{d_1^2 \cdot 4\pi}\right)\left(\left[1 - e^{-\mu/\rho \cdot \rho t}\right] F\right)\left(\frac{De}{d_2^2\ 4\pi}\right) \quad \text{(eq. 3.2.2-1)}$$

where

z = atomic number of x-ray anode material

V = anode voltage

I = anode current

E = effective energy of the x-ray entrance beam

A = area of sample size on test specimen

d_1 = distance between anode and sampled region on test specimen

D = area of detector

e = efficiency of detector

d_2 = distance between sampled region and detector

μ/p = interaction cross-section for photoelectric effect

pt = areal density of copper (grams per square centimeter)

F = fluorescence yield

The first term in parentheses is the source flux in terms of x-rays per second. It is based on the formula of Compton and Allison[1], and utilizes an effective energy of the incoming beam.

The second term in parentheses is simply the solid angle of the sampled region in the test specimen as seen from the source, normalized by 4(pi). Multiplication of the source strength by this term yields the number of x-rays per unit time that reach the sampled region.

The third term contains the probability for photoelectric interaction and ultimate release of a fluorescent copper K-line photon. Multiplication of this factor by the previous terms yields the total number of fluorescent copper K-line x-rays emitted from the sampled region per unit time.

The fourth term contains the solid angle of the detector as seen from the source, normalized by 4(pi). Also included is the efficiency of detection of these fluorescent x-rays. This term is the overall detection efficiency for all the fluorescent copper K-line photons produced in the sampled region.

Multiplication of the previous terms by this factor yields the number of fluorescent x-rays actually detected per second.

We have made many simplifying assumptions concerning average (or effective) energies, ignoring certain characteristic lines present in the x-ray anode and other complicating factors. While these "complicating factors" will have an effect on the outcome, to the extent that the estimate is to be trusted (approximately a factor of 2), the assumptions are valid.

For nominal values of these variables, the number of photons per second in the detector is approximately 5000 for a sampled region of 1 square millimeter.

The implications for performance of the system are addressed in the following subsection.

3.2.3 Performance prediction for x-ray fluorescence

The implication of this result and Poisson statistics indicate that a 1-second measurement on an area of 1 square millimeter of this treated fabric will yield a measure of the amount of copper present to a precision

of 1.4%. This precision is inversely proportional to the square of the sampled region. Thus, a sample of 0.25 square millimeters (0.020 inches square) would have a precision of 2.8% if the measurement is to be made within 1 second. Time enters the equation for precision in a similar way: To double the precision, we must quadruple the time. These relationships can be summarized in the following relationship:

Square-root (precision) x area x time = constant

This generic equation is statistical (Poisson), and is applicable for all such systems.

If this measurement is made over a large area containing many threads, e.g., 25-100 square millimeters, discontinuities in individual threads, in thread-to-thread variations get averaged out. Of course, by doing this we also lose the good spatial resolution inherent in going to the very fine areal discrimination. Conversely, if we maintain fine resolutions, e.g., 0.010 inches square, there is always a question over what region of the thread was the measurement made. Thus, a copper content determination made over a tiny spatial element of fabric will be uncertain as to fractional content. If the region included a cross-over between two orthogonal threads, then the fraction of copper will be lower than if the measurements were made over a single layer of thread. A method for addressing this problem of knowing where we are is discussed in the next section.

3.2.4 Applicability of the technique

This x-ray fluorescence technique should be particularly applicable in several cases, but we must first solve the problem of knowing where we are making the measurement.

We propose that this be done by a simultaneous transmission measurement of the sample. Even though the cloth is relatively transparent to the 10 keV and higher energies, there will be a flux high enough to measure the amount of cloth present to a precision of better than 3%. This measurement on the transmitted beam can be made simultaneously with a current-integrating x-ray detector.

The x-ray fluorescence technique will be useful under these circumstances:

1. The detector must be able to discriminate the fluorescent x-rays from any background.
2. There must not be any other high-Z material present that could interfere with the measurement.
3. The underlying material must be relatively transparent to the fluorescent K radiation. Otherwise a signal weighted by depth in the underlying material will result.

As we discovered in the testing phase, nickel salts used to dissolve the copper-8-quinolinolate made this technique less than perfect for this application.

The x-ray fluorescence technique will be relatively slow to implement on any kind of production basis unless sparse sampling is allowed, or unless averages over large regions are allowed.

3.3 X-ray dual energy techniques

Dual energy techniques were first introduced in medical x-ray diagnostic technology nearly two decades ago (Judy[2]).

The essence of the technique can be explained in a single paragraph: A test specimen is made up of components that have different elemental

constituencies. These different constituencies can be separated into two groups, a high-atomic number group and a low-atomic number group. The aim of the examination is to discriminate the amounts of matter in each group as a function of position. Thus, such a technique is valuable for determining how much bone mass (calcium) is present in a patient with osteoporosis. Two x-ray attenuation measurements are made on a single test specimen. The two measurements are made at different energies, one much higher than the other. Experimentally, we observe that the low-energy beam is attenuated to a much greater extent that the high-energy beam in both low-Z and high-Z components, but the high-Z attenuation is far more severe: The high-Z component has a much higher contrast between low and high energies than the low-Z component. We use the low-Z component to "normalize" the data, and the differential attenuation to find the amount of high-Z material present. When the high-energy and low-energy beams are lines, i.e., containing little spectral spread, this technique is referred to as dual photon absorptiometry (DPA). A description of this interaction mechanism is shown graphically in figure 4, taken from the Nord[3] paper.

The copper in the copper-8-quinolinolate is the high-Z component. Everything else is the low-Z component. Analytically, we can work this out following Nord's derivation. Nord uses monoenergetic sets of energies; we have generalized the results to include the spectrum of x-ray energies that would emanate from an x-ray generator. That is the reason for all the integrals over energy. (Note, in Nord's paper there is an error in the formula for the areal density of the low-Z (s) component.)

Transmitted intensity is related to incident intensity exponentially:

$$\hat{I} = \int I(E)dE = \int I_o(E)\, e^{-\mu/\rho(E)\sigma}\, dE \qquad \text{(eq. 3.3-1)}$$

where μ/ρ = gamma attenuation coefficient

σ = areal density of material

The gamma attenuation coefficient is a function of x-ray energy and the elemental constituency (atomic number — Z) of the test specimen. The two transmission equations are:

$$I^L = \int I_o^L(E)\, e^{-\mu_s^L/\rho\,\sigma_s}\, e^{-\mu_b^L/\rho\,\sigma_b}\, dE \qquad \text{(eq. 3.3-2)}$$

$$I^H = \int I_o^H(E)\, e^{-\mu_s^H/\rho\,\sigma_s}\, e^{-\mu_b^H/\rho\,\sigma_b}\, dE \qquad \text{(eq. 3.3-3)}$$

The superscripts L and H indicate the two energies (low and high) over which the two transmission measurements are made. The subscripts s and b denote the low-Z and high-Z materials, respectively. (The origin of this notation is in the medical usage: s for soft tissue, b for bone.)

The two equations in two unknowns, the areal densities of the high-Z and low-Z components, can be solved for those quantities directly:

$$*\hat{}\,\mu/\rho(A) \equiv \frac{\int *I_o^A(E)\,\mu/\rho(E)\,dE}{\int *I_o^A(E)\,dE}$$

$$\sigma_b = \frac{(*\hat{}\,\mu/\rho_s^L / *\mu/\rho_s^H)\ln(*\hat{}I^H/*\hat{}I_o^H) - \ln(*\hat{}I^L/*\hat{}I_o^L)}{(*\hat{}\mu/\rho_b^L) - (*\mu/\rho_s^H)(*\mu/\rho_s^L)/(*\hat{}\mu/\rho_s^H)} \qquad \text{(eq. 3.3-4)}$$

$$\sigma_s = \frac{\ln(*\hat{}I^L/*\hat{}I_o^L) - (*\hat{}\mu/\rho_b^L)/(*\hat{}\mu/\rho_b^H)\ln(*\hat{}I^H/*\hat{}I_o^H)}{(*\hat{}\mu/\rho_b^L)/(*\hat{}\mu/\rho_b^H)(*\hat{}\mu/\rho_s^H) - (*\hat{}\mu/\rho_s^L)} \qquad \text{(eq. 3.3-5)}$$

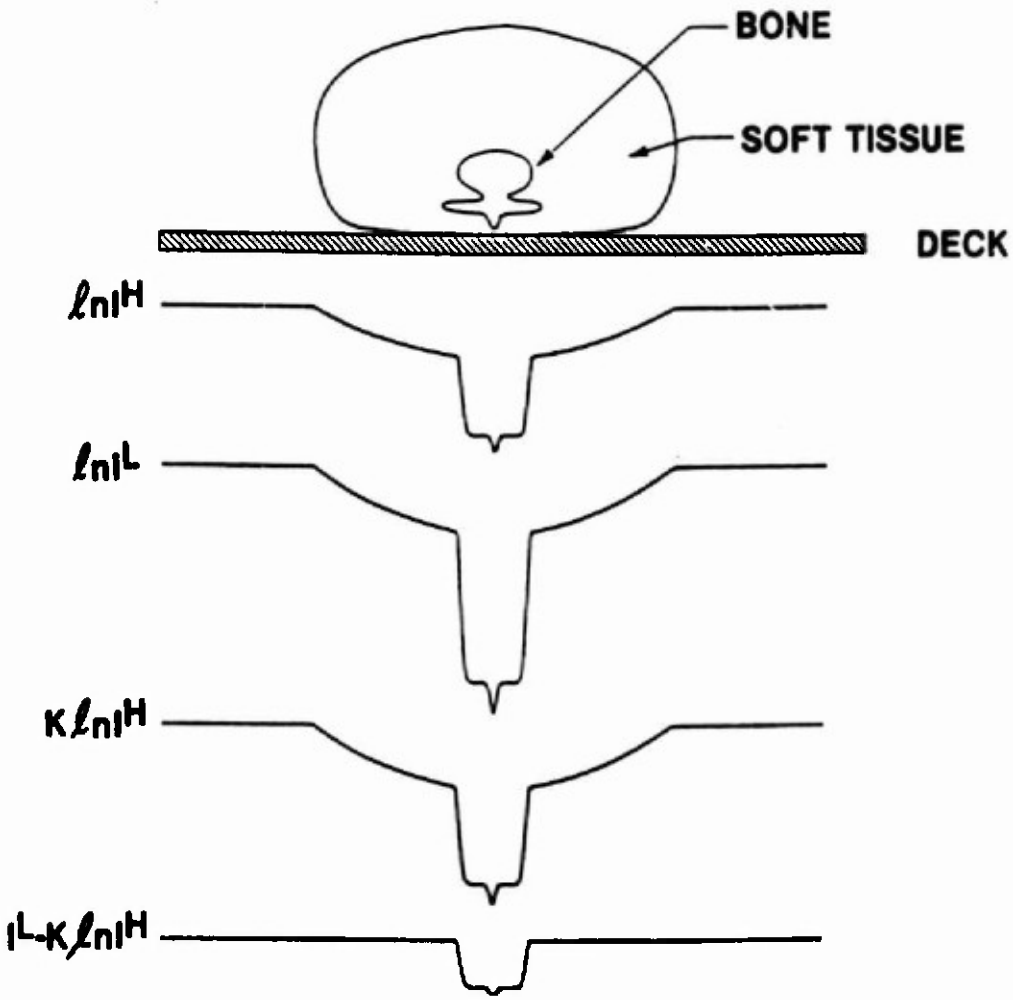

Figure 4. Graphic of x-ray dual-energy technique in the medical context.[3] Photon intensity profiles illustrating how the computation works. The top two traces show the raw data for a typical scan. The lower two traces show how the low-Z (i.e., soft tissue) effects can be subtracted away.

All other quantitities can be derived or measured independently. (While the notation seems cumbersome, its use stems from the restrictions set by the use of the particular spreadsheet which was used in the calculations described in the next section.)

We must now determine sensitivity of the technique to the number of photons, the spectrum of the x-ray generator and the sensitivity of the detector in deriving the fraction of copper-8-quinolinolate in a small region of the textile.

3.3.1 Calculation of dual energy response

The calculation task was broken into a number of subtasks. These included:

Determination of an initial x-ray spectrum.

Modelling the textile including the density variations of the copper-8-quinolinolate.

Transmission calculations through the treated cloth.

Calculation of detection efficiency as a function of voltages of the x-ray generator.

Calculation of the expected signal as a function of the amount of copper-8-quinolinolate relating to the different voltages and the sensitivity of the determination to errors in measurement.

Multiple linear regression analysis model for the relationship between the amount of copper-8-quinolinolate and the measured quantitities to determine best x-ray energies (generator voltages).

Performance predictions.

The entire calculation through the multiple linear regression analysis model was performed in a scientific spreadsheet. These calculations were done on spectral bins corresponding to wavelengths (rather than energy as shown in the previous subsection) since many of the programs in a commercial package were already set-up in that configuration. These files were maintained on a Lotus-1-2-3 compatible spreadsheet, and utilized programs available form SCIENCE.WKS for x-ray transmissions.

The initial x-ray spectrum was modeled on a tungsten anode as discussed in Gilfrich and Birks,[4] Birks,[5] and in Criss and Birks[6]. The spectrum included continuum radiation, the K and L lines of the tungsten anode (as applicable), and the effects of the beryllium window on the x-ray tube. Spectra were calculated at a number of different voltages. A sample is shown in Figure 5.

The textile was modeled as pure cellulose, and the copper-8-quinolinolate was modeled exactly. The only variables were the amounts of the cellulose and the copper-8-quinolinolate that were to be measured. Mass attenuation coefficients for each are shown in Figure 6. When multiplied by the (-) areal density for each component and exponentiated, the result is the transmission as shown for the cellulose component in Figure 7 (and shown analytically in equation 3.3-1. The fungicide component differs only slightly from full transmission, and so it is not shown here.

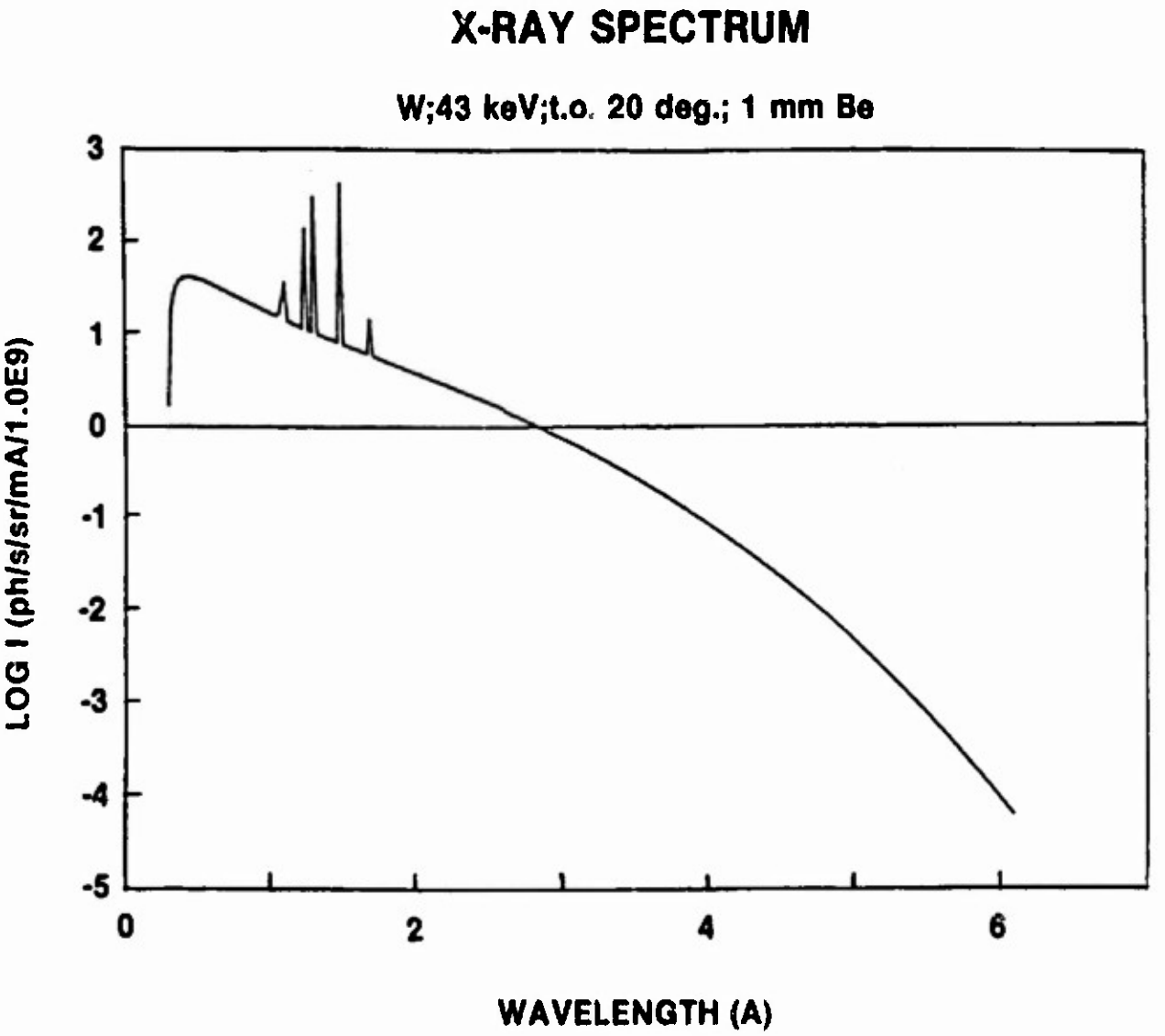

Figure 5. Sample x-ray spectrum computed as a function of wavelength. This particular sample is calculated at an anode voltage of 43 kV, with a beam take-off angle of 20 degrees, and a 1 mm thick beryllium window. The output is shown as the logarithm of the number of photons per second per steradian, per milliamp of emission current.

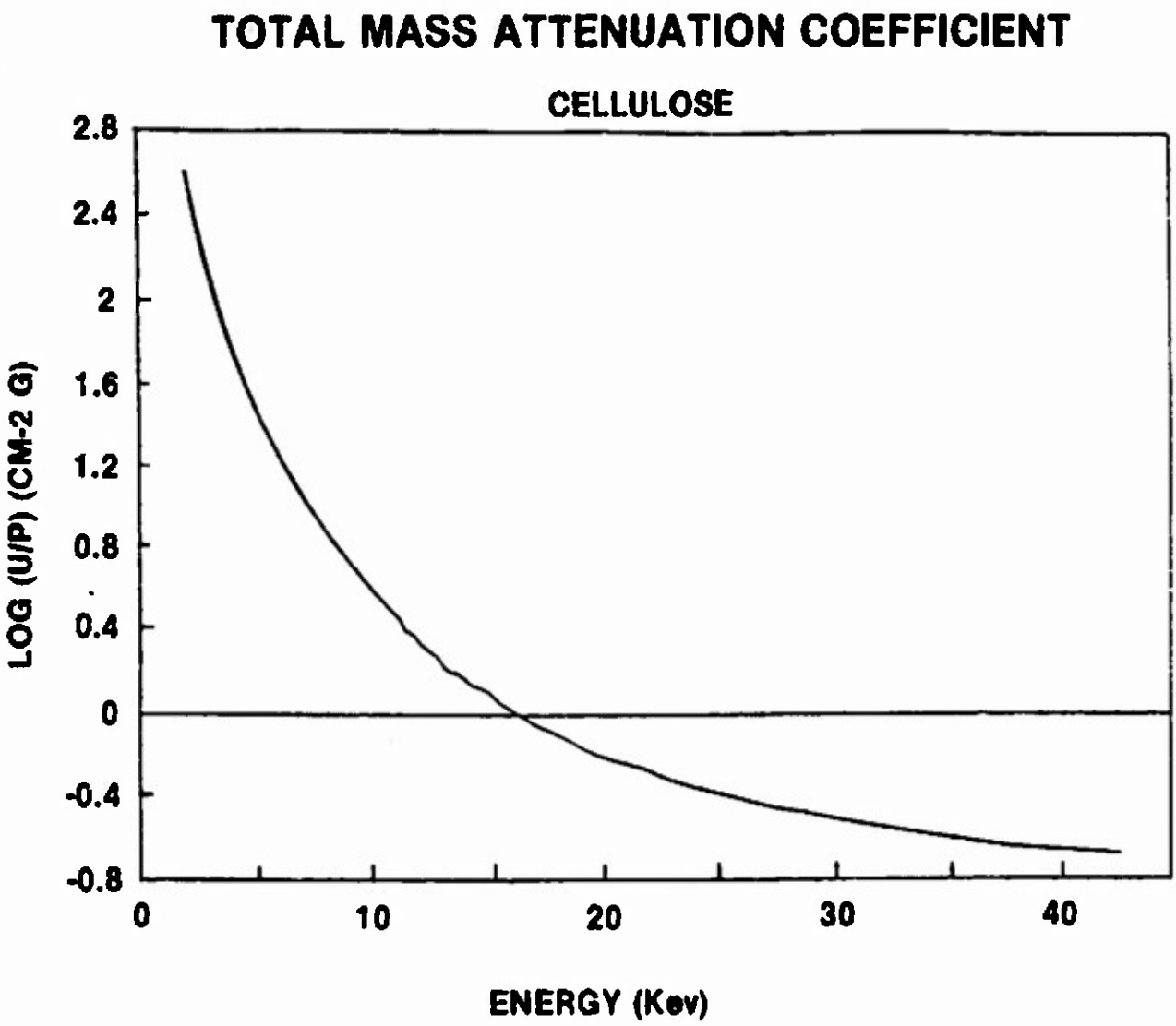

Figure 6a. The total mass attenuation coefficient for cellulose as a function of energy. The ordinate is in units of the "mu/rho" — cm^2/gram.

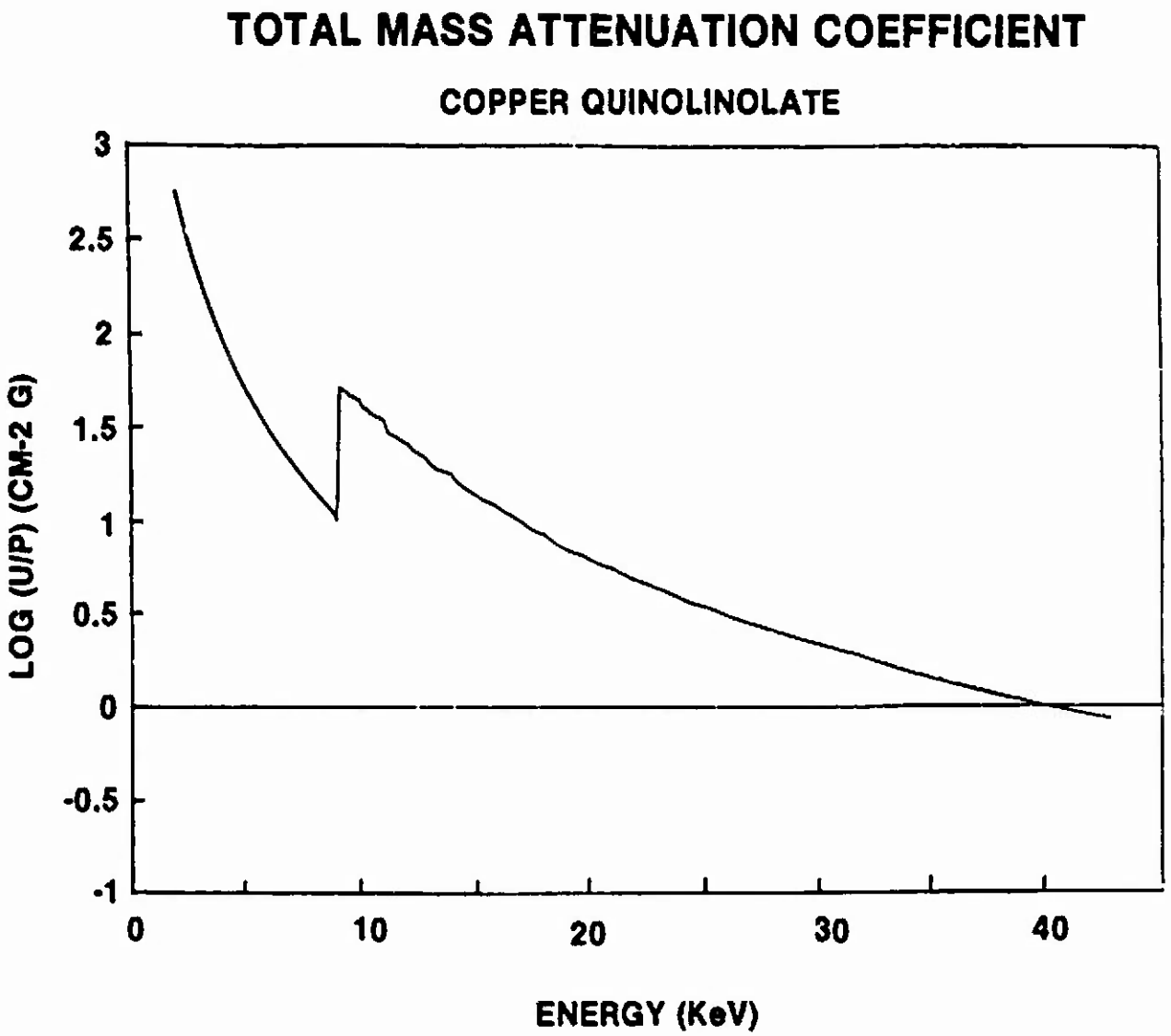

Figure 6b. The total mass attenuation coefficient for copper-8-quinolinolate as a function of energy. The ordinate is in units of the "mu/rho"--cm^2/gram.

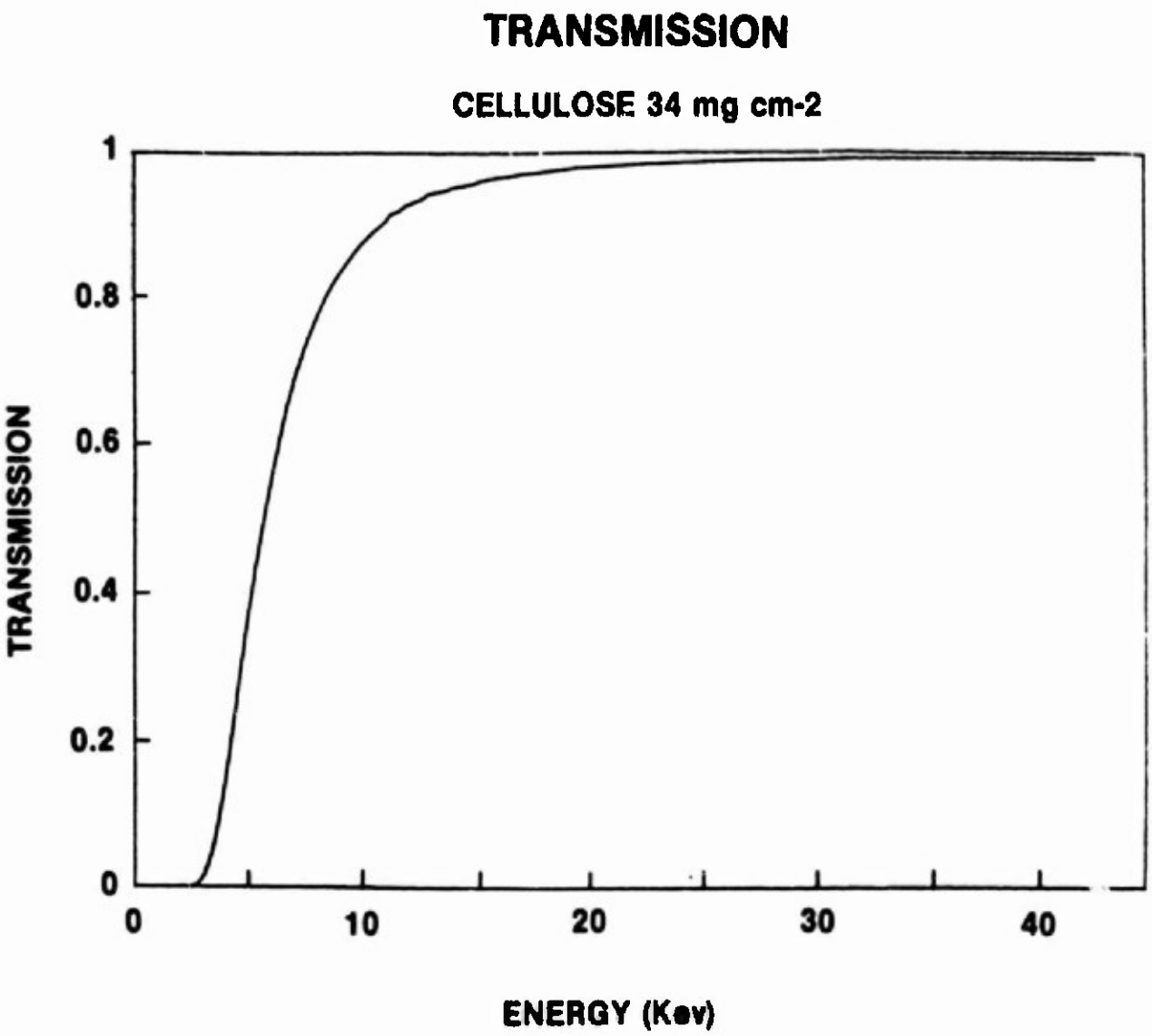

Figure 7. Calculated transmission of the cotton textile 283g (10 oz.) based on a pure cellulose constituency. On this scale, the change in transmission due to the copper is barely discernible.

The next step is the calculation of how much flux is actually seen by the detector: the integrated x-ray flux through the modeled cloth and fungicide. This is done on a bin-by-bin (wavelength or energy) basis, and the result weighted by the energy at that bin and summed. This is a measure of the total energy deposited in the counter (assuming 100% detection efficiency -- a good assumption in this energy interval) per unit time. Figure 8 shows the results of such a calculation for a particular set of conditions.

The resulting signal is shown in figure 9 for a variety of combinations of tube voltages. (For this particular set of conditions, the high voltage is always taken as twice the low voltage. This is not necessary, but for any practical x-ray high voltage source, it entails only using the center tap vs. the end-taps on the primary transformer winding.) The highest signal, however, does not necessarily imply the greatest sensitivity of the response to the two voltages. The 25/12.5 kV combination yields the greatest signal of the combinations tested.

```
  40.00 kV       ^I(0) = 2.1607E+12   ^I =   1.8722E+12 ph s-1 sr-1 as-1
cellulose        ^sI(0) = 4.8736E-03   ^sI =  4.4736E-03 watt sr-1 as-1
mass density:    copper q mass density:       s^u/p(C)=    2.8062
   34.0 sq cm-2              0.068 sq cm-2  s^u/p(Q)=   15.3950

  35.00 kV       ^I(0) = 1.5942E+12   ^I =   1.3845E+12 ph s-1 sr-1 as-1
cellulose        ^sI(0) = 3.3115E-03   ^sI =  3.0003E-03 watt sr-1 as-1
mass density:    copper q mass density:       s^u/p(C)=    3.2439
   34.0 sq cm-2              0.068 sq cm-2  s^u/p(Q)=   17.4340

  30.00 kV       ^I(0) = 1.1078E+12   ^I =   9.3268E+11 ph s-1 sr-1 as-1
cellulose        ^sI(0) = 2.1034E-03   ^sI =  1.8730E-03 watt sr-1 as-1
mass density:    copper q mass density:       s^u/p(C)=    3.8325
   34.0 sq cm-2              0.068 sq cm-2  s^u/p(Q)=   19.9318

  25.00 kV       ^I(0) = 7.0486E+11   ^I =   5.7968E+11 ph s-1 sr-1 as-1
cellulose        ^sI(0) = 1.2145E-03   ^sI =  1.0556E-03 watt sr-1 as-1
mass density:    copper q mass density:       s^u/p(C)=    4.6585
   34.0 sq cm-2              0.068 sq cm-2  s^u/p(Q)=   22.9396

  20.00 kV       ^I(0) = 3.8761E+11   ^I =   3.0699E+11 ph s-1 sr-1 as-1
cellulose        ^sI(0) = 5.9894E-04   ^sI =  5.0190E-04 watt sr-1 as-1
mass density:    copper q mass density:       s^u/p(C)=    5.9409
   34.0 sq cm-2              0.068 sq cm-2  s^u/p(Q)=   26.4729

  17.50 kV       ^I(0) = 2.6224E+11   ^I =   2.0157E+11 ph s-1 sr-1 as-1
cellulose        ^sI(0) = 3.8070E-04   ^sI =  3.1039E-04 watt sr-1 as-1
mass density:    copper q mass density:       s^u/p(C)=    6.9293
   34.0 sq cm-2              0.068 sq cm-2  s^u/p(Q)=   28.3415

  15.00 kV       ^I(0) = 1.6009E+11   ^I =   1.1753E+11 ph s-1 sr-1 as-1
cellulose        ^sI(0) = 2.1603E-04   ^sI =  1.6921E-04 watt sr-1 as-1
mass density:    copper q mass density:       s^u/p(C)=    8.4147
   34.0 sq cm-2              0.068 sq cm-2  s^u/p(Q)=   30.0545

  12.50 kV       ^I(0) = 8.2225E+10   ^I =   5.5539E+10 ph s-1 sr-1 as-1
cellulose        ^sI(0) = 1.0049E-04   ^sI =  7.3333E-05 watt sr-1 as-1
mass density:    copper q mass density:       s^u/p(C)=   11.1056
   34.0 sq cm-2              0.068 sq cm-2  s^u/p(Q)=   31.2710

  10.00 kV       ^I(0) = 3.1202E+10   ^I =   1.7347E+10 ph s-1 sr-1 as-1
cellulose        ^sI(0) = 3.2120E-05   ^sI =  1.9700E-05 watt sr-1 as-1
mass density:    copper q mass density:       s^u/p(C)=   17.6493
   34.0 sq cm-2              0.068 sq cm-2  s^u/p(Q)=   32.8402
```

Figure 8. Sample output of calculation program. This yields integrated results on the basis of both photons and total energy transmitted through the test specimen. The nontraditional symbols, e.g., ^ #I, arise because of the limited character set allowed by the Lotus 1-2-3 spreadsheet input. This nontraditional character set is followed uniformly in the text.

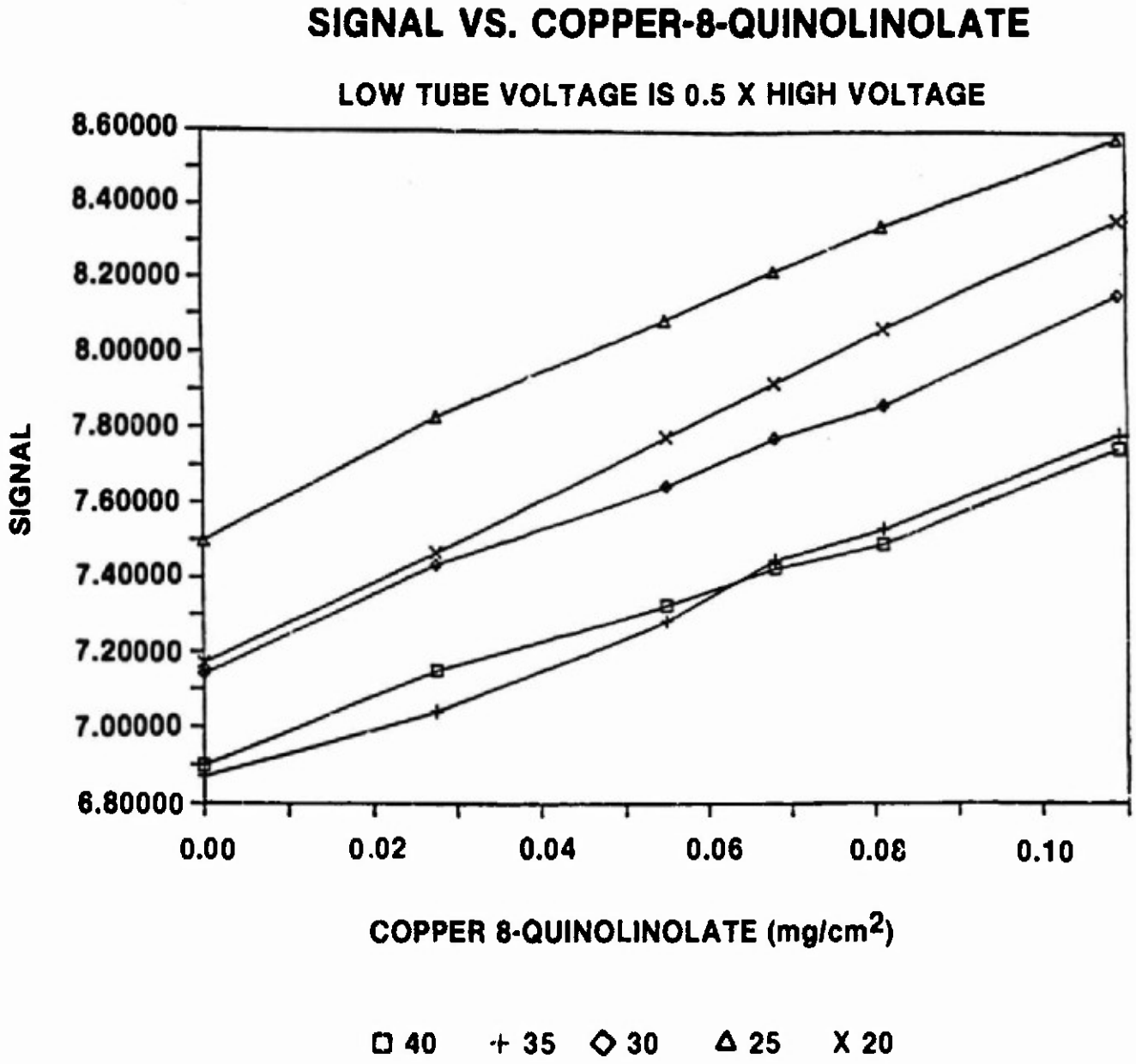

Figure 9. Gross signal predicted as a function of amount of copper-8-quinolinolate for various different combinations of x-ray generator voltages.

The only question that remains is the sensitivity to the accuracy of the measurement. The question of accuracy is one of how many x-ray photons are actually being generated per unit time for each of the different x-ray generation voltages and configurations; this is statistical accuracy. Thus, for instance, while the 25/12.5 kV may yield the highest signal, it may not offer the best slope, i.e., the best contrast. The amount of signal present may be feeble compared to a different voltage exhibiting less favorable sensitivity, e.g., 30/15 kV. (The analogy is in measuring the thickness of a piece of glass. If the measurement is made with visible light, there's plenty of signal, but poor contrast. If the measurement is made with UV, there's plenty of contrast, but practically no signal. In fact, the best radiation with which to measure the thickness of glass is usually x-rays, the energy being dependent on the thickness and accuracy required.)

As it turns out, the best combination for this series of assumptions is 20/10 kV as shown by figure 10. (Using any lower energies begins to involve self-absorption effects, and so we have used this energy as a practical low-energy cutoff.)

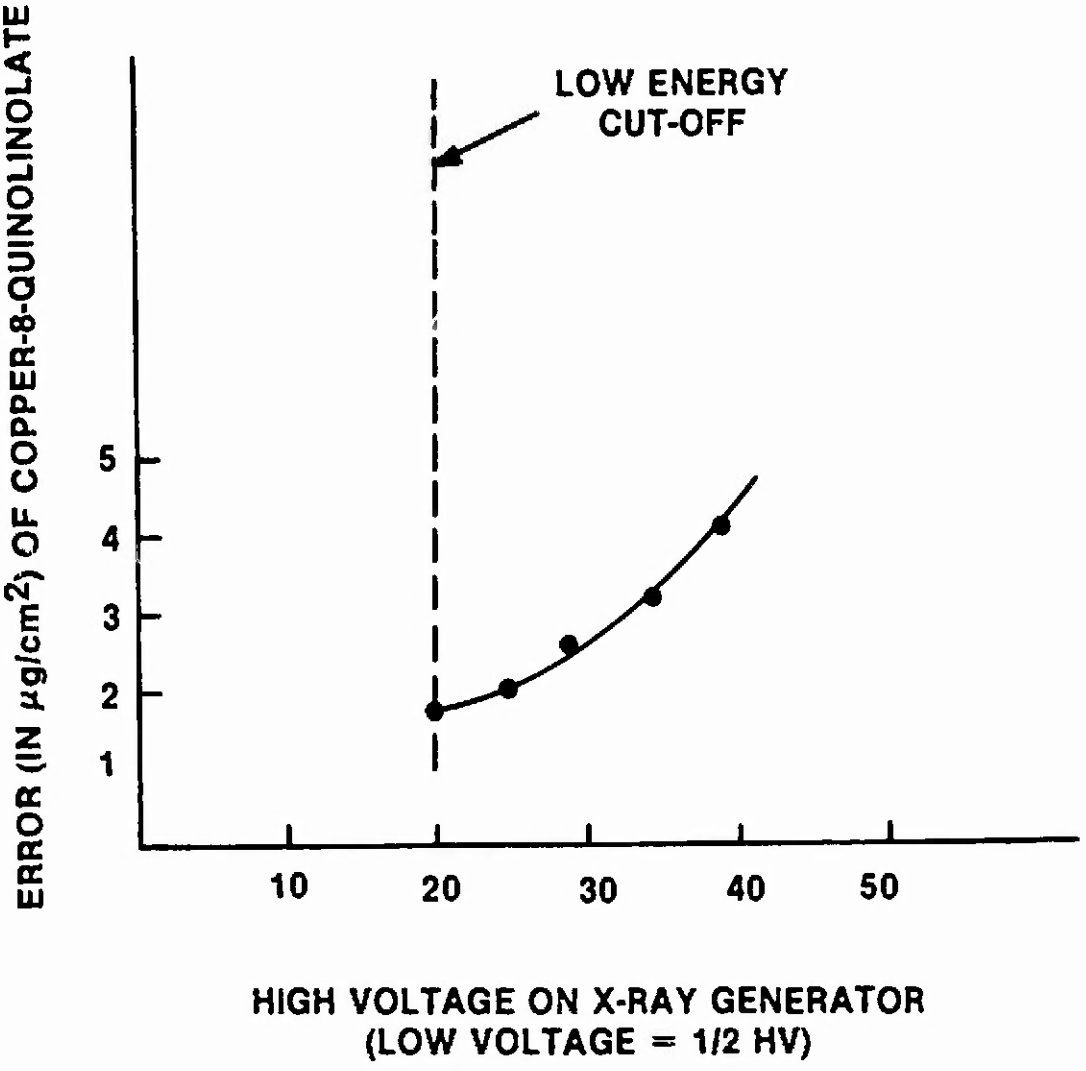

Figure 10. Best possible values for error in determination of amount of copper in micrograms/cm^2 as a function of x-ray generator voltage.

3.3.2 Performance prediction for dual energy technique

This is perhaps the hardest number to provide. The reason is that performance is critically dependent on an entire chain of assumptions involved in the system design. For the system conceptual design, a strawman design based on a standard x-ray diffraction source geometry, we calculated that the nominal amount of copper in copper-8-quinolinolate (0.068 mg/square centimeter) could be determined to a precision of +/-0.007, i.e., 10% in 1 second. The area of the measurement is 0.25 mm square (0.010 inch square). This is the same order of magnitude response as the fluorescence calculation yields. Since the dual energy technique is so sensitive to the assumptions, it was decided to stop the calculations at this point and proceed with a set of real measurements. These are described in section 4.

3.3.3 Applicability of the dual energy technique

The technique is well-summarized in the article by Nord.[3] The great advantage of the dual energy technique is that it is applicable over much greater ranges of thicknesses and effective atomic numbers of textiles and treatment agents. Thus, while fluorescence scattering measurements are practical only for reasonably thin fabrics and high-Z treatments, dual energy techniques are practical over much lower-Z treatments, and over very thick samples. (Dual energy medical diagnostic units find the amount of calcium present in the backbone. This attenuation is very high; indeed, the human gut presents the most attenuating region for any medical x-ray examination.)

So phosphorus-based compounds could be examined on thick leather, as an example. Indeed, the technique can be used to examine the distribution of

copper-based preservatives in wood samples, for which a feasibility experiment has already begun, based on the initial calculations made early in the program.

Compared to the fluorescence, the advantage of the dual energy technique is that there are many transmitted x-ray photons to measure, rather than having to dig out every photon from the noise. The disadvantage is that these transmitted photons must be measured to a very high precision. This is seen in the results of the dual energy measurements in section 4.

3.4 Infrared techniques

An alternative to x-ray examination for nondestructive testing is inspection with other wavelength bands. One of the most attractive of these bands is the infrared (IR) band. X-ray examination is cumbersome by standards of other types of inspections. With x-rays, there is always a radiation hazard, the equipment is expensive relative to other types of inspection, and there is considerably more effort involved in educating personnel, both from usage and safety perspectives. The important aspects for sensible implementation of IR are two-fold: The textile base must have an IR pass-band, and the copper-8-quinolinolate must have a measurable absorption within the textile pass-band.

The primary difference in detection schemes for IR vs. x-ray is in the detection of the organic quinolinolate via IR vs. copper via x-ray.

The disadvantage in IR detection is that every different combination of base and treatment materials must be examined for the combination of fabric pass-band and fungicide absorption within the pass-band.

There are a number of IR approaches that can be applied. These are discussed in the next section.

3.4.1 IR methods of approach

There are a number of sensible subcategories of IR approach. They are all based on Fourier Transform Infrared (FT-IR) techniques, which are discussed at length in Griffiths and de Haseth[7] and in the series edited by Ferraro and Basile[8,9]. The techniques that seemed fruitful in the initial stages were in the mid- and far-infrared bands.

Mid-IR (5000-500 cm^{-1}) techniques include transmission, attenuated total reflectance (ATR), reflectance-absorbance (R-A) and diffuse reflectance (D-R). Far IR (400-50 cm^{-1}) techniques include transmission and D-R.

(A word about units: Common IR usage dictates description of the energy in terms of wave numbers, whose unit is inverse centimeters [cm^{-1}]. The radiation that has this wave number has a wavelength equal to the reciprocal of the wave number. Thus, the boundary between mid-IR and far-IR, typically taken to be 500 cm^{-1}, is 0.002 cm = 200,000 Angstroms.)

Transmission. Transmission techniques are fairly straightforward. The sample is placed in one leg of a path of a Fourier transform IR spectrometer, and the transmission is measured as a function of wavenumber.

Attenuated total reflectance (ATR). This technique is a subgroup of internal reflection spectroscopy. The technique is based on maintaining an interface between the test specimen and a crystal of known index of refraction and geometry. An infrared beam is passed into one end of the crystal and makes its way down the crystal, alternately bouncing off the crystal/specimen interface and the crystal/air interface. The characteristics of the specimen at the crystal/specimen interface determine

the magnitude of reflection and the sampling depth on the test specimen (as a function of wave number). ATR is primarily a surface or near-surface phenomenon. Thus, in combination with a large amount of copper-8-quinolinolate found in a transmission measurement, high ATR readings for the fungicide would indicate that the materials were resident on the outside of the fabric. Conversely, low ATR readings would indicate that the fungicide had been largely absorbed.

Reflectance-Absorbance (R-A). Reflectance-absorbance measurements are made at grazing incidence. The usual rules of electric-field boundary conditions apply. (See Golden's article, "Reflection-Absorption Spectroscopy" in Ferraro and Basile[9]). The angle of incidence is set equal to the angle of reflection, and absorbance measurements are made. The R-A technique does not depend on a contact measurement as does the ATR technique. R-A does, however, measure the same type of surface effect as does ATR.

Diffuse Reflection (D-R). D-R measurements are specifically made under conditions where the angle of observation of the test specimen is specifically not equal to the angle of incidence, i.e., there is no "reflection" in the D-R signal. D-R is typically accomplished at angles far closer to normal incidence than the R-A measurements. The D-R measurements are more difficult to interpret theoretically, since they are sensitive to a combination of scattering, absorption, reflection, and internal transmissions. D-R measurements result from a combination of surface and bulk effects.

These are the specific techniques that could be used to examine the copper-8-quinolinolate treated samples. The response of the fungicide on

an underlying cellulose base could not be reliably calculated, or any subsequent performance predicted for a system employing FT-IR principles. It turns out that performance for these techniques could be measured directly, and that is exactly what we have done. The experiments are discussed in Section 5.

3.4.2 Applicability of the IR techniques

If the IR techniques provide sufficient data on the fungicide-treated fabric, this is clearly a more desirable inspection scheme than one based on x-rays. IR equipment is cheaper and easier to maintain than x-ray equipment, presents no radiation safety hazards, and typically scans much faster than does an x-ray based system.

3.5 Other techniques

Other techniques fall into two categories, direct approaches dependent on measuring the amount of copper or the quinolinolate portion of the copper-8-quinolinolate, and indirect approaches that measure a derived materials property of the treated textile.

Insofar as direct measures are concerned, no other wavelength bands present reasonable inspection schemes for these textiles and the fungicides in any contexts outside narrow research tools. While Raman IR techniques were also studied, solidified forms of the fungicide would most likely broaden the response bands to the point of loss of fungicide identity, and this approach was quickly abandoned.

Indirect measures would include, for instance, measurement of intensity and spectrum of visible light transmission, ultrasonic wave attenuation and speed, and stress-strain curves. Visible light solutions are complicated by other factors, unfortunately, because the intrinsic variability of the

base textile causes tremendous variations in transmitted light. An ultrasonic approach measures acoustic impedance, and thus could provide a good measure of the penetration of the fungicide, if there is sufficient spread in the acoustic signatures between treated and untreated samples. The ultrasonic approach, though indirect, is especially attractive because of the possibility of accomplishing near total inspection (rather than sampling) of the fungicide-treated textile in a production environment. This approach has been experimentally verified and is discussed in Section 8.

3.6 Conclusions of the theoretical investigations

The results of these initial studies indicate that both x-ray and infrared approaches should be investigated experimentally. Time-scales for measurements could be as short as milliseconds, and fine spatial resolutions are possible. It is quite clear that the x-ray technique should work, but that the implementation would not be easy. The IR alternative is too attractive to ignore. The experiments are discussed in sections 4 and 5 for x-ray and IR techniques, respectively.

The ultrasonic approach, though indirect, also bears investigation because the technique is easy to implement and because the technique can handle large volumes of inspection. Section 8 discusses the ultrasonic approach in detail.

4.0 EXPERIMENTAL VERIFICATION (X-RAYS)

The results of the calculations shown in section 8 indicated that experimental verifications were necessary. Since both fluorescent and dual-energy techniques both appeared to be viable contenders for incorporation into a machine, we decided to maintain all x-ray approaches as long as possible into the program. X-ray tests of treated and untreated

cotton duck samples were run in three separate series of tests.

Summary of x-ray tests. The first set of tests were conducted for feasibility purposes, to see if there was indeed any differential absorption between treated and untreated samples. These tests (for dual energy investigations) were conducted at Arnold Greene Testing Laboratories (AGTL) in Natick, MA. The AGTL tests were relatively trivial to conduct. These tests provided cause for optimism, but were not conclusive.

The second set of tests were performed at Hologic, Inc., Waltham, MA, a manufacturer of dual-energy equipment for medical diagnostic purposes. The results of these tests were extremely encouraging, and a final experiment was designed and conducted in a customized configuration that was constructed by Skiametrics at MIT. These results yield quantitative measures of performance for both fluorescent x-ray and dual-energy x-ray-based inspection systems.

4.1 Initial feasibility experiments

Arnold Greene Testing Laboratories provides x-ray imaging (on film) of various classes of test specimens. AGTL x-ray generators will operate at voltages as low as 40 kV. While this was clearly much higher an x-ray generator voltage than was desirable, these were the only facilities available for a quick, preliminary test. Moreover, the film-based tests were not expected to yield enough signal-to-noise in the image to actually measure the amount of copper present based on dual energy techniques. This test was undertaken, primarily to see if the gross image of the cloth could be seen.

A test specimen, composed of pieces of fungicide-treated cotton duck and untreated duck, was prepared and a number of contact x-ray film images were made of the test specimen at 40 kV and 80 kV. Under good radiographic

film-reading conditions the individual threads could be seen in both 40 and 80 KV films, the contrast being slightly better in the 40 KV films, exactly as expected. The data were then digitized on a standard real-time closed circuit TV CCD-based film digitization system, and the data plotted on a pixel-by-pixel basis. A sample of a profile from a single line of pixels is shown in Figure 11. The left half of the profile shows the intensity across the untreated sample, the right half of the profile shows the intensity across the treated sample.

Superposed on the profile is an average of the slope in the region immediately to the left and right of the boundary. This change over the boundary showed that a certain degree of gross differentiation between treated and untreated samples could be seen, even with film. The high spatial frequency peaks and valleys are consistent with the thread spacings on the sample (21/cm); on this scale, the profile covers approximately 2.5 centimeters (1 inch) in 500 pixels.

Thus while differential absorption could be observed, there was not enough data to yield either good predictions of how much flux would be required nor the sensitivity of the technique.

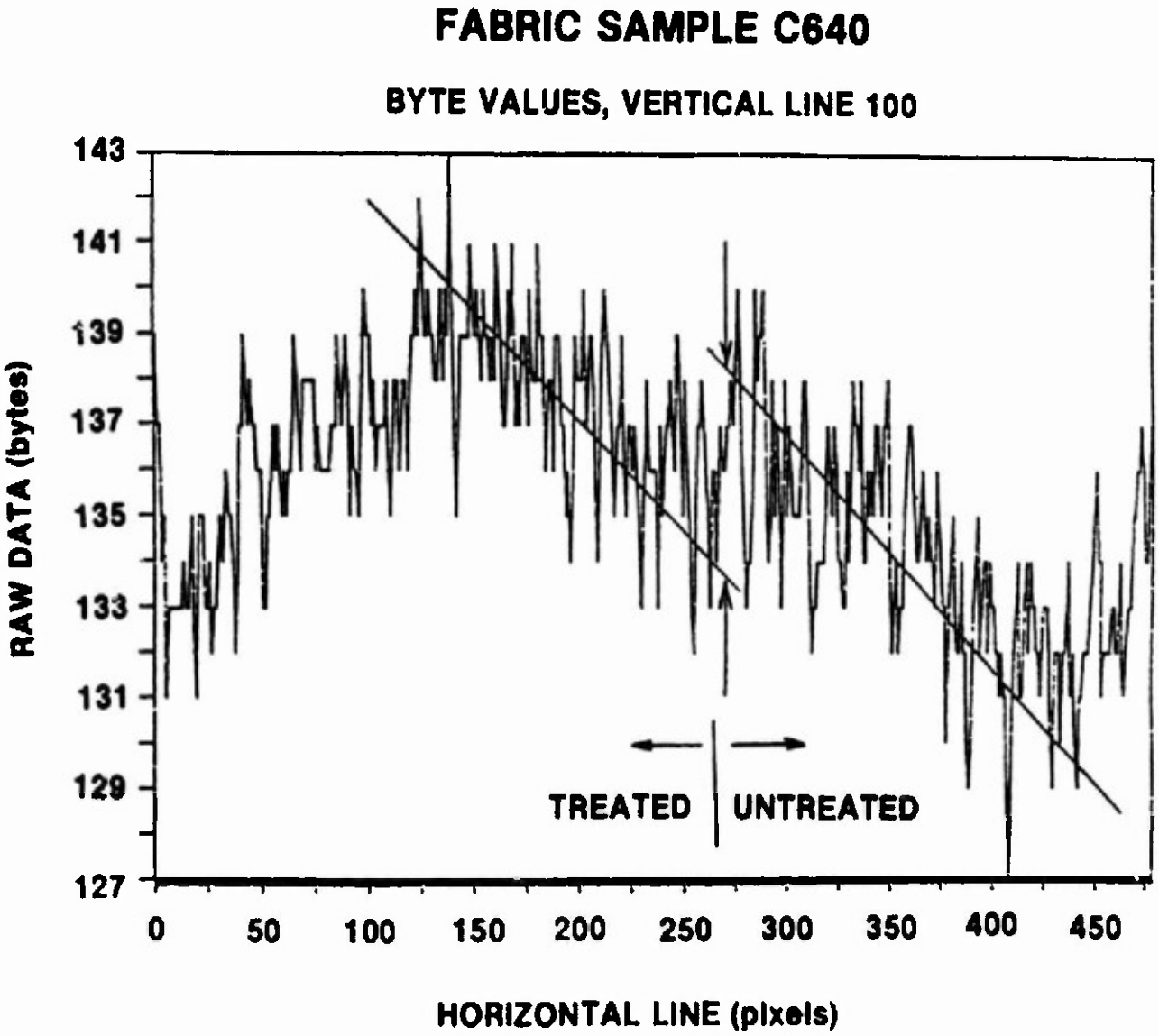

Figure 11. Single line profile of digitized film of x-ray (40 kV) image of cotton duck fabric sample. The region to the left is treated with the fungicide, the region to the right of the center is untreated. The spikes are consistent with the warp. Large scale structure is due to unevenness of the beam. Transition between treated and untreated region is comparable to the magnitude of the differences due to warp spikes.

4.2 Dual x-ray energy imaging test

Based on the results of the initial test, we decided that a dual energy imaging test was appropriate. An imaging test at a spatial resolution consistent with a thread dimension would truly prove the technique. Unfortunately, dual energy imaging equipment is usually not readily available. Such a system must be designed and constructed for specific purposes, and the application for that system is usually narrow. We were, however, aware of a system that has good spatial resolution and is currently being used in a medical context: an imaging bone densitometer.

Hologic, Inc., of Waltham, MA, is a manufacturer of medical instrumentation for measurement of bone density. This instrumentation is based on dual-energy x-ray techniques. The Hologic system operates at 70 and 140 kV, and is excellent for finding the areal density of calcium to a precision of 0.5% or better with spatial resolution of approximately 0.7 pixel/mm.

We elected to try using the Hologic bone scanner on the treated and untreated fabric samples. A single layer of the cloth produced no significant differences in results between the two. This is not surprising in view of the fact that the x-ray generator voltages of 70/140 are far too high to detect, let alone measure, the amount of copper present at an expected level of 0.000068 grams/cm^2.

However, when the fabric was folded 8 times, and the test repeated, there was a significant difference. Treated and untreated samples were clearly distinguishable. This image is shown in Figure 12. This was the first time that the dual energy technique had been used to make an image in high-Z in this fabric. Moreover, the energy was absolutely inappropriate

for making this kind of measurement. Nonetheless, we had an image where the copper-8-quinolinolate treated duck was clearly seen, and that image was different from the untreated section. This was most encouraging, and paved the way for the next set of experiments.

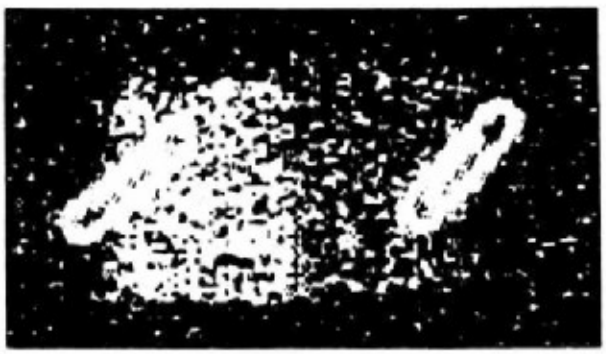

Figure 12. The first dual energy image taken of the two duck samples, one copper-8-quinolinolate impregnated, the other untreated. In this first test, even though the energies were inappropriate (70 and 140 kV), the samples, folded 8 times to enhance the effect, were decidedly different. A paper clip is seen in each image. The image to the left is sensitive to the high-Z components.

4.3 Customized dual-energy x-ray experiments

Now that the technique was shown to produce (admittedly coarse, at this point) Z-maps from the x-ray attenuation measurements, a set of experiments at appropriate energies was necessary. These experiments must examine the test specimen with a more realistic energy probe and at a finer spatial resolution. The results of these experiments should imply a set of operating conditions, a measure of sensitivity of the technique to the amount of copper present, and eventually a system design and performance expectation.

4.3.1 Components and configuration

The experiment required an x-ray source, a detector, a specimen holder and a means for repeating positions on the test specimen to a precision of 10-20% of the effective spatial resolution of the system. An acceptable configuration was also necessary.

X-ray source. To this end a number of adjustable voltage, high current x-ray sources were investigated. The best x-ray generators in the energy range of interest (below 40 kV, as discussed in section 3) are those used for x-ray diffraction and fluorescence studies. A source of this type was located in MIT's Center for Materials Science and Engineering. The source utilized for these experiments is a conventional sealed-tube GE/Diano(R) diffractometer source. The source can be operated at continuously adjustable voltages ranging from 8 kV to 60 kV and at currents of 1 and 10 milliamps. (Higher currents are possible, but swamping effects in the counter ruled them out for these experiments.) This source was operated with a molybdenum anode (Z-42) with a beryllium window. The molybdenum anode was chosen over the conventional (and more efficient tungsten

standard) because of the complication of the tungsten L lines whose energies are quite close to the copper K edge. The tungsten L-lines actually straddle the copper K edge at 9.0 keV, the L-alpha and L-beta being at 8.4 and 9.7 KV, respectively.

Detector. Ideally, these are counting experiments, where the statistical precision of the measurement can be sharpened as long as the requisite amount of time is devoted to data acquisition. (In principle, current [i.e., integrated flux] measurements can be repeated a number of times to arrive at the same precision, but the experiment is easier to do in a counting mode. The weighting for attenuation purposes is slightly different for the two approaches.)

The two detectors that are appropriate are either proportional counters or scintillation counters. Either of these types of detectors provided single photon counting capability. The xenon-carbon dioxide proportional counter with beryllium window was the best detector for these low energy measurements because the effective cut-off of the detector was at such a low energy — approximately 2-3 keV. A 2-inch (51 mm) diameter side-window sealed proportional counter (LND Model 4546) was used for these purposes.

The alternative of the beryllium-windowed scintillation counter employing a sodium iodide crystal and photomultiplier tube (PMT) does not extend to quite as low an x-ray energy as does the proportional counter, because of the intrinsic low-level noise of the PMT. Even though the scintillation counter can handle a much higher counting rate than the proportional counter, and can be used in the current mode, for these initial studies, the proportional counter was a better choice.

Test specimen and manipulating fixture. The test specimen was constructed of two strips of copper duck, one treated with copper-8-quinolinolate, the other untreated. These strips were mounted on an optical translation stage so that various points on the cloths could be placed in the path of the x-ray needle beam and reexamined to a spatial precision of 0.001 inch (0.03 mm).

Configuration. The configuration employed is shown in Figure 13. The beam was collimated to a pinhole of approximately 0.008 inch (0.020 cm), the x-ray illumination spot being confined to a similar dimension by proximity focussing.

The distance from source spot to pinhole was 5 inches (125 mm), and from pinhole to sample 0.1 inch (3 mm), making for a source unsharpness of 0.001 inch (0.03 mm) on the test specimen.

The detector was mounted 2.4 inches (62 mm) behind the sample. For various energies, an aluminum filter was sometimes used to harden the beam or cut the rate to acceptable limits for the proportional counter.

4.3.2 Measurements

The copper-8-quinolinolate treated cotton duck samples were measured in transmissions at the energies shown in Table 1. A number of control points were also obtained on untreated cotton duck and on a copper foil.

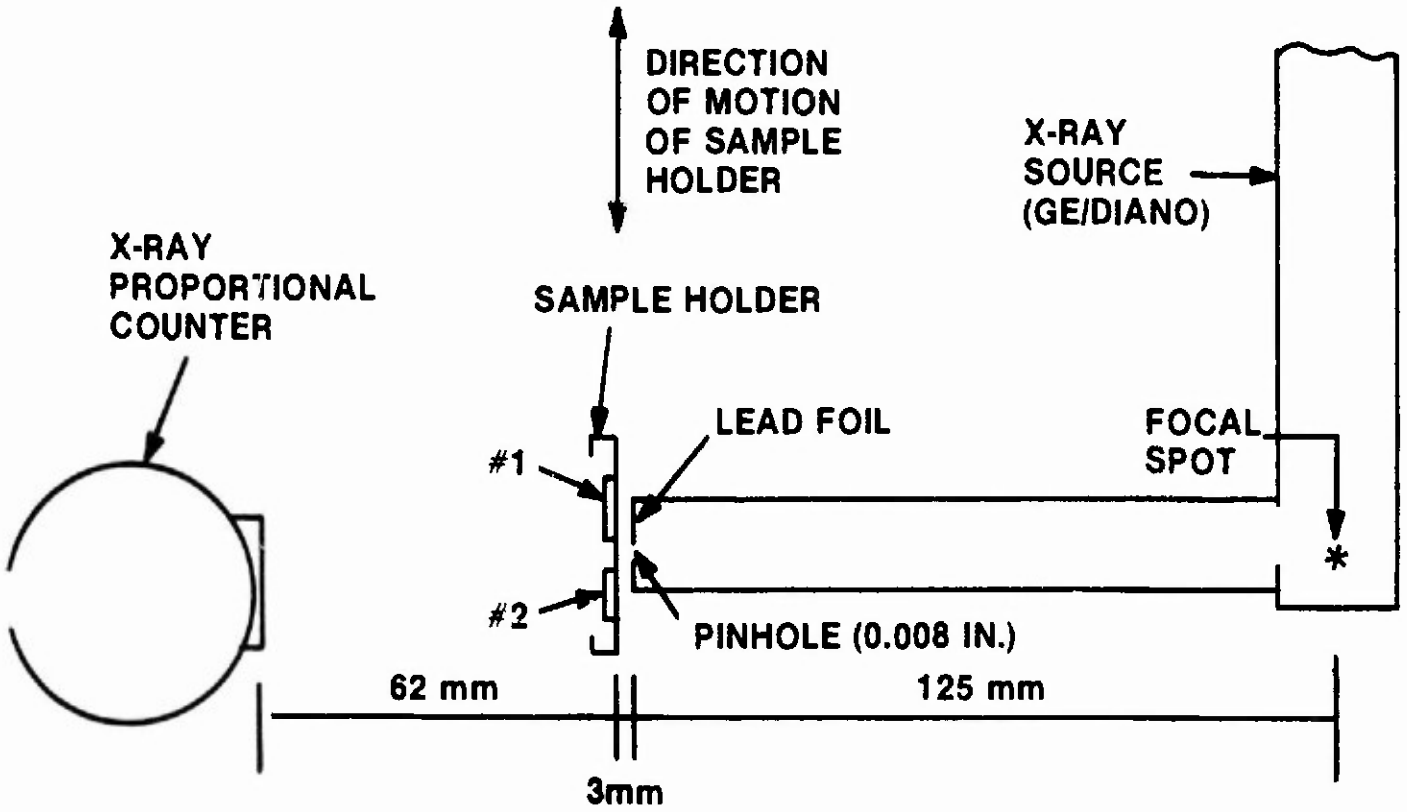

Figure 13. Test configuration for dual energy experimental investigations. The output of the x-ray proportional counter was fed to a conventional preamp/amplifer and then to a pulse height analyzer for integration and analysis.

TABLE 1a. Measured Transmission of Copper-8-Quinolinolate Treated Cotton Duck Samples.

POSITION	8 kV	10 kV	20 kV	30 kV
1-control	0.7071	0.7766	0.9732	0.987
(uncoated duck)	0.0014	0.0014	0.0028	0.003
2-control	0.5764	0.7319	0.9549	0.975
(uncoated duck)	0.0012	0.0011	0.0027	0.003
3-control	0.5781	0.6385	0.9510	0.9805
(uncoated duck)	0.0012	0.0017	0.0027	0.003
4-Cu-8	0.6549	0.6972	0.9647	0.982
	0.0013	0.0019	0.0027	0.0028
5-Cu-8	0.6947	0.7367	0.9610	0.9848
	0.0013	0.0019	0.0020	0.0028
6-Cu-8	0.6421	0.7426	0.9558	0.9829
	0.0020	0.0019	0.0020	0.0028
7-control	0.1577	0.1788	0.2372	0.5100
(0.001 in Cu-foil)	0.0005	0.0008	0.0022	0.0018

NOTES:

1. First three samples are controls of 10 oz (283g) cotton duck. Samples 4, 5, and 6 are copper-8-quinolinolate treated pieces. Sample 7 is a piece of 0.001 inch thick copper foil (0.0228 grams/cm^2 areal density).

2. Top number of each pair is the transmission. Lower number is statistical precision of that number.

3. These measurements were made with a pinhole of diameter 0.008 inches (0.20 mm). For measurements in Table 1b, pinhole size = 0.05 inch (1.3 mm).

TABLE 1b. Measured Transmissions of Copper-8-Quinolinolate Treated Cotton Duck Samples. (Large Pinhole).

POSITION	9 kV	18 kV
8-control	0.782	0.971
	0.006	0.006
9-Cu-8	0.761	0.965
	0.006	0.006

4.3.3 Results and discussion

The results and sensitivities are shown in Table 2. The main conclusion is that very thin coatings of the high-Z component can be measured to a precision of a 10-20% over small regions, given enough time to make the measurement. We were limited in these measurements to count rates of approximately 5000 per second, but that was only so that we could actually observe the spectra as they arrived, consistent with the intent of using the proportional counter.

The most irksome problem is the tremendous amount of precision required in obtaining this result. These dual-energy techniques require a precision of approximately 1-3 parts in 1000 or better to yield good sensitivity and reasonable errors for measuring the high-Z component. The problem arises because of the inconstancy of x-ray sources. Detectors are certainly up to the task of providing all the precision that is required, and the outputs can be routinely digitized and added according to standard statistical rules.

This precision can be accomplished in one of two ways: The first is in using an x-ray source monitor. This is simply a second detector that monitors the unattenuated beam at a position just off-center from the needle-beam that is used to examine the test specimen. The output of this monitor detector is used as a divisor of the output of the specimen detector (skiametric) so that the net signal is compensated for source variations. The second is in using a reference standard that is included in the machine and which is used as internal calibration on a time scale that is short compared to the intrinsic source drift time. (This second scheme is employed by the Hologic osteoporosis system.)

TABLE 2. Copper Fractions

POSITION/ SAMPLE	VOLTAGE PAIR-kV	FRACTION COPPER	SENSITIVITY*
4-Cu-8	10/20	0.002 0.001	0.0004/0.001
	8/20	0.002 0.001	0.0004/0.001
5-Cu-8	10/20	0.0035 0.0005	0.0004/0.001
	8/20	0.0040 0.0005	0.0004/0.001
6-Cu-8	10/20	0.0041 0.0005	0.0004/0.001
	8/20	0.0030 0.0005	0.0004/0.001
9-Cu-8	9/18	0.002 0.001	0.0004/0.001

*Sensitivity is defined as the change in the fraction of copper measured as a function of change in measured transmission. To the degree that this is measurable, the sensitivities are identical for all measurements at these energies. Were higher voltages used, the sensitivities would decrease.

NOTES:

1. Any calculations that used 30 kV as one of the pairs exhibited very little sensitivity to the amounts of copper present.

2. The presence of other high-Z elements, detected during the x-ray fluorescence tests, may have skewed these results significantly.

In any case, measurements whose precision is commensurate with accuracy requirements for high-Z determination can be acquired in a data acquisition time of about a second per sample. This should translate directly to a production or research machine.

4.3.4 Complications

In the course of the fluorescence measurements described below, it became clear almost immediately that copper was not the only high-Z component present. Also present were manganese and nickel, the latter in an abundance comparable to the copper. The nickel component is particularly distressing because it is so close to the copper on the periodic table, and the absorption edges lie practically next to one another, at least insofar as the dual energy technique is concerned and bremsstrahlung is the dominant form of x-ray energy. The problem is that the technique cannot distinguish the copper from the nickel; they are both detected as "high-Z". Further discrimination of these two in a dual energy mode needs a combination of special filters and the use of an x-ray line that falls between the two K-edges.

This problem falls outside the original system requirements. If the nickel (or other high-Z component) can be isolated, accounted for independently, or (best of all) be eliminated from the sample, then the dual energy technique appears to have great promise. If the amount and distribution of contaminants are high, then dual energy techniques are not, by themselves, appropriate.

4.4 Fluorescent investigations

One final x-ray test on the test specimen was run. This was a fluorescent x-ray examination, and employed the configuration shown in Fig. 14. The same GE/Diano x-ray source which was used for the dual-energy experiments was used for these fluorescent tests. The pinhole was removed and a much larger area -- approximately 0.1 inch (3 mm) square of the test specimen — illuminated. The detector used for this experiment was an Ortec SiLi detector operating at liquid nitrogen temperature. SiLi detectors have far better energy resolution than do proportional counters, although they cannot be used at the same x-ray count rates as can other detectors. For fluorescence feasibility studies, however, solid-state detectors are excellent, because they have such good energy resolution.

The samples which were examined were the untreated copper duck and the copper-8-quinolinolate treated sample. The untreated duck showed no evidence of any high-Z fluorescence peaks, except for a minuscule arsenic peak, apparently a constituent of the underlying glass slide, at 10.5 kV. The treated sample showed a large copper component, exactly as expected. However, also present in sample were a nickel peak, which was present at virtually the same intensity as copper, and manganese, which presented one-third to one-half the copper intensity.

Cross-sections for fluorescent interactions are sufficiently similar for the copper and nickel so that the relative numbers of counts in each peak translate almost identically into relative elemental abundances. The implication is that there is about as much nickel present as there is copper in the samples examined.

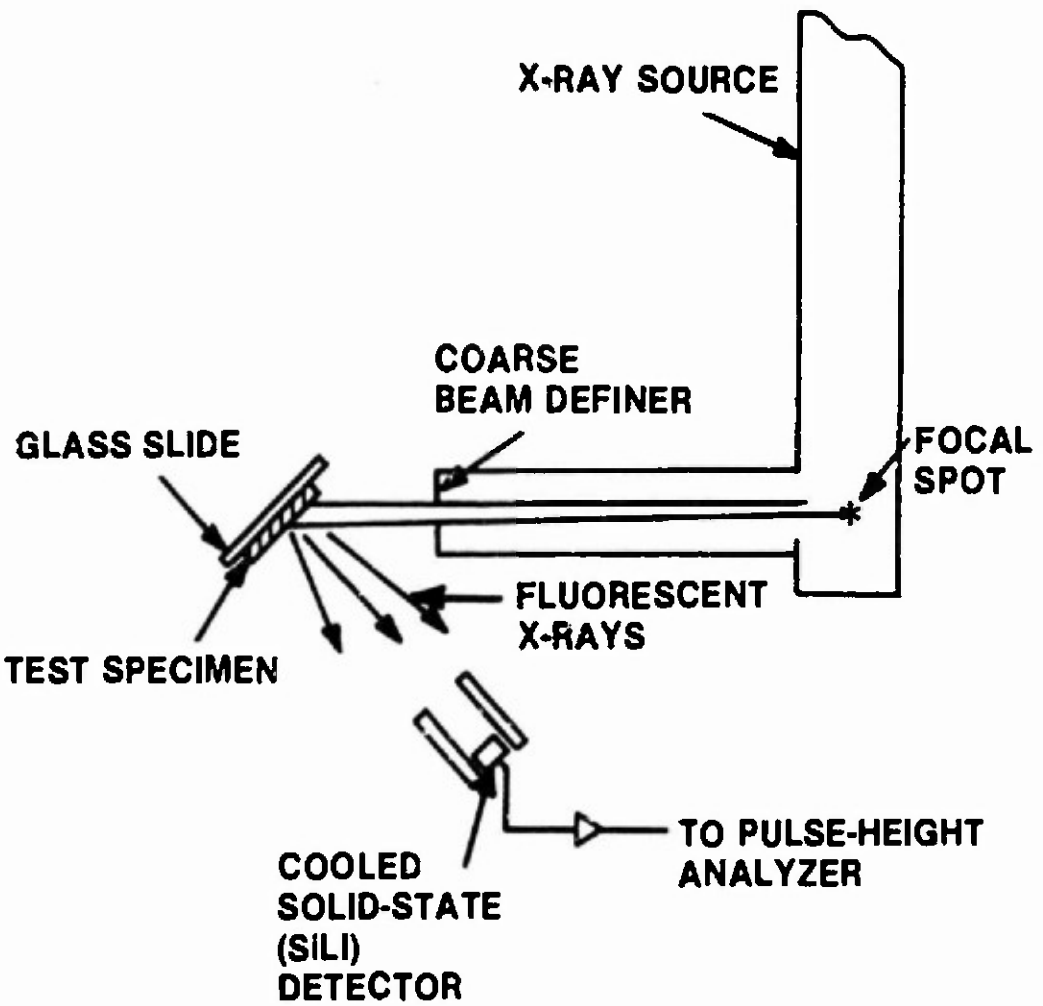

Figure 14. Configuration for x-ray fluorescence measurements. The solid-state x-ray detector was cooled to liquid nitrogen (77 K) for these measurements.

Subsequent discussions with the Army revealed that the copper-8-quinolinolate is frequently dissolved in a nickel-salt bath, and that is probably the origin of the nickel seen in the fluorescent experiment.

The count rates for these peaks fell in the 200-300/second vicinity, indicating that a measure of the total amount of copper in the sample could be gotten to a precision of better than 10% in a second or less, even with this experimental set-up which was not optimized for recovery of the fluorescent flux. By making an effort to maximize the solid angle of the detector, as seen from the illuminated area, the time per measurement could be decreased by a factor of 10 to 100. Thus, a reasonable sample rate is something on the order of 10-100 samples per second over regions 10-100 mm^2.

4.5 Applicability of the x-ray techniques; performance predictions

The dual-energy techniques will perform over a greater variety of thicknesses of materials than will the fluorescent technique, and will be able to yield precisions of 10% per measurement or better in a time scale of approximately a second. This will cover a region of 0.010 inches (0.25 mm) square. If the region of coverage is a larger area, then the inspection time will decrease in inverse proportion to the area. Thus, an area of 0.040 inches square (1 square millimeter) could be sampled in approximately 60 milliseconds. With nominally available hardware (section 6), the practical limit of the dual energy technique is probably about 16 milliseconds per measurement of copper fractional content. For monitoring purposes, this is an ideal speed, because continuous measurements can be made on-line over a region 0.2-0.4 inches (5-10 mm) in linear extent (along the direction of motion of cloth), assuming a standard 18 inches/second

(46 cm/second) travel rate. The dual-energy technique depends on Z-separation of a higher Z-component from a lower Z-component. If there is substantial contamination by unwanted high-Z elements, then the technique will measure the sum of the amounts of high-Z materials.

The dual energy technique will measure the relative presence of elements with Z's as low as 11 or 12. This measurement of relative presence (rather than absolute presence only) is important because of the spatial inhomogeneity of any fabric sample. Thus, a measure of 0.00070 grams/cm^2 of copper over an average of many threads is exactly what is expected. But the local variation on a spatial scale comparable to or finer than the spatial period of the thread would yield quite a range of values around that mean, values consistent with total penetration of the copper-8-quinolinolate fungicide of the fabric. It is a function of how much material is present in the sampled region. A relative measure yields the appropriate 0.2% (or whatever it turns out to be) independent of how much of the material happens to be in the beam. This is a much more meaningful measure of how well the application process is working.

The fluorescent energy approach requires a much higher energy source than does the dual energy technique, but this is not a significant item except for greater radiological safety considerations in the vicinity of the machine. Fluorescence measurements can be obtained at a rate of 10-100 samples per second over regions of size 10-100 mm^2. Fluorescence measurements can be used for finding the absolute amount of copper, and the amount of copper relative to other high-Z elements. Fluorescence measurements can be used at the same standard rate of 18 inches/second (46 cm/second) of textile travel in a monitoring mode.

The fluorescent energy approach will yield only an absolute measurement and is subject to the inhomogeneity factor described above. Fluorescence techniques are much more likely to succeed only where the measurement is obtained over an area containing many threads.

Fluorescence approaches work only where the x-ray fluorescence energy of the elemental trace material (e.g., copper) in question is calcium (Z=20) or higher.

The combination of fluorescence and dual-energy measurements yields unambiguous fractional amounts of copper present.

5.0 EXPERIMENTAL VERIFICATION (IR)

In this section, we discuss the detection of the copper-8-quinolinolate (1.0% by weight) on cotton duck 339g/m^2 (10 oz/yd^2) by Fourier transform infrared (FTIR) spectroscopy. In these preliminary studies, a sample of the treated and untreated fabric (supplied by technical monitor) have been examined in the mid-infrared (5000-500 cm^{-1}) by transmission, attenuated total reflectance (ATR), reflectance-absorbance (R-A), and diffuse reflectance (D-R). A spectrum of a neat sample of the fungicide was also produced and is presented here. Detection of the copper compound in the far infrared region (400-50 cm^{-1}) was also studied by transmission and D-R.

5.1 Experimental apparatus

All mid-IR spectra were recorded at a resolution of 8 cm^{-1} with a Digilab (Digilab Division of Bio-Rad, Cambridge, MA) Model FTS-15/90 FTIR equipped with a wide band mercury-cadmium-telluride (MCT) detector and operated at a moving mirror scan speed of 1.2 cm/second. The source aperture was set to 18 mm and unattenuated for analysis of the fabric. In the case of transmission, R-A and D-R, the incident beam was highly

attenuated by the sample, but increased amplifier gain allowed observation of the interferogram. Single beam energy spectra for the various sampling modes have been included below and may be used to estimate the relative throughput. The spectra are plotted from 5500-400 cm^{-1} transmission bandwidth of the optical system without sample (empty beam) and are given in Figure 15.

Studies in the far IR were conducted with a Digilab Model FTS-40V FTIR spectrometer with an evacuated optical bench, 6 micrometer mylar beam splitter, mercury arc source and triglycerine sulfate (TGS) detector. The bandwidth of this spectrometer is 500-50 cm^{-1}.

5.2 Transmission

We expected that the mid-IR spectrum of the cotton duck would be dominated by absorbances due to the cellulose. The structure of cellulose and inspection of standard spectra indicated, however, that transmission windows might exist below 900 cm^{-1} through which the out-of-plane bending modes of quinoline might be observed.

The experiments were carried out by placing a piece of the fabric sample at the focus of a 3X beam-condensing transmission optic. A circular spot (about 6 mm in diameter) on the fabric was interrogated.

In Figure 15, a transmission spectrum obtained by ratio of two untreated duck single-beam spectra (top, 16 scans co-added) is compared to a transmission spectrum produced by ratio of treated to untreated single beams (bottom, 256 scans co-added). The untreated/treated spectrum shows transmission windows only in the regions where organic molecules typically do not absorb (i.e., around 4400 cm^{-1} and 2000-1800 cm^{-1}). Even the low frequency region, where the quinoline out-of-plane bending modes would

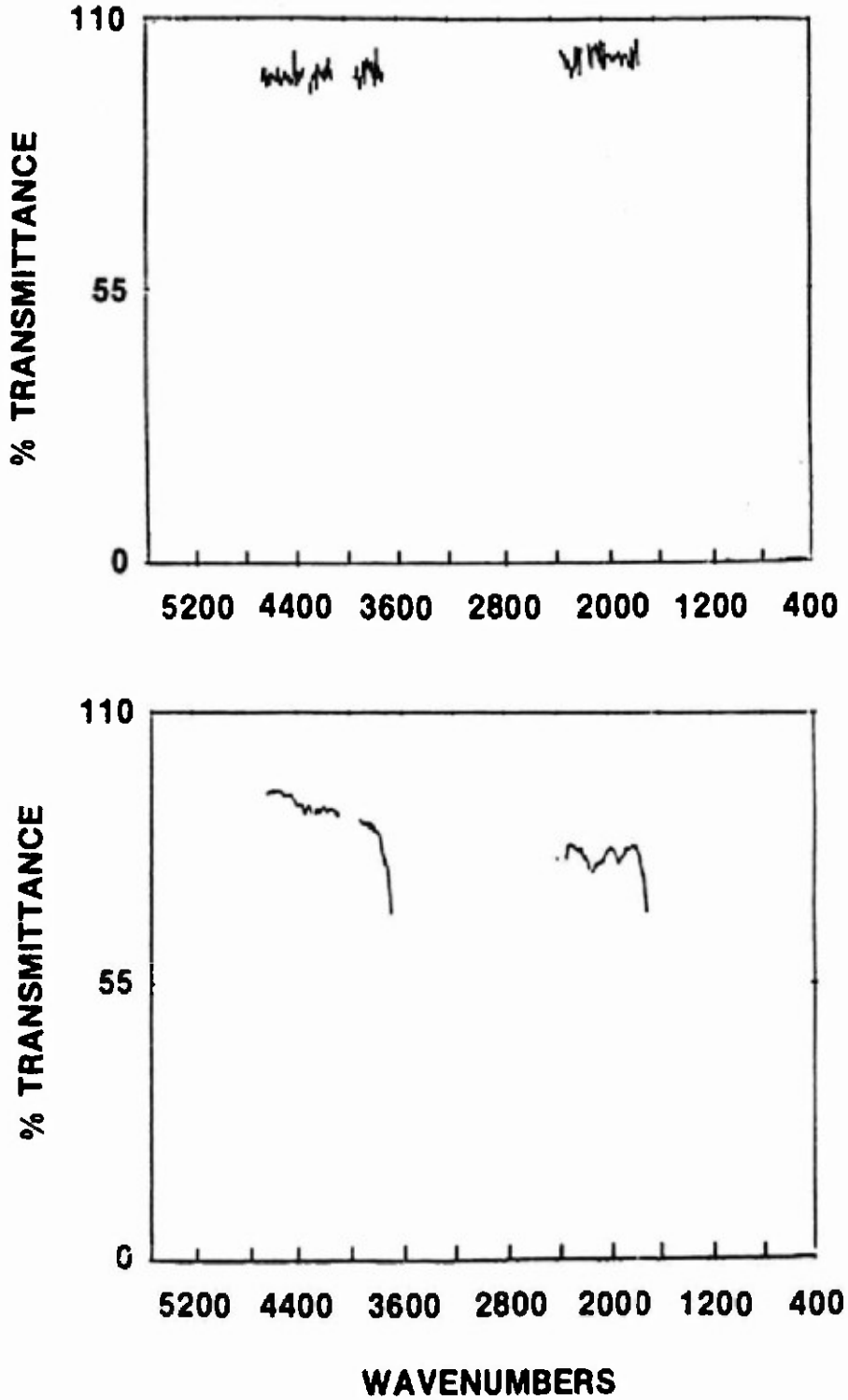

Figure 15. Transmission spectrum (top trace) obtained by ratio of two untreated duck, single-beam spectra. This ratio establishes region where sufficient transmission exists. Bottom trace shows ratio of treated to untreated single beams.

be found, is opaque. The treated/untreated spectrum indicates new absorbances in what appears to be the high-frequency edge of a peak around 3600 cm^{-1}, and again, around 1600 cm^{-1}. The peak maxima, however, are not observed since they occur in the opaque region of cellulose absorbance. The purpose of displaying spectra resulting from different amounts of a signal averaging is to provide an estimate of the noise level at different sampling times. The top spectrum, with 16 scans co-added can be collected in about 3 seconds, while the bottom spectrum, which resulted from 256 scans, required about 55 seconds (this includes data reduction and processing time, which may account for as much as half of the total time). In Figure 16, the single beam spectra obtained from an empty sample beam (top), the treated duck (middle), and the untreated duck (bottom) are shown. The bandwidth for the optical system is approximately 5200-480 cm^{-1}.

5.3 ATR

Detection of the fungicide layer was also attempted by ATR. In this technique, the spectrum of surface films may be obtained by placing the sample in contact with an infrared crystal of relatively high refractive index. The IR beam is focussed on one end of the crystal at the proper angle for total internal reflectance. As the beam travels down the crystal, it reflects off the inner walls; at the point of reflection, an electric field is produced outside the crystal boundary. This field may then be absorbed by the contacting sample. Selection of the crystal material, its length-to-width ratio and the angle of incidence allows the penetration depth of the external field into the sample and the number of reflections to be varied. Both of these factors, as well as the wavelength

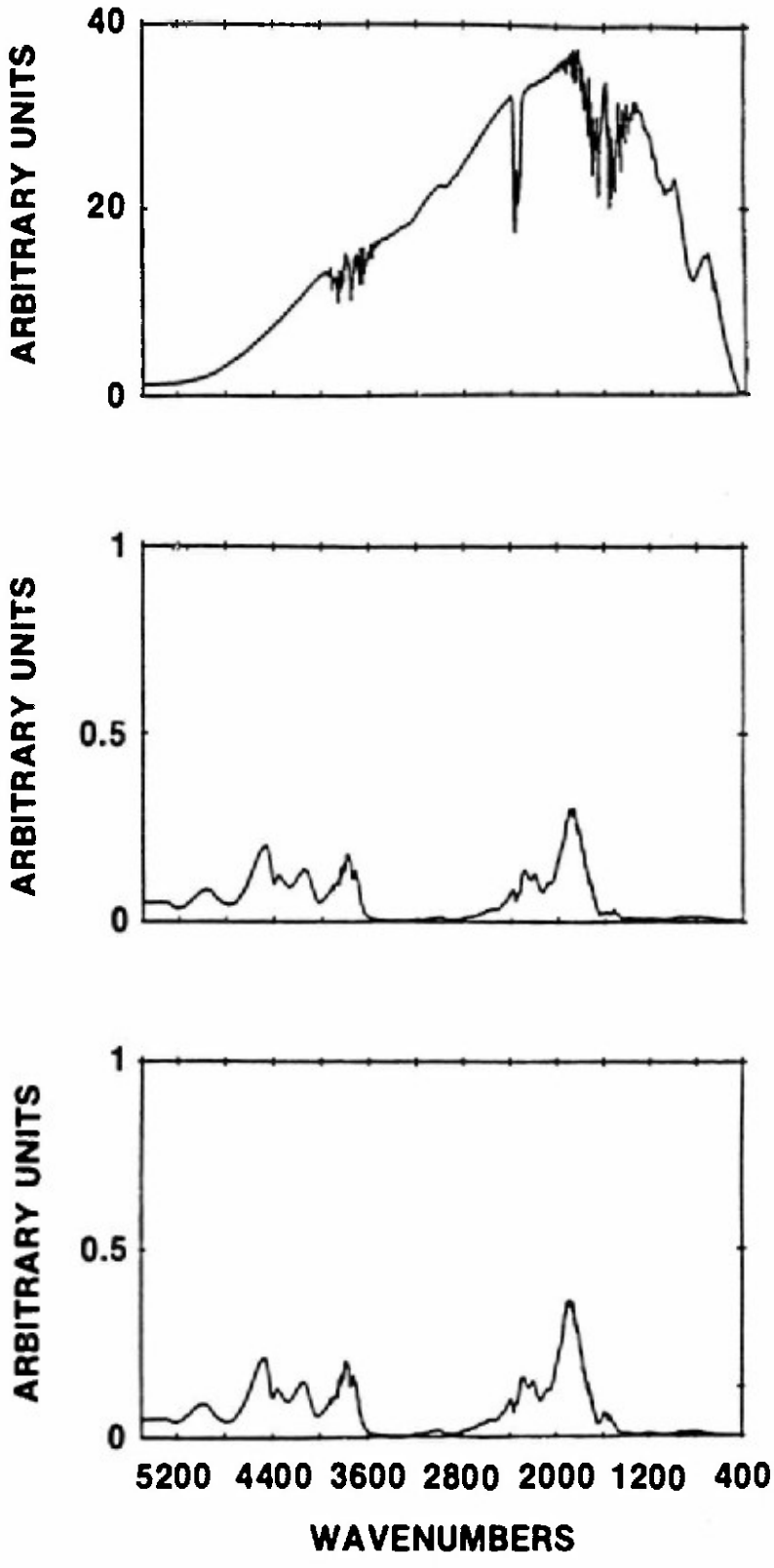

Figure 16. Single beam transmission spectra for empty sample beam (top), treated cotton duck (middle), and untreated duck (bottom). Spectral resolution was 8 cm^{-1}.

of the IR, affect the pathlength of the beam through the sample and, therefore, the observed absorbance intensity.

In the experiments presented here, a 6 cm long by 3 mm wide, parallelogram-shaped KRS-5 crystal was used at a 45 degree incident angle. The resulting penetration depth is 0.12 x (wavelength) and the number of reflections is 14. This yields a pathlength of about 16 micrometers at a wavelength of 5 micrometers (sample material was placed on both sides of the crystal). Two 1 cm x 6 cm strips of the fabric to be analyzed were placed in contact with the sides of the KRS-5 crystal. For each spectrum, 2048 scans were co-added.

In Figure 17 the ATR spectra of the treated (top) and untreated (bottom) fabric, ratioed to a blank crystal face are shown. Both spectra have the same band patterns with the most characteristic absorbance found between 1100-800 cm^{-1}. This region of the coated fabric spectrum is shown in more detail in Figure 18.

The position of these bands corresponds to a strong absorbance also found in the standard spectra of cellulose (see Aldrich Library of FTIR Spectra) and may be correlated with vibrational modes of the C-O-H functionality.

5.4 R-A and D-R

The last set of experiments conducted in the mid-IR region was detection of specular reflectance or R-A and D-R. For the R-A data, a 3X beam-condensing reflectance optic was used to focus the beam to a 6 mm diameter spot on the fabric. For D-R, a sampling optic which focussed the beam to about a 1 cm diameter spot was used. The standard spectrum of copper-8-quinolinolate was obtained by placing the neat powdered sample

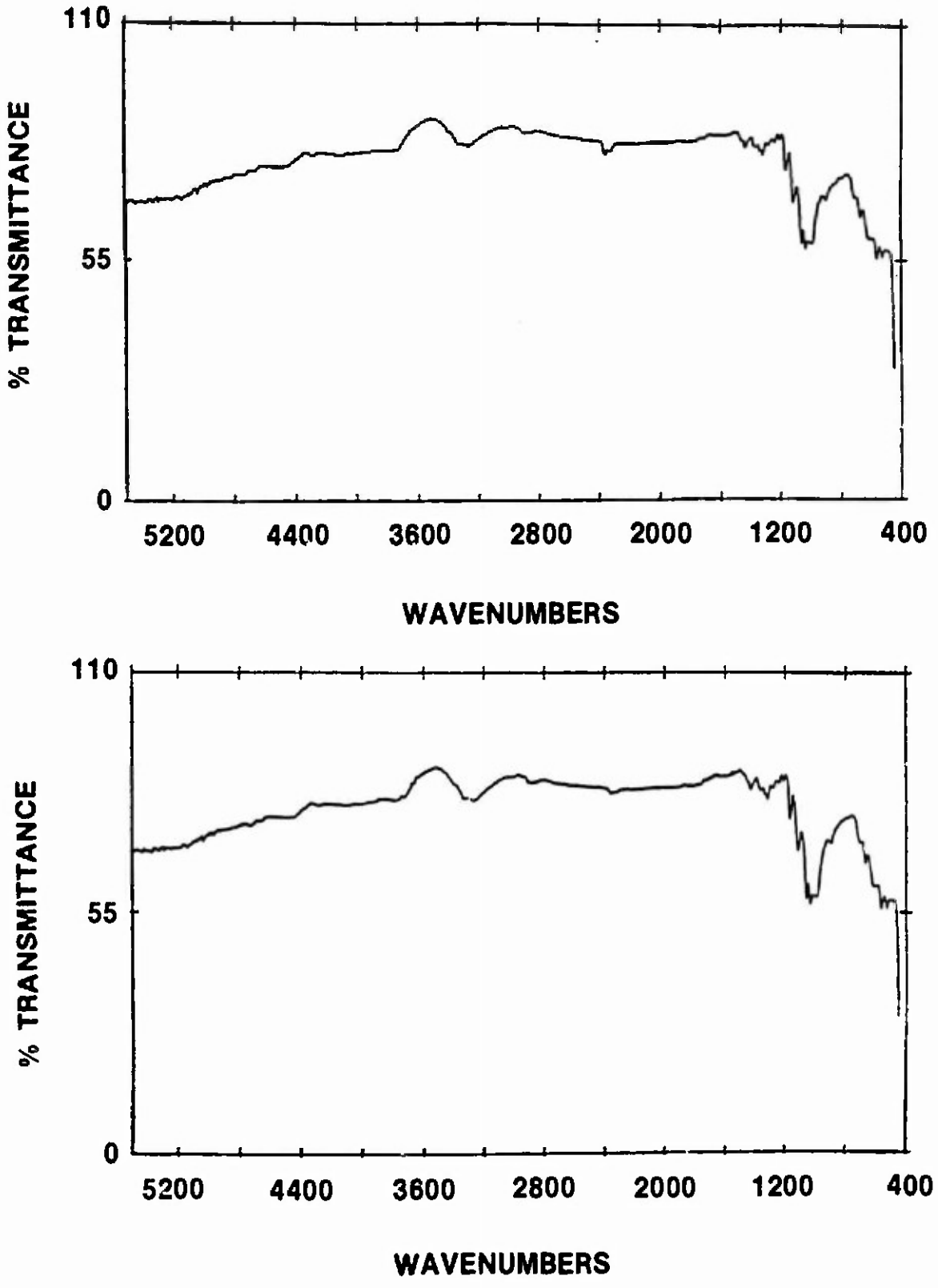

Figure 17. ATR spectra of the treated (top) and untreated (bottom) fabric, ratioed to blank crystal face.

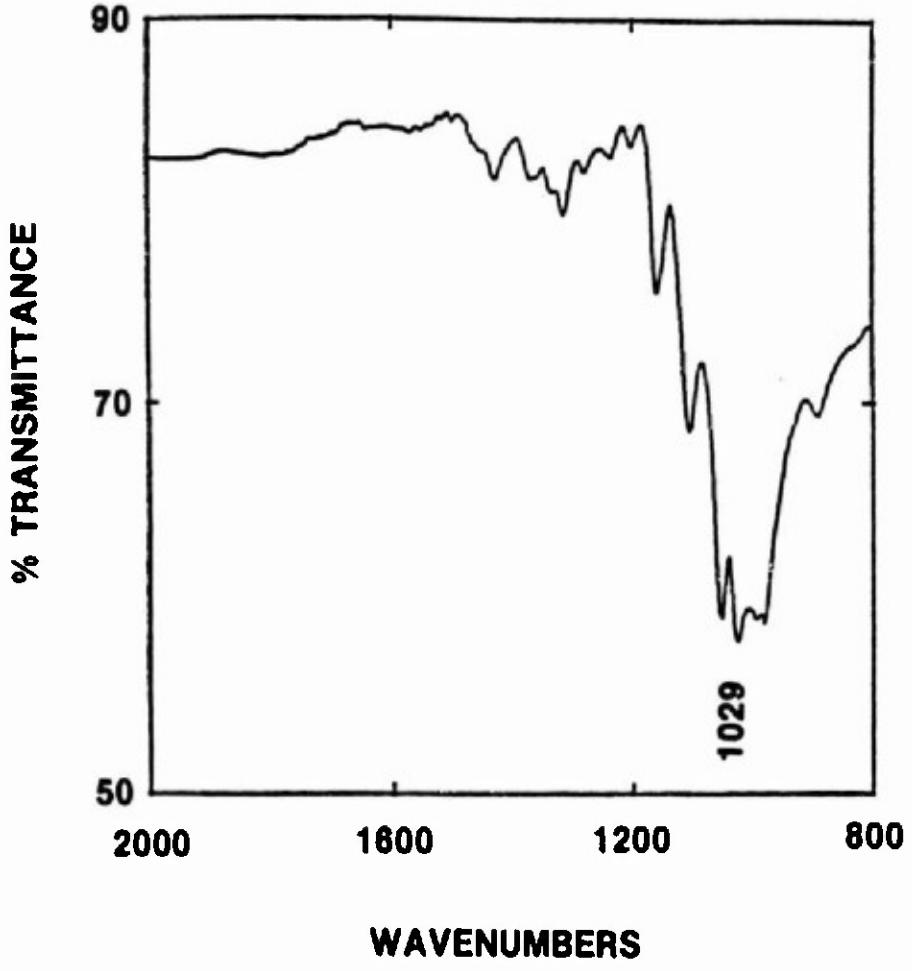

Figure 18. A more detailed look at the absorbance pattern in the 1100-800 cm^{-1} wavenumber region.

(used as received from our Army technical monitor, purified by recrystallization) on the germanium surface of an aluminum-coated germanium crystal. This optical configuration allows transmission-like spectra (free of absorbance bias) to be obtained in a R-A sampling mode (Gagel and Biemann[10]).

The R-A spectrum of untreated cotton duck ratioed to untreated cotton duck is shown in Figure 19 (top, 16 scans). The opaque regions occur in areas which are similar but not identical to those found in the transmission data. The most important difference is in the increased throughput in the reflectance mode observed in the region from 1600-1400 cm^{-1}. In the lower trace (256 scans) of Figure 19, the R-A spectrum obtained by ratio of the treated duck to the untreated duck is shown. A strong band of the treated duck to the untreated duck is shown. a strong band at 1573 cm^{-1} is observed in this spectrum, but is not present in the untreated/untreated data nor in any of the spectra obtained by the methods previously discussed.

In Figure 20, the spectrum of a neat sample of copper-8-quinolinolate is shown and in Figure 21, this standard spectrum (upper trace) and the treated/untreated R-A spectrum (lower trace) are compared in the region from 2000-1400 cm^{-1}. The absorbance band at exactly 1573 cm^{-1} is detected in both spectra. In Figure 22, the single beam spectra are shown for the untreated (top) and treated (bottom) duck.

The band at 1573 cm^{-1} is also observed when the sample is studied by D-R spectroscopy. Figure 23 shows the treated/untreated (top) and single beam (bottom) D-R spectra. Also observed in these spectra is a new peak at 1743 cm^{-1}. These spectra are the result of 256 co-added scans; clearly, good data could be obtained with far less signal averaging.

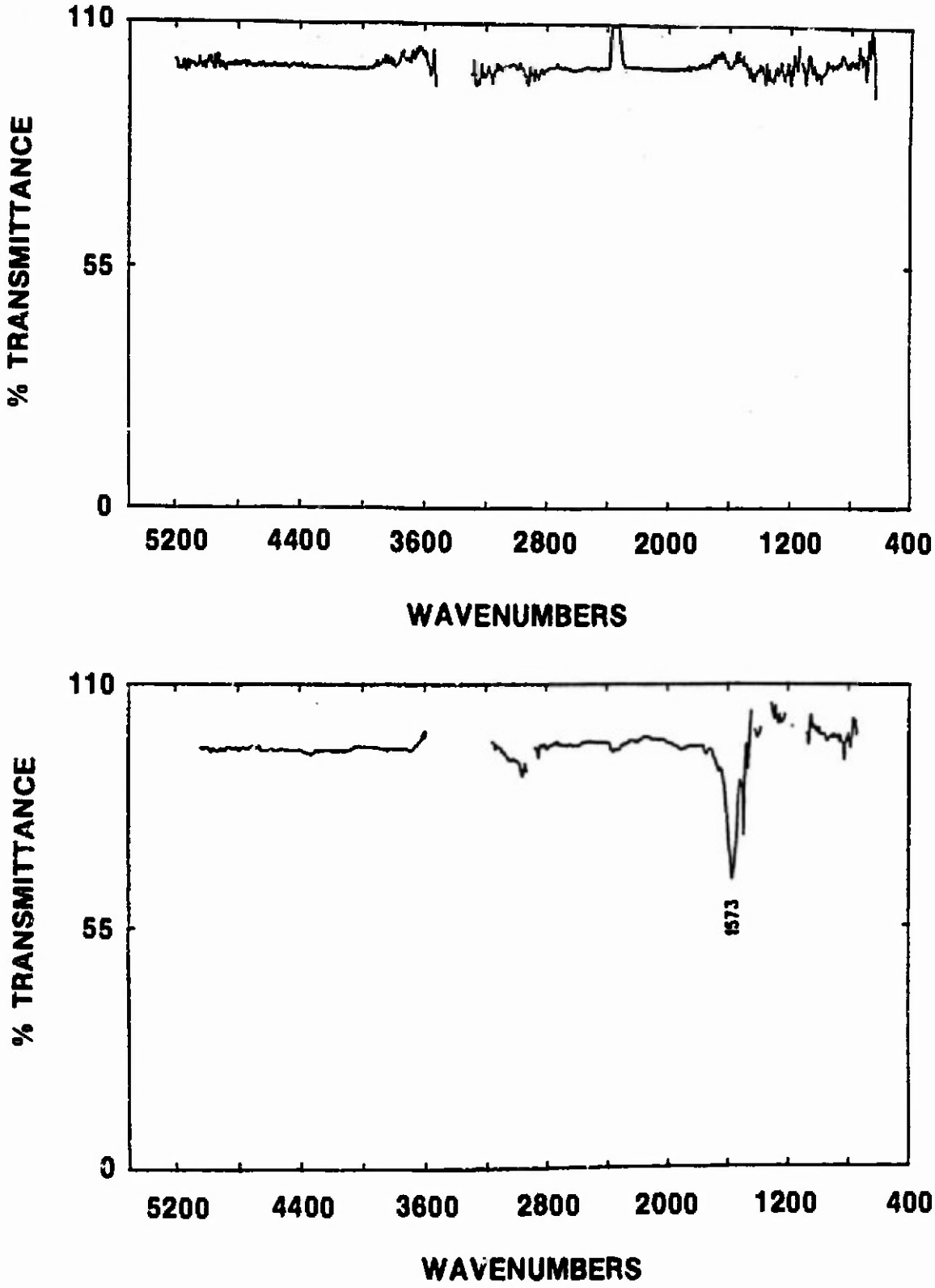

Figure 19. Reflectance-absorbance spectrum of untreated cotton duck ratioed to untreated cotton duck (top). R-A spectrum of ratio of treated duck to untreated duck is shown in bottom trace.

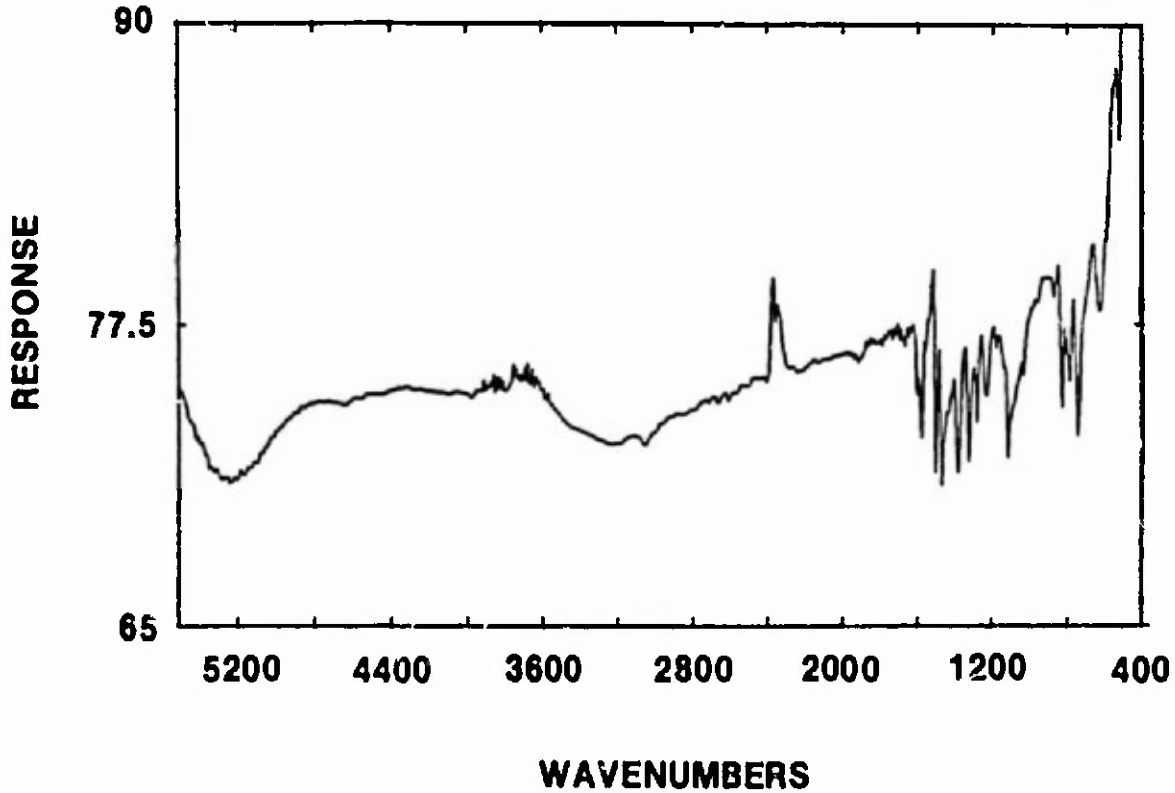

Figure 20. Spectrum of a neat sample of copper-8-quinolinolate.

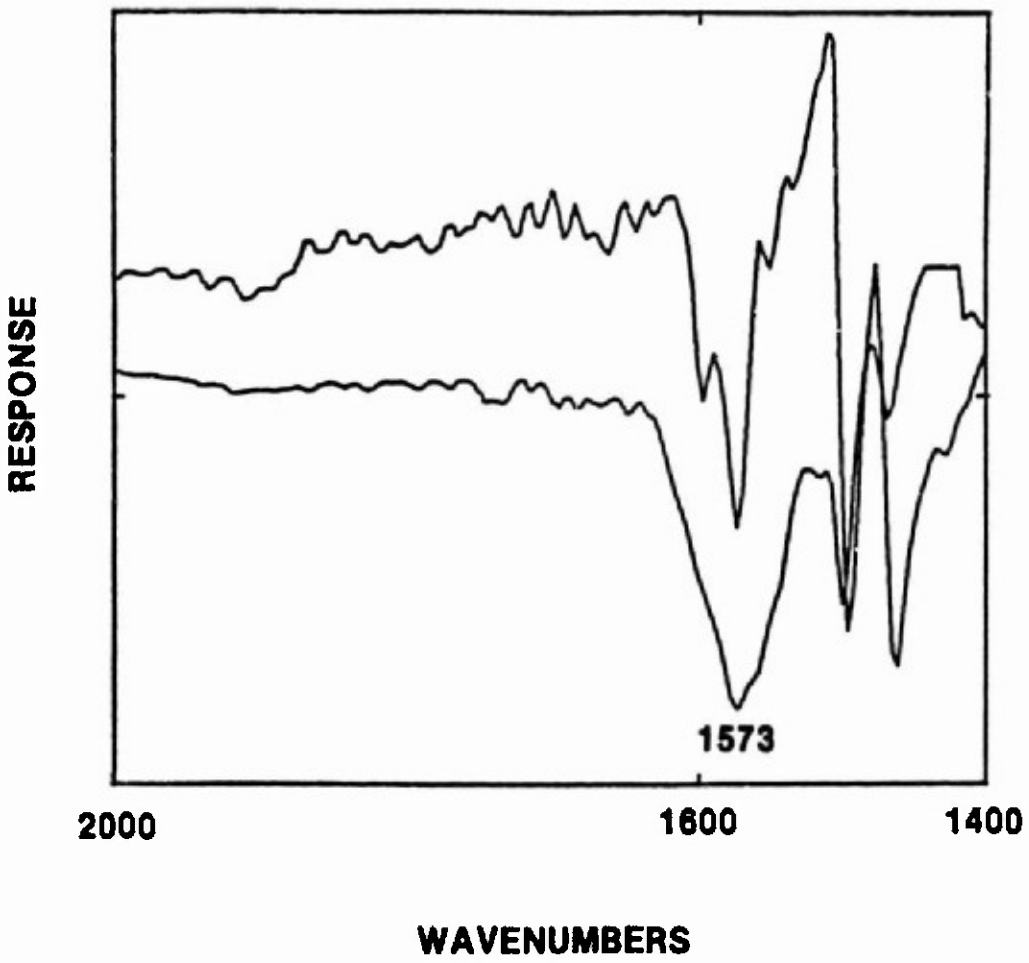

Figure 21. Spectrum of neat sample of copper-8-quinolinolate at high resolution shown in upper trace. Lower trace shows the treated-to-untreated ratio for comparison in this 2000-1400 cm^{-1} band.

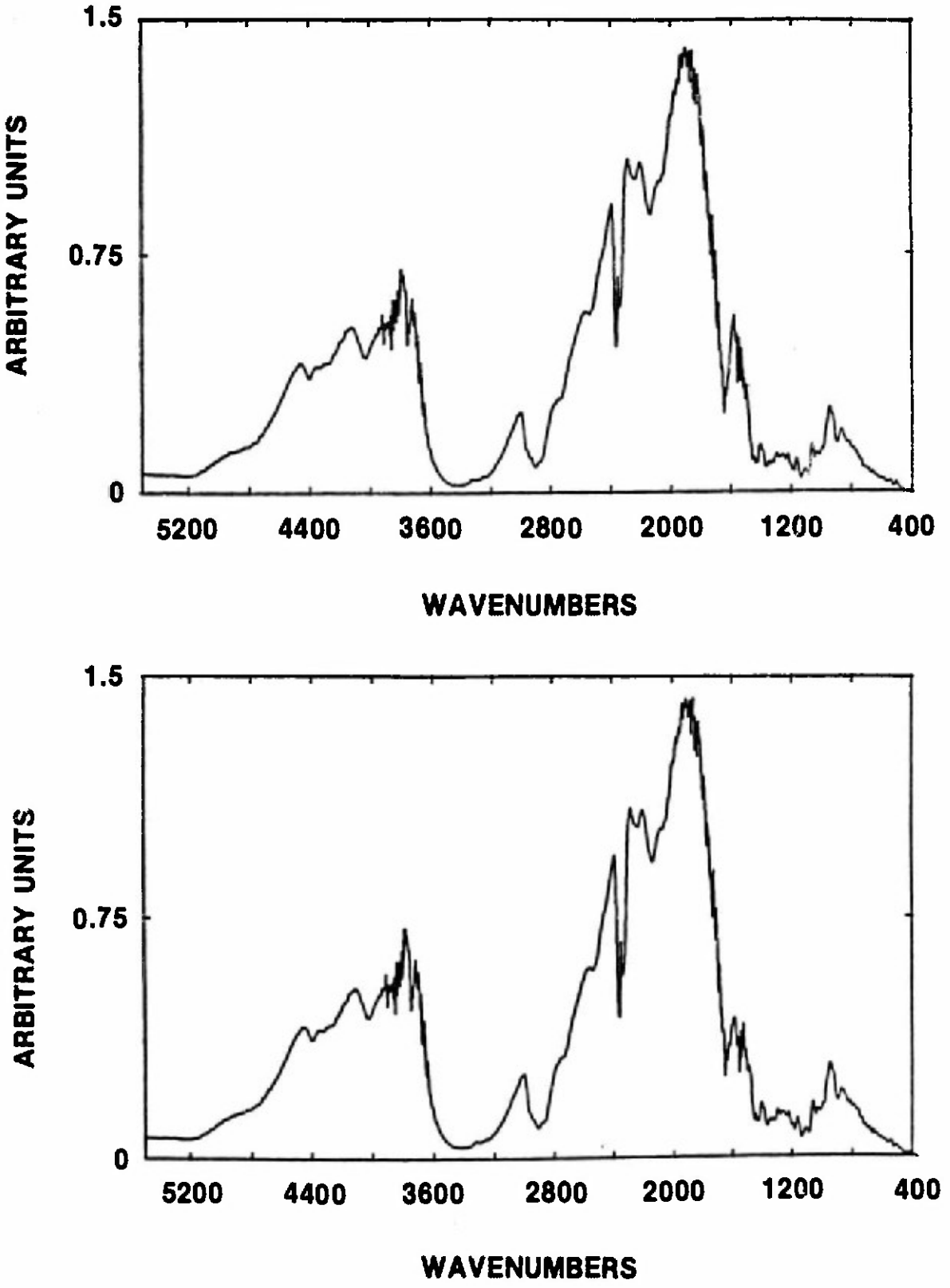

Figure 22. Single beam reflectance-absorbance spectra for untreated (top) and copper-8-quinolinolate treated (bottom) samples.

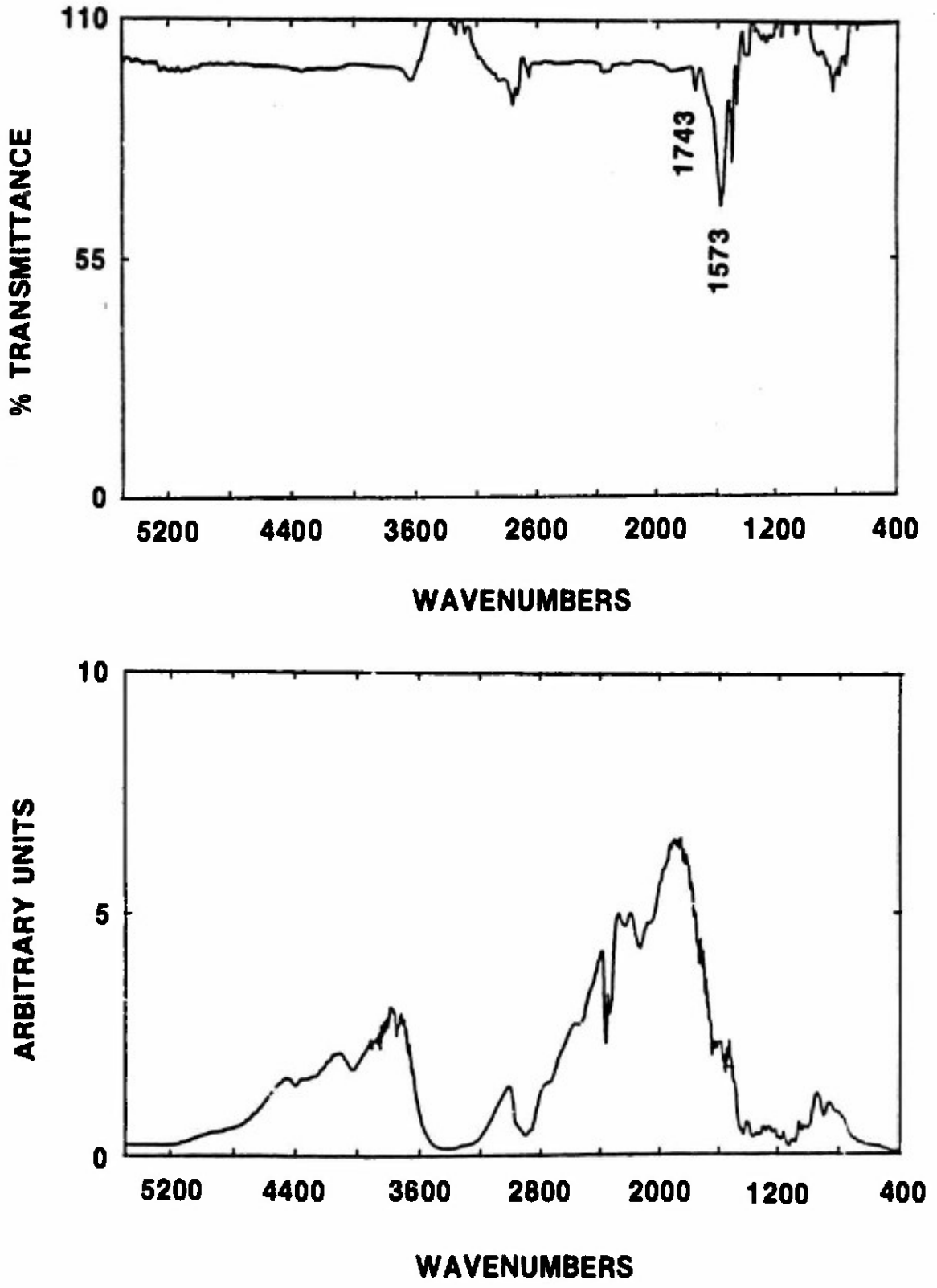

Figure 23. Diffuse reflectance spectrum of treated/untreated samples (top) and single beam spectrum (bottom).

5.5 Far IR

Inorganic and organometallic compounds are known to give rise to absorbance bands in the low frequency region, bands that result from the vibrational modes involving the metal atom. Differentiation of the treated and untreated fabrics might be possible if unique absorbances due to the copper fungicide complex could be observed in the far IR. In Figure 24, the single beam spectrum from an empty beam and the ratio of two empty beam spectra (the "hundred percent line") show the transmission region of the far IR spectrometer. In Figure 25, the infrared transmission spectrum of the neat copper complex, taken in a nujol mull (a pulverized paste) between polyethylene plates is given. From this spectrum it is apparent that the fungicide has absorbance bands in this region. This spectrum shows good correspondence with data reported by Ohkaku, et al.[11].

Attempts to obtain a transmission spectrum of the compound on the cotton duck failed. Throughput was so highly attenuated that an interferogram could not be observed. It might be possible to detect the transmitted radiation with the use of a liquid helium cooled InSb detector placed close to the sample, but such results would not be available using the conventional equipment described in section 5.2.

The fabric samples were found to be reflecting. Figure 26 shows the single beam spectrum (top) from treated duck and the ratioed spectrum of treated to untreated duck (bottom) obtained with a reflectance optic, which collects both specular and diffuse reflectance. While the sample did provide sufficient far IR throughput for statistically significant data to be collected, no absorbance bands that could be correlated with the fungicide were detected.

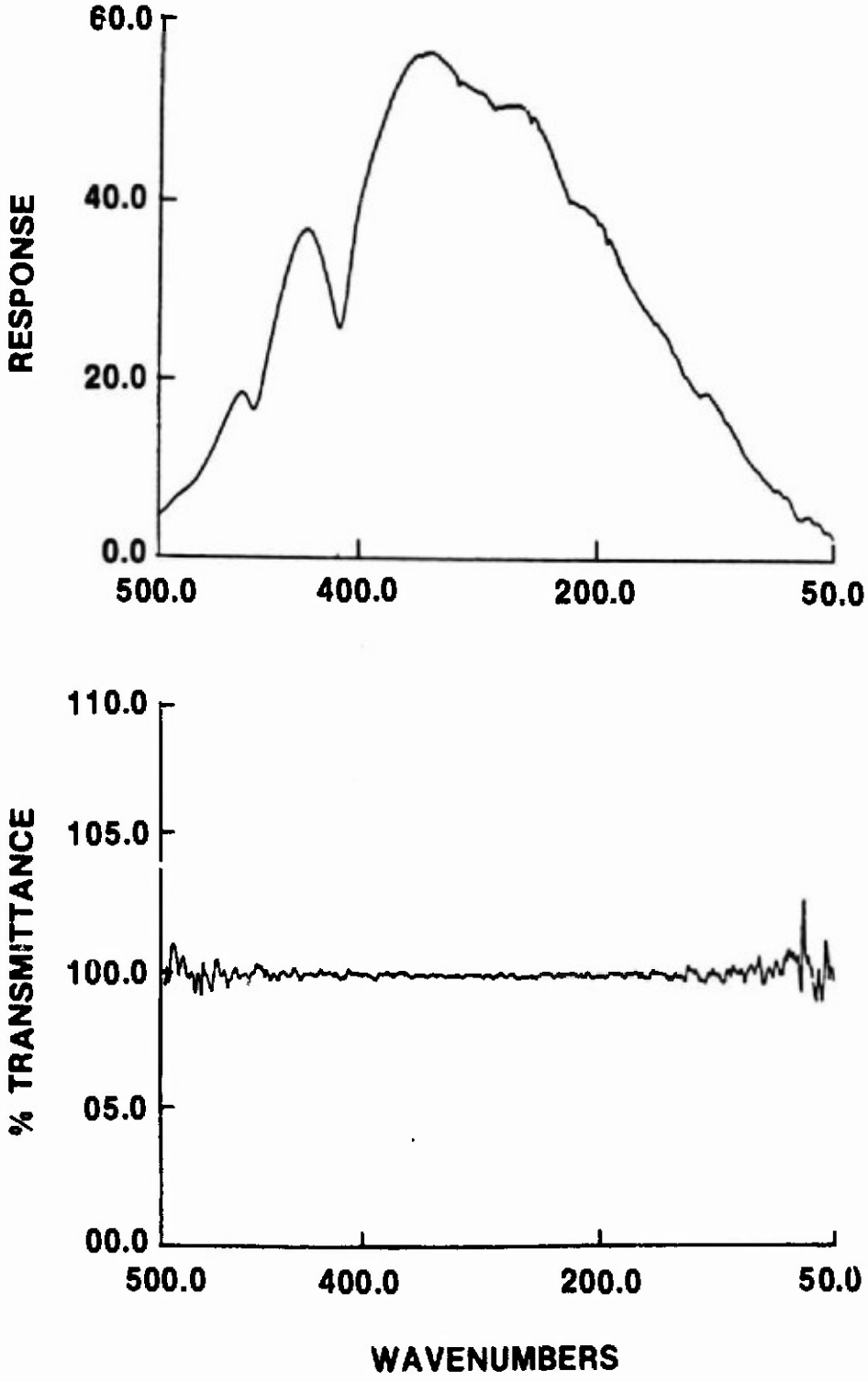

Figure 24. Single-beam spectrum of an empty beam in the far IR (top). Ratio of two empty beam spectra shown in bottom trace.

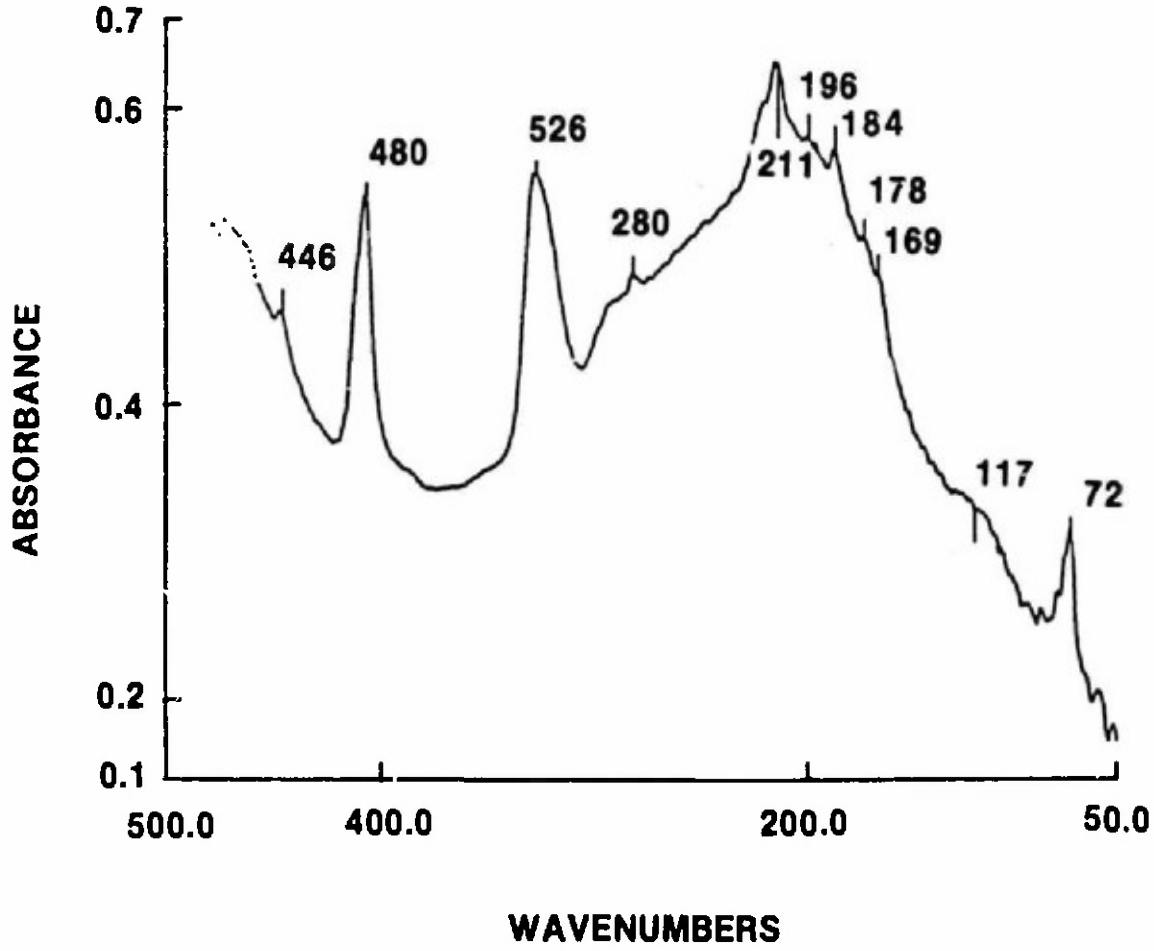

Figure 25. Far IR transmission spectrum of a neat sample of copper-8-quinolinolate in a nujol mull.

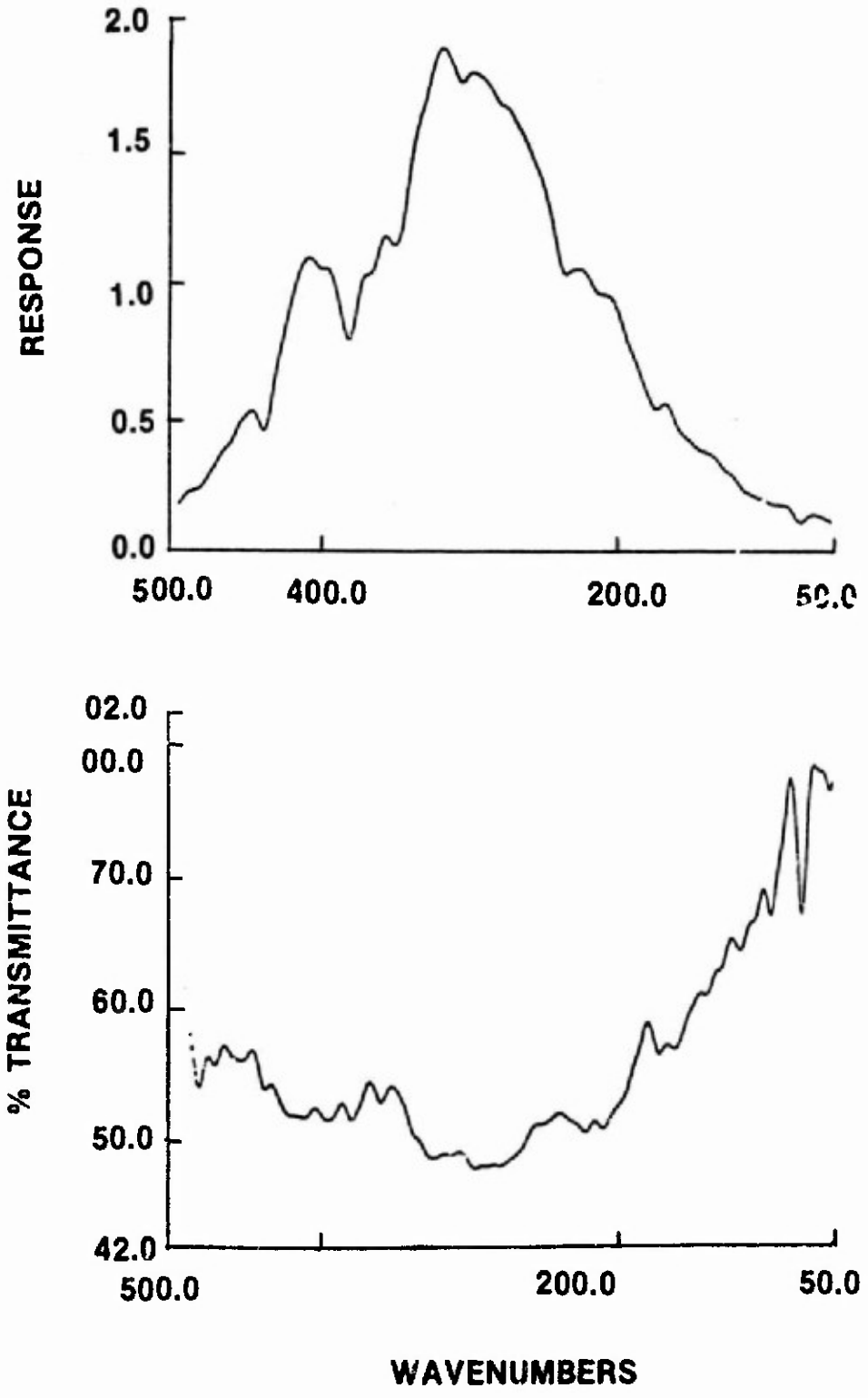

Figure 26. Single beam far IR spectrum from treated duck (top), and ratioed spectrum of treated to untreated duck (bottom). The response is the summed response of D-R and P-A signals.

5.6 Discussion of initial IR experiments

Copper-8-quinolinolate can be detected on cotton duck fiber by IR absorbance at 1573 cm^{-1}. The signal may be observed by R-A or by D-R spectroscopy. The fact that this band is detected in the reflectance modes but not transmission or ATR is probably due to pathlength considerations. For transmission, the pathlength through the cellulose is too long, which results in mostly opaque regions -- including the region around 1573 cm^{-1}. In the transmission spectrum of treated/untreated (Figure 15), the side of an absorbance band can be seen at approximately 1600 cm^{-1}; this may be due to the peak at 1573 cm^{-1}.

In the ATR experiment, no unique bands are observed which could be correlated with the fungicide, even though over 2000 scans were signal averaged, and the region about 1573 cm^{-1} closely studied. The short pathlength in the ATR experiment (only 16 micrometers) resulted in throughput over the entire mid-IR without opaque regions. The fact that the fungicide is not detected is interesting from the perspective of modeling the distribution of the compound on the cellulose. Since the ATR experiment interrogates the sample layer only to its penetration depth, the presence of a surface layer atop the fabric should be preferentially detected in the treated fabric spectrum versus the cellulose bands (unless the thickness of the layer is less than the penetration depth or the layer component is an unusually weak absorber). We observe that the cellulose bands are of roughly the same intensity in both untreated and treated spectra, and the fungicide is too weak to be seen at all. The copper-8-quinolinolate is probably not a layer atop the fibers, but rather the cellulose provides a matrix in which the compound is trapped. This matrix model could also lead

to dipolar interaction between the cellulose and copper-8-quinolinolate, which could broaden the absorbance bands of the fungicide when observed in situ. Consistent with this model, the comparison of the R-A spectrum and the neat sample spectrum (Figure 21) shows some broadening.

In reflectance spectroscopy the pathlength of the incident beam through the sample is less easily predicted, but the data show that the pathlength falls between that of transmission (the thickness of the cloth) and ATR (16 micrometers).

The far IR studies provided no information which could be used to identify the fungicide treating on the fabric. Although copper-8-quinolinolate has absorbance bands in the FIR, analysis in this spectral region is apparently not sufficiently sensitive to detect the compound in situ on the fabric by reflectance spectroscopy; in transmission, the sample is too highly scattered to allow good data collection.

5.7 Future IR studies and potential

Design of a dedicated mid-IR absorbance detector for determining the presence or absence of the fungicide is feasible, based on the experiments already performed. Design of a method that yields quantitative information on the level of treating needs more experimentation. In particular, a calibrated set of cloths, treated to a known amount would be useful to test the accuracy and reliability of the method. Experiments to aid the selection of the best optical configuration (D-R vs. R-A, angle of incidence studies, optimum spot size, scan rate, continuous analysis operation) would need to be carried out. We have, however, conducted experiments sufficient to establish viability of the technique, and, subject to the recommended experiment below, we have accomplished that.

Provided that the continuous motion experiment works, we now have sufficient experimental data to provide a design of detail sufficient for generating a mature Phase II program plan and reliable cost estimate.

One potential problem would be irregular scattering effects from spot to spot on a textile fabric. The arguments against this possibility are: (1) The fabric is of a regular weave and thus should yield a similar scattering spectrum anywhere on the cloth (down to a certain spatial resolution) and (2) baseline relative absorbance could be observed to minimize any such effects. To check this possibility, the R-A studies described above were carried out twice, on different days using different pieces of fabric from the same cloth. Baseline relative reflectance at 1573 cm^{-1} differed between the two measurements by only 1.7% of the total response. A simple experiment in which the fabric is continuously moved across the beam focus as spectra are repeatedly collected would conclusively resolve this question. This experiment was undertaken and is reported below.

Use of the copper-8-quinolinolate absorbances in the FIR may be possible even though they were not detected in the experiments described here. Further investigations require a more sensitive detector. Even if this could be accomplished, from a practical standpoint the FIR has several disadvantages for use in a dedicated, on-line detector. Sensitivity in the FIR is generally lower than that in the mid-infrared and because water vapor absorbs strongly over the entire FIR band, measurements are usually made in an evacuated (about 1 torr pressure) sampling compartment. Another discouraging factor is that the most sensitive of the FIR family of detectors requires cooling with liquid helium (compared to liquid nitrogen or room temperature detectors in the mid-IR).

5.8 Continuous analysis demonstration

Since the goal of these studies is to develop a method to monitor the quality of the fungicide treatment in the fabric, an experiment that mimics the operation of an on-line infrared reflectance detector was performed.

The configuration is shown in Figure 27. A circular strip from a piece of treated fabric was fixed to the perimeter of a support disk. In two regions, the copper-8-quinolinolate treated duck was removed and replaced by sections of untreated cloth. Next, the disk was placed in the sample compartment of a Fourier transform infrared spectrometer; the beam was focussed onto the cloth and the disk was rotated by a motor drive while reflectance spectra were continuously collected. The pattern of the cloth samples (which were fixed to the aluminum disk using two-sided tape with care taken so that there were no blank spots) is shown in Figure 27. The beam in this analysis was first focussed on an untreated "reference" region, then, when rotated (counter-clockwise at 1/30 RPM), treated, untreated, and, again, treated cloth regions were interrogated. This imitates the analysis of a fabric sheet which is defective by having a spot that has been left untreated.

The optical configuration for detection is shown at the bottom of Figure 27. This method is similar to that used to obtain reflectance spectra of compounds which have been deposited from a high performance liquid chromatograph, as described by Gagel and Biemann[12]. Eight scans were co-added before transforming each spectrum, implying a resolution time of about two seconds. The beam diameter was about 6 mm. The untreated "reference" region covered about a 1 cm length of the disk perimeter, and

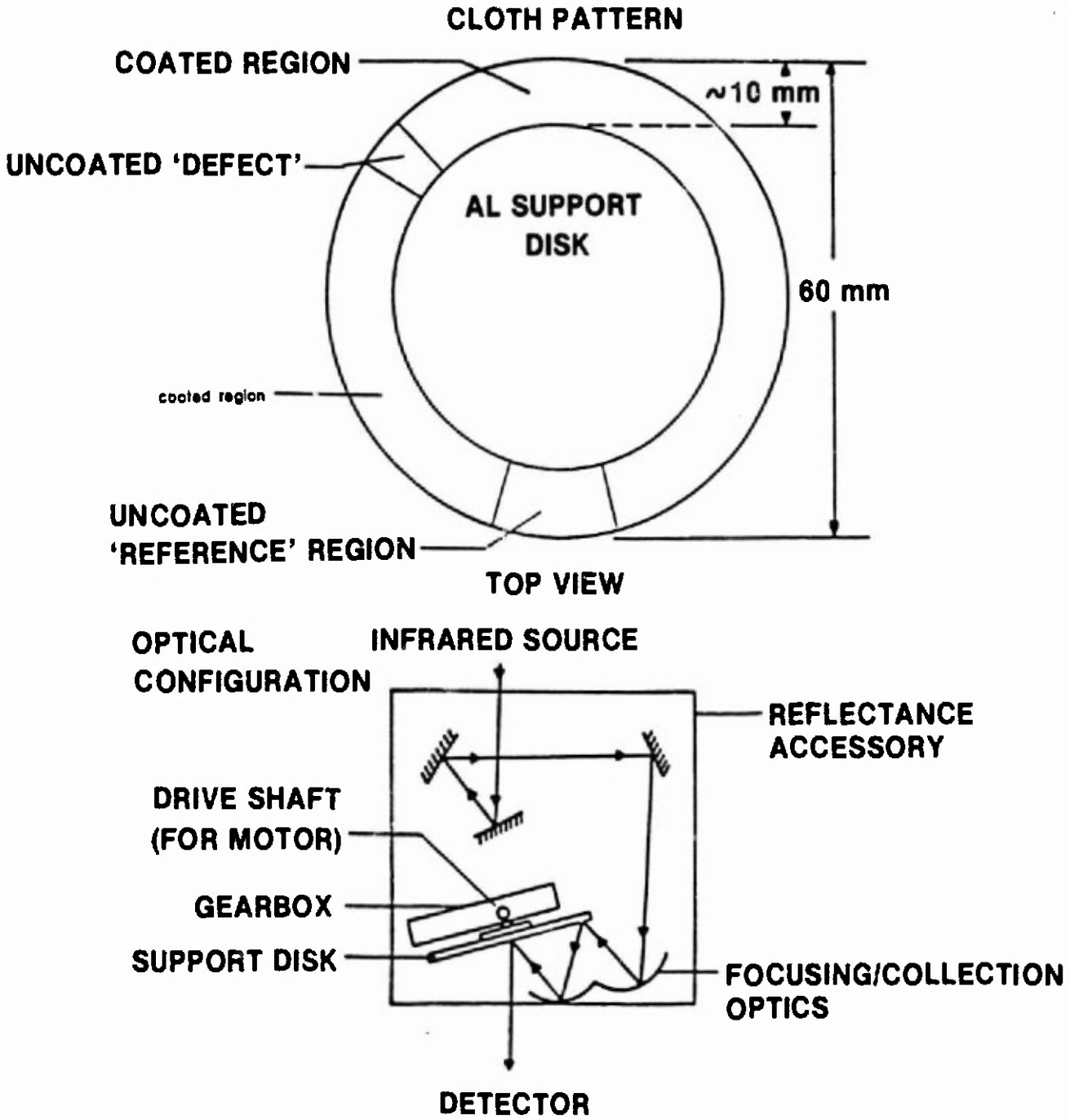

Figure 27. Configuration for continuous analysis demonstration.

the second untreated strip, representing the "anomaly", was approximately 6 mm long.

Figure 28 shows a tracing of the baseline relative absorbance at 1573 cm^{-1} over the 30 minute analysis period (one disk revolution). These data are characterized by zero absorbance at the beginning of the run as the reference region passes through the beam, followed by a sudden rise in absorbance as the first section of treated duck is detected. The rapid drop in absorbance starting at about 10 minutes corresponds to the untreated anomaly region. This is followed by a return to high absorbance, indicating detection of the second treated region, and this high absorbance persists until the disk completes the revolution and returns to the reference strip at about 29 minutes. The small-scale variations — the noise — is actually quite small, on the order of 1% or so. If the magnitude of these variations is allowed to relax to 10%, the data time could be shortened by a factor on the order of 100. These scans could be collected in a time of about 0.25 seconds per interrogation spot. Thus, continuous on-line measurements of fabric traveling by at the standard 13 inches per second (46 cm per second) speed would yield quinolinolate measurements to a precision of 10% and with spatial resolutions of about 5 inches (13 cm). Alternatively, the fabric travel could be buffered so that it is stopped periodically for 1/4 second to make this measurement with a finer spatial resolution.

Figures 29 through 32 show four spectra, taken at points labeled A-D on Figure 28. In Figures 29 and 31 (points A and C in Figure 28), the spectra obtained from the untreated regions are shown to be absent of the fungicide absorbance at 1573 cm^{-1}, while the spectra in Figures 30 and 32 (points B

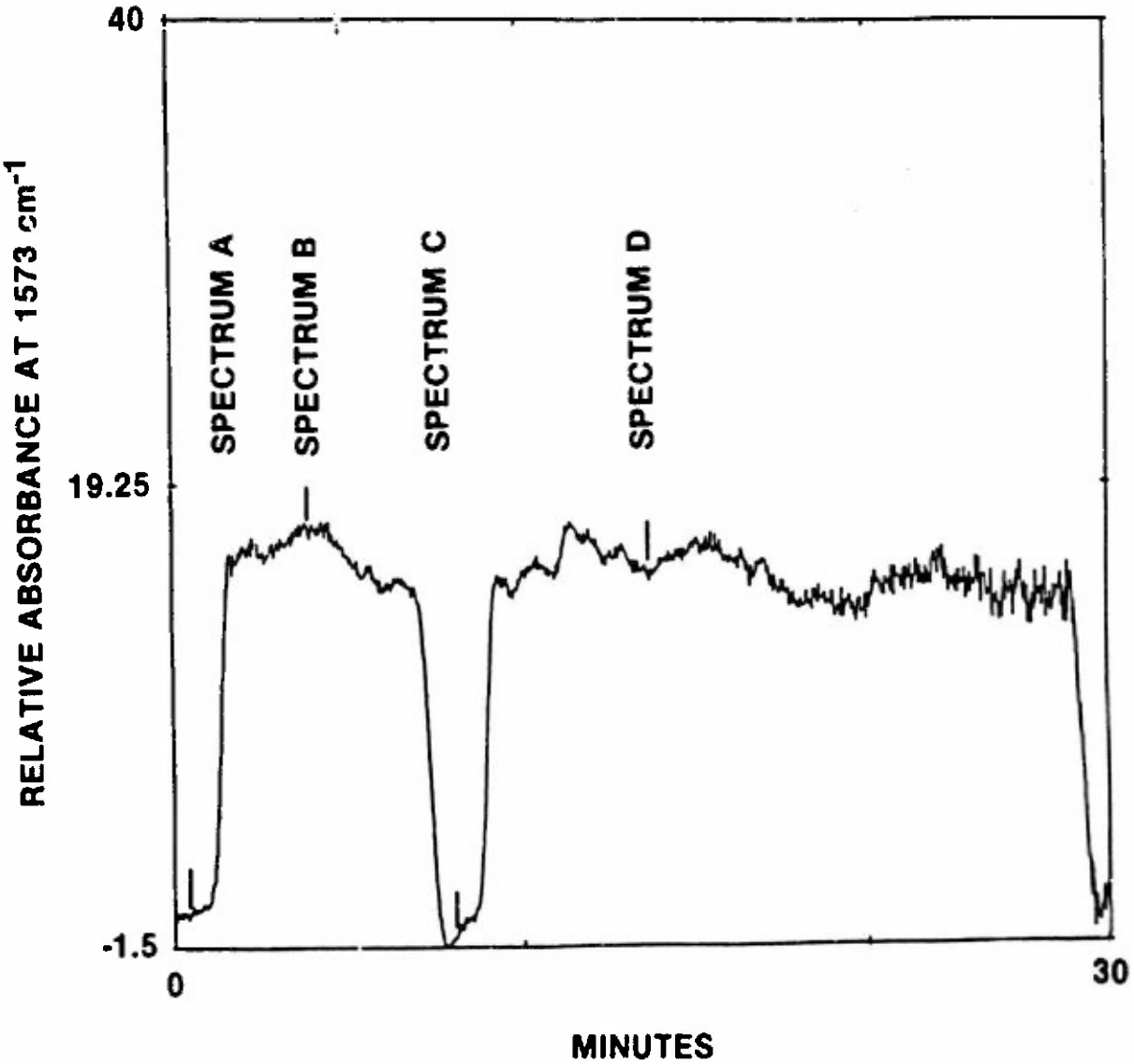

Figure 28. Relative absorbance at 1573 cm^{-1} as the test specimens were rotated through the IR sample beam. Spectra were obtained at the four positions indicated.

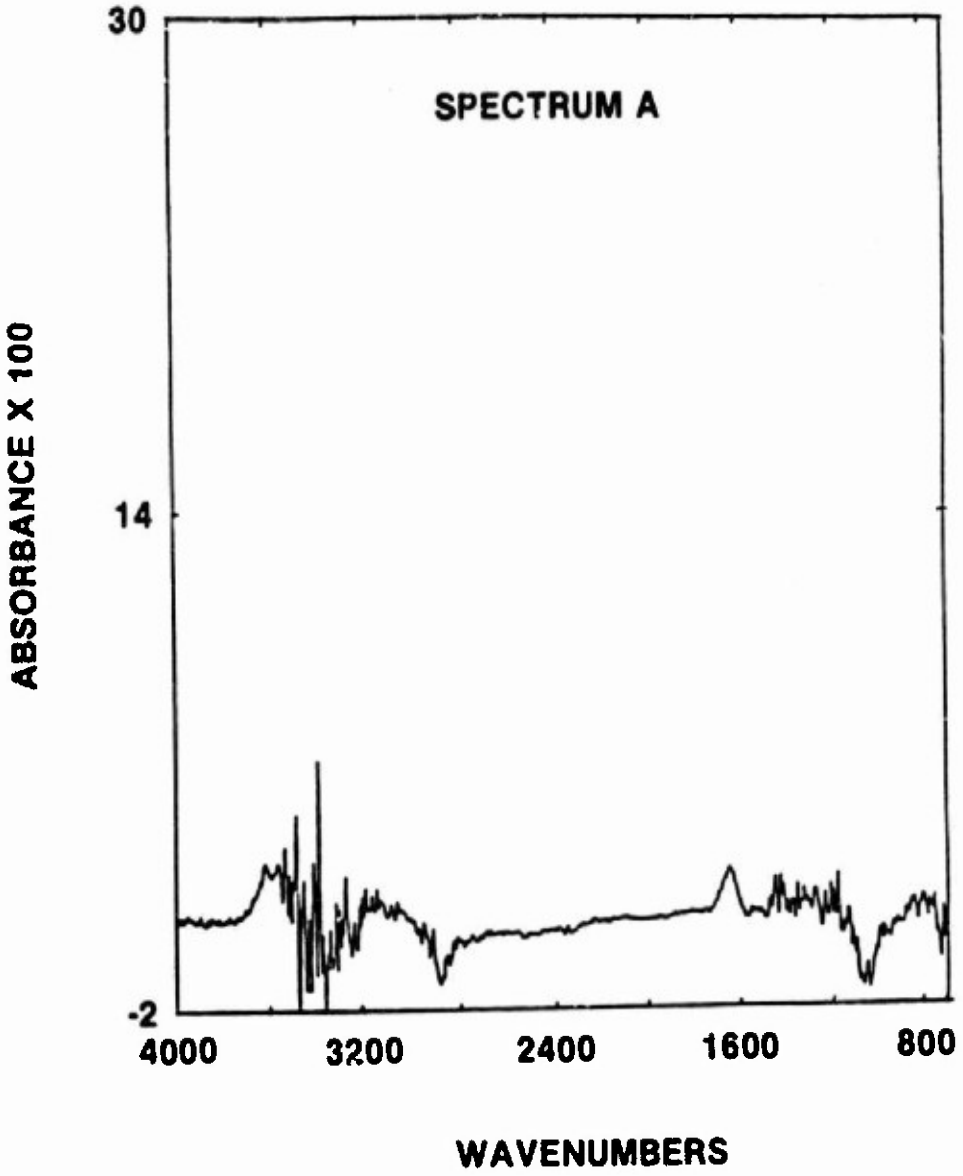

Figure 29. The first of the four spectra (A, B, C, D) taken at the times indicated on Figure 28. No evidence of the feature at 1573 cm^{-1} is seen.

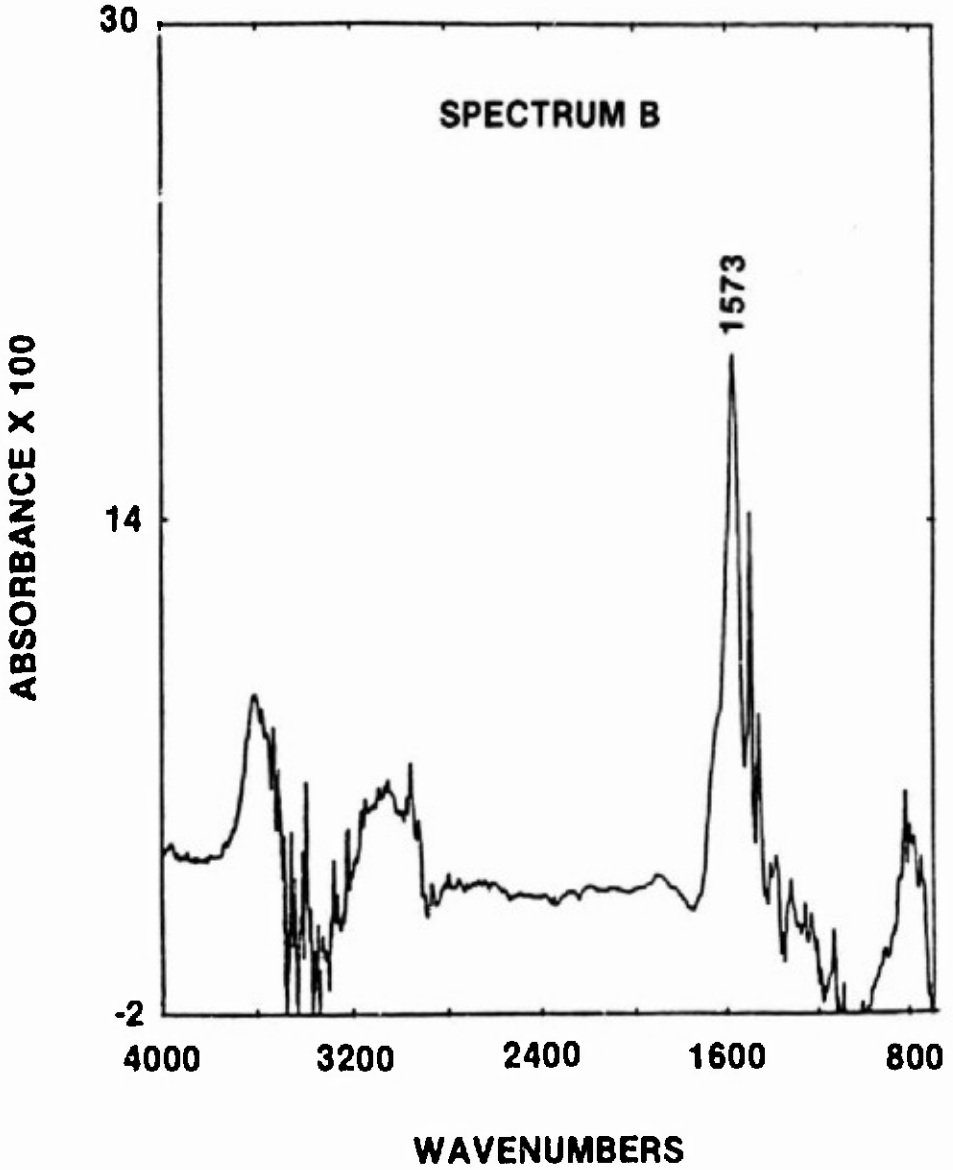

Figure 30. Spectrum B, showing the strong feature at 1573cm^{-1}.

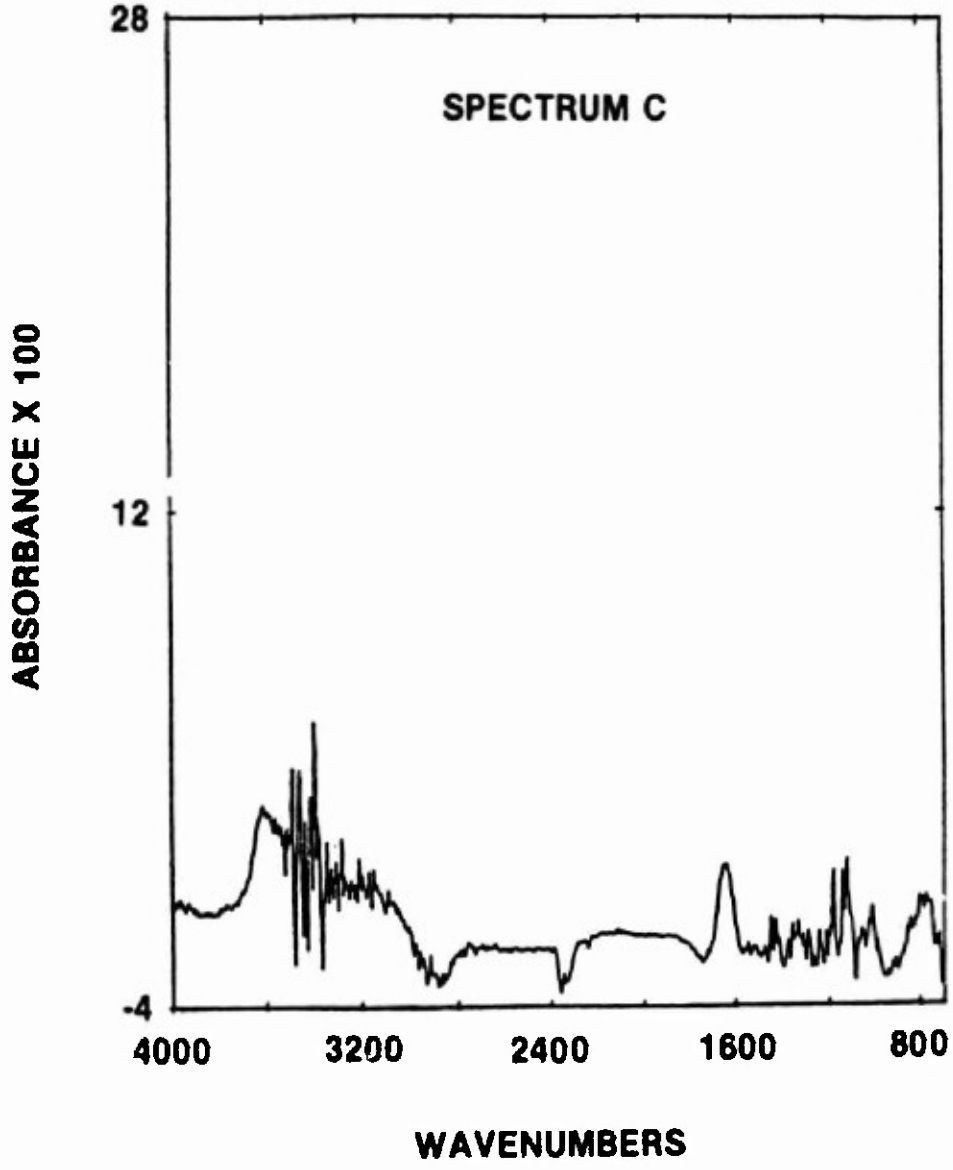

Figure 31. Spectrum C in absorbance. No feature is seen at 1573 cm^{-1}.

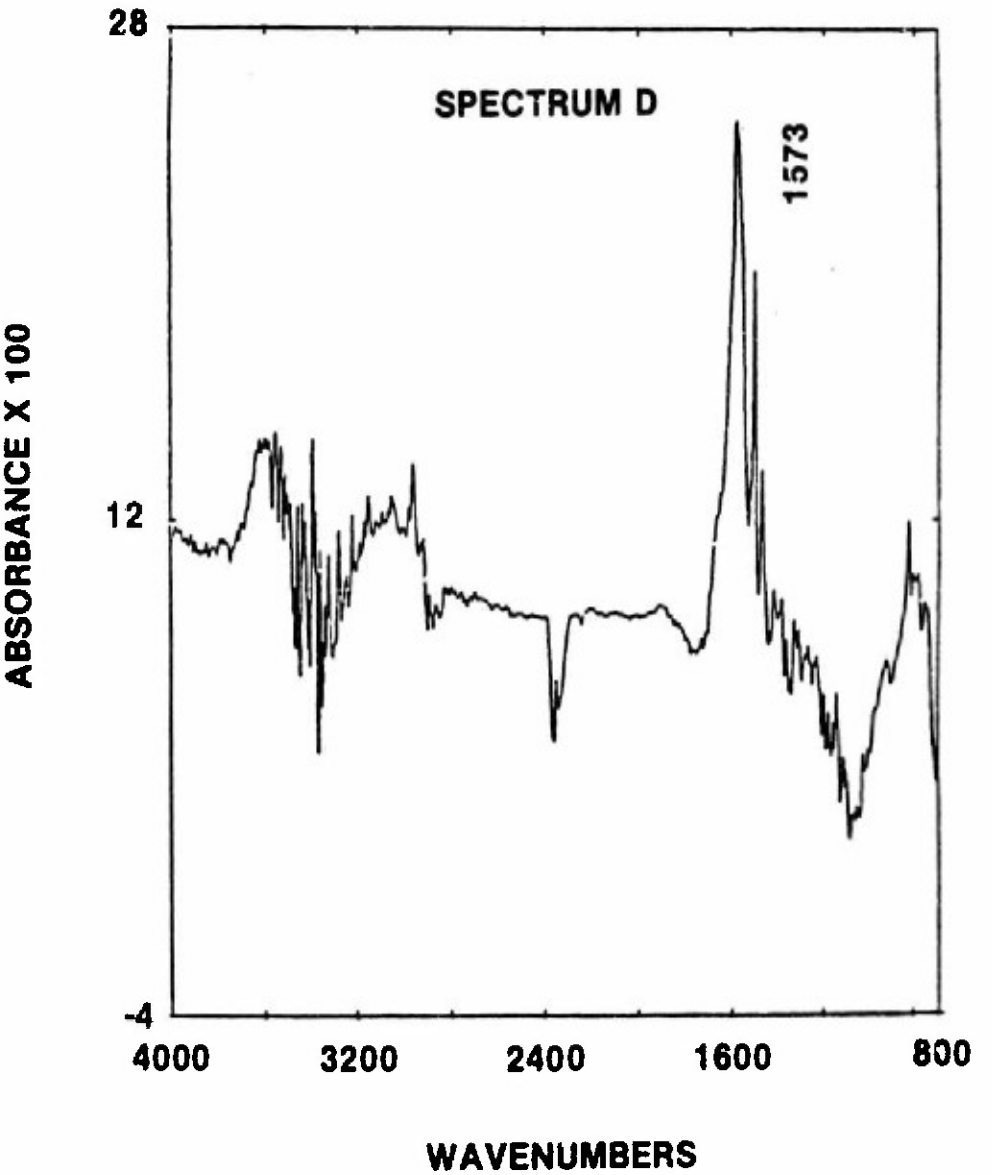

Figure 32. Absorbance spectrum at position D, showing feature at 1573 cm^{-1}.

and D in Figure 28), which are from the treated cloth, exhibit this characteristic band.

This simple experiment demonstrates how an on-line reflectance detector can be used to monitor fungicide treatment quality. The high signal-to-noise ratio of the spectra obtained indicates that much higher fabric speeds could be used for simple detection. Alternatively, it may be preferable to spot test fabric sheets in a noncontinuous manner. The best embodiment would ensure fungicide treatment compliance; optimizing analysis speed is left for future consideration (see Section 7 on IR system design).

Also notable is the relatively small noise and drift levels of the absorbance signal throughout the run. Despite the crude method by which the sample was fixed to the support, the absorbance drift was only +/-15% of the total signal. (This is the large scale drift -- the actual noise present in the measurement is on the order of 1% or so.) It is likely that a dedicated device could greatly improve upon this by ensuring that the sample is held flat (most likely by stretching the fabric slightly) and by passing the cloth through the beam in a direction consistent with the weave. A system design is shown in Section 7.

6.0 SYSTEM DESIGN (X-RAYS)

According to the results of Section 4, the experimental verification, there are still two viable candidates for implementation of an x-ray based inspection system. Both fluorescence and dual energy techniques offer distinct advantages (as well as the IR solutions, a system design for which is given in Section 7).

The main advantages of fluorescence techniques include:

— one-sided inspection

-- unambiguous determination of absolute high-Z elemental abundances

The advantages of the dual-energy techniques include:

— fine spatial resolution capability

— relative amount of high-Z determination

— ability to work in very thick samples

— ability to detect elements down to an atomic number of 11 or 12, much lower than that allowed by fluorescence

Either machine will probably be used in a sampling manner, if employed in a production context. In a research context, the dual energy technique is more useful, due to its fine spatial resolution capability in situations involving inhomogeneous samples. Many fungicides use high-Z-based compounds, e.g., copper, phosphorus, or chromium, and the dual-energy technique allows investigation of migration of these compounds under a variety of circumstances.

There is a reasonable basis for belief that the dual-energy technique will ultimately be more versatile than the fluorescence technique, even though the fluorescence offers unambiguity (as long as a solid-state detector is used). Indeed, because of the configuration of the basic machine, it may be possible to add the capacity to make fluorescence measurements (thin samples only) simultaneously with the acquisition of the dual energy data.

6.1 Machine configuration

The machine design is based on the Hologic configuration. This system is set up so that it can perform at three preselected pairs of x-ray

energies. The system can be used to monitor copper or other high-Z elements, and can be used to monitor high-Z thicknesses up to and including leather and wood blocks, materials which are entirely outside the realm of fluorescence detection. The advantage of using this configuration is that all the design, integration and implementation work has already been done and paid for. The modifications required to make this machine perform in an energy regime appropriate for textiles and treated materials are small compared to the effort necessary to build a machine from first principles and components.

The system configuration is shown in Figure 33. A commercial system is shown in Figure 34. A self contained x-ray source mounted beneath the test samples provides alternating x-ray pulses at a preselected pair of voltages, e.g., for copper-8-quinolinolate on cellulose this would be a set of low voltages, e.g., 10/20 kV. The x-ray detector is mounted above the test specimen. Controlled by an internal computer, the x-ray source and detector move across the test specimen in an X-Y raster pattern. The x-ray beam is extremely well collimated so that only a thin needle-beam passes through the test specimen. In the path, as shown in the figure, is a calibration disk containing various x-ray absorbing materials. This rapidly rotating disk allows automatic measurements to be made on materials identical to those being measured. Every picture element is referenced to these calibration materials. This calibration scheme is what allows the amount of various elements to be so well determined, relative to other methods. When the x-ray beam is detected it contains information about the x-ray absorbing characteristics of both the test specimen and the

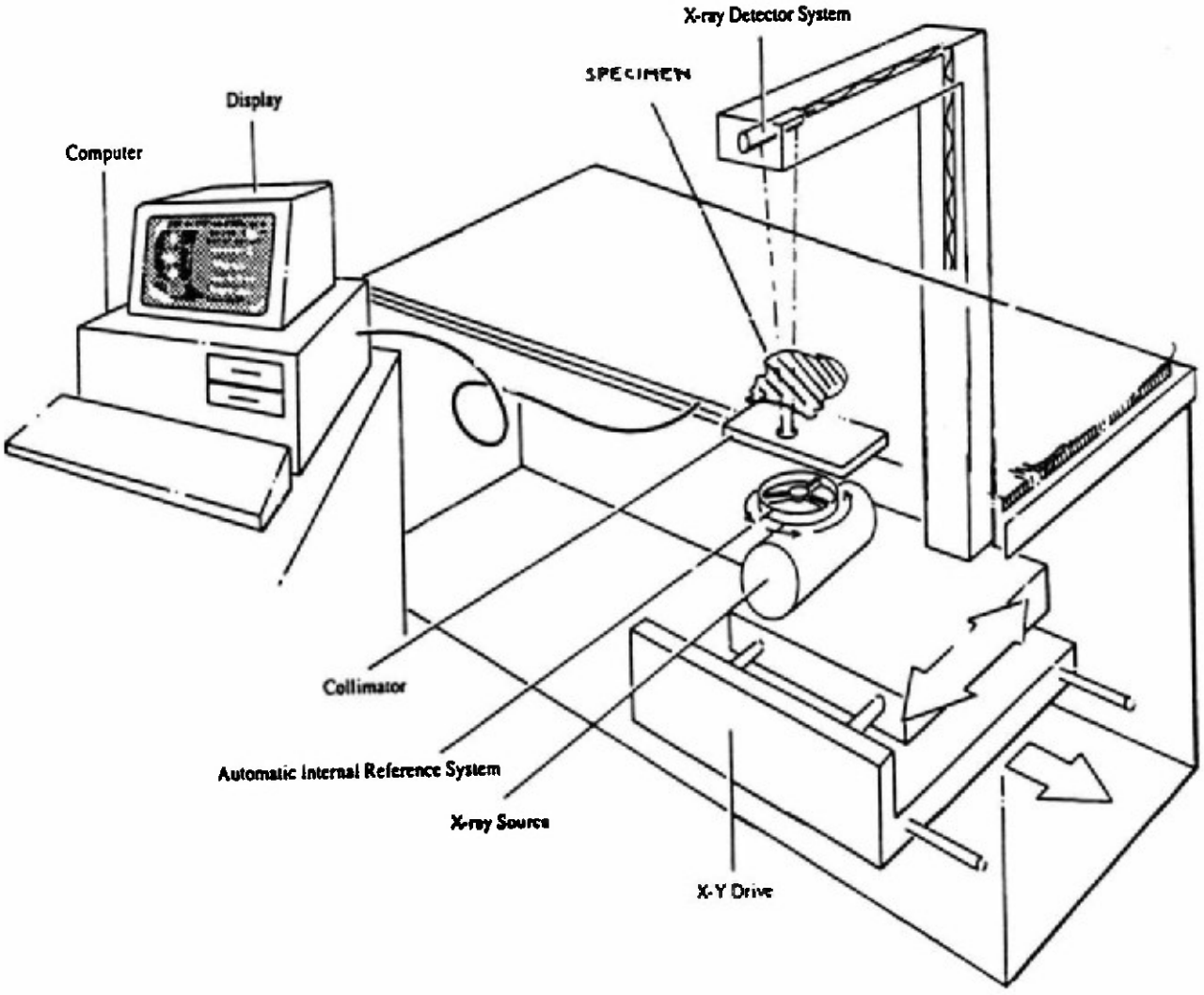

Figure 33. Machine configuration for dual energy x-ray testing.

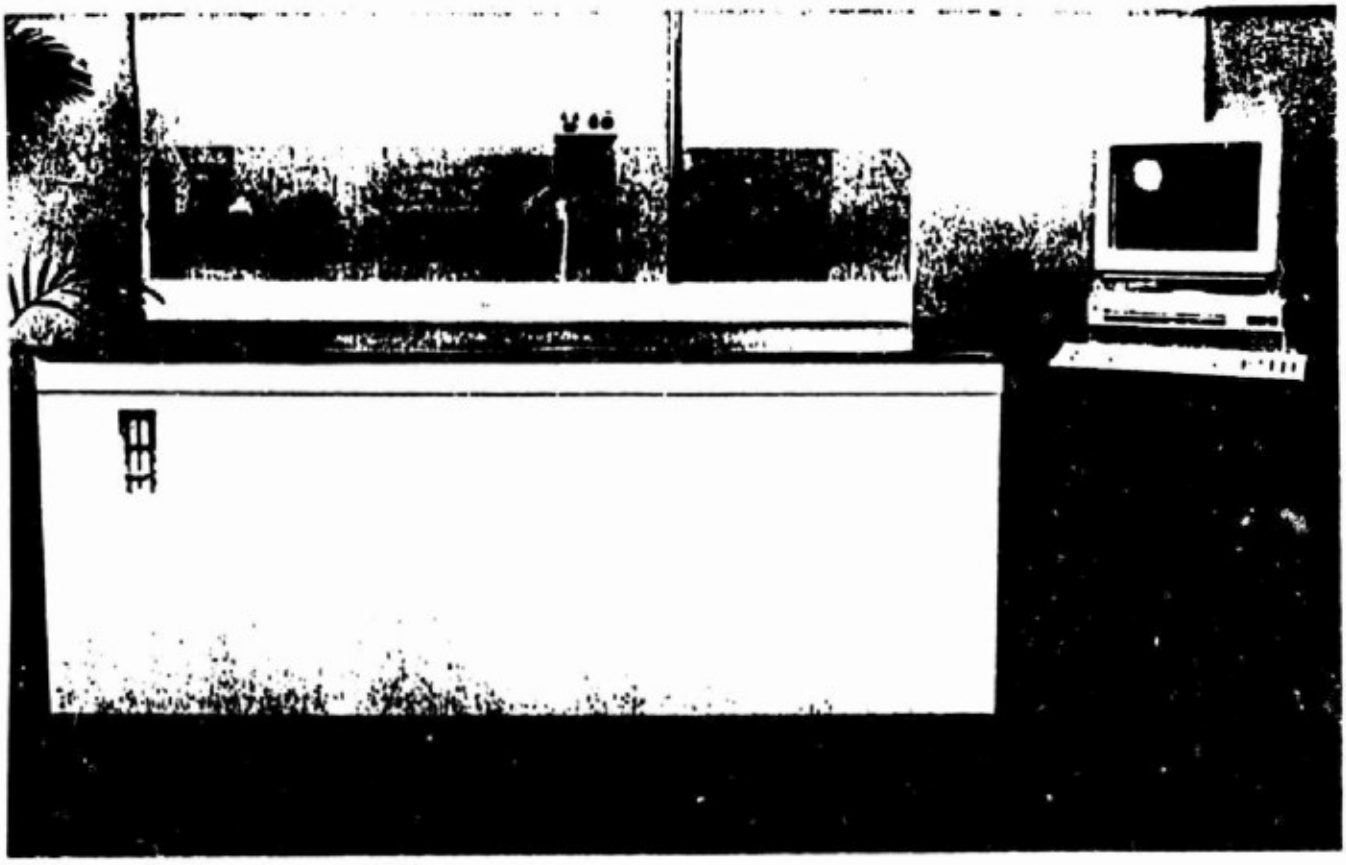

Figure 34. Existing Hologic machine.

calibration materials at each of the two excitation energies. The analog-to-digital converter digitizes this information and sends it to the computer for analysis.

X-ray source.

The x-ray source is a standard Lohman industrial (nonmedical) tube used for fluoroscopic examinations. These tubes are rugged, reliable, and relatively inexpensive. The only difference over the standard configuration may be an examination of different glass envelopes for the tube. The reason is that some of the lower energy x-ray flux, which may be desirable for examination of the thinner less-attenuating test specimens, may be absorbed in a standard glass envelope.

X-ray detector

The x-ray detector is a standard scintillation detector utilizing a combination of cadmium tungstate and photomultiplier (PMT). This combination gives not only the intrinsic high dynamic range offered by the more standard sodium iodide/PMT pair, but a fast recovery time (lack of afterglow) so that the second of two adjacent absorption measurements is not poisoned by the results of the first. The machine design essentially puts all the spatial resolution into the collimation scheme, and the detector need have no spatial resolution capability at all.

Calibration wheel

The main problems in establishing dual-energy absorptiometry for accurate measurements of the amount of specific materials (i.e., weighted by atomic number as described earlier) is the lack of good x-ray source stability and the polychromaticity (resulting in variable beam-hardening — change of spectral shape) of the x-ray beam. (For samples which are

optically thin to the radiation being used as the probe, this second issue is not as important. Copper-8-quinolinolate on cloth falls into this category.)

The design of the Hologic device incorporates an automatic internal reference system, as shown in Figure 34. The calibration wheel has alternating sections of materials consisting of the high-Z and low-Z components, and these materials are scanned between each pixel, in combination with the test specimen. It is the continuous calibration that makes the system work so well.

Software and analysis, visual image display

The system contains a high resolution image display (1 mm x 1 mm pixels, standard size), an automatic analysis program to eliminate imprecision due to operator intervention, a full adjustable region-of-interest (ROI) so that an individual test specimen can always be analyzed in the same way using the same ROI. This is necessary to achieve high precision in cases involving stepped treatment of a sample. The system contains a "compare" capability allowing the operator to review the current image alongside the image obtained on the same specimen at a previous time.

The software is menu-driven, although it need not be operated in that mode. The calibration and quality control software can be changed to accommodate the needs of thin/small samples for nondestructive testing, rather than medical uses.

All raw data are automatically archived so that should any change be made in calibration procedure, the old data can be reanalyzed with the new algorithms.

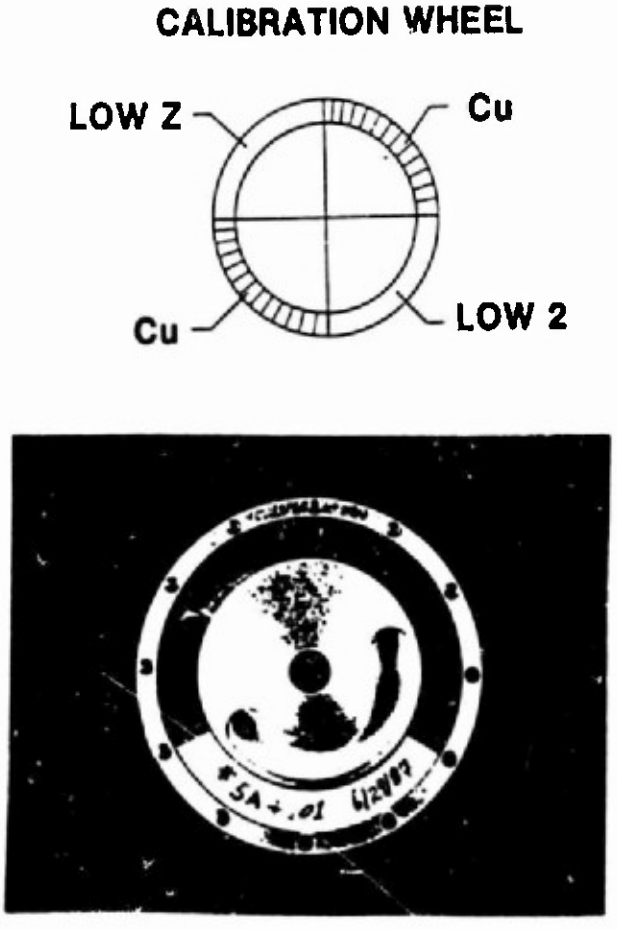

Figure 35. Sketch and photo of calibration wheel assembly.

Performance characteristics

The current performance characteristic allows the areal density of the high-Z component to be found to a precision of 0.4%. We expect that this precision will be degraded somewhat (we estimate a factor of 2-5, making the precision 1-2%) as the machine is used for these nondestructive testing purposes.

A single sample (approximately 120 x 140 mm, 1 mm pixels) should be scannable in a time of 5 minutes. This would yield a picture of all the copper along the line of sight in each of the pixels — a distribution of copper in area.

The distribution of copper as a percentage of the total amount of material present requires another calculation, and this can be accommodated by a change of software as well. The data must be gathered in order to make the copper measurement. The precision of the measurement of the low-Z component must also be set (it will be on the order of the precision of the high-Z component); the percentage of the high-Z component will be somewhat less precise — something on the order of half as precise as the absolute value. The percentage figure, of course, is what's required for determining whether a given test specimen has met its specification. (This ignores the contaminant problem encountered with the nickel.)

Thin samples can be examined by fluorescence simultaneously with the acquisition of the dual energy data. This requires a separate detector and data channel. While the system is not currently set up for these functions, this capability will be examined during the Phase II program. The reason for consideration of this option is that the spatial resolution capability has already been included, and the incorporation of a

fluorescence detector would be relatively easy. While we cannot guarantee that this approach will be implemented in the Phase II system, it can be added as an option in Phase III commercialization. It certainly is very simple to add a nonimaging x-ray fluorescence detection scheme. This would allow the presence of gross amounts (e.g., 1 part in 1000 or so of the copper content) of contaminants (of differing Z's) to be identified, and to ascertain whether the dual energy measurements had been contaminated.

In summary, then, the following design changes are required to the Hologic machine:

1. Different set of operating voltages is needed. Hologic design can be modified so that three separate sets of voltages can be programmed into the system with little redesign.
2. Different calibration samples are needed. The system design allows substitution of various, different calibration materials as necessary.
3. Software modification would be required to accommodate these changes.
4. Possible incorporation of fluorescent x-ray detector should be considered.

Interface

The interface itself is already established and determined by the set-up of the Hologic machine. For the most part, this is an operator interface, a data interface, and a test specimen interface. The operator interface has been described primarily through the software and menu-driven display. The data interface is a quantitative output in two forms: (1) paper hardcopy of already-analyzed data in image format, and (2) magnetic media output for both the raw data, and the image data, which are saved in

a file on an internal hard disk and read out to a standard 5-1/4 inch PC diskette for archival storage or further processing. The test specimen interface is a simple bed where the specimen is placed. In this machine, the test specimen interface is identical to that of a patient. In a production machine, the interface is more similar to the apparatus shown in the next section.

Other issues

This section addresses the machine change issues. Concurrent with these matters is a calibration and use program, which makes the system useful in the fungicide/textile and other relevant NDT roles. This issue is addressed in the Phase II program plan, Appendix A.

This machine is to be used in a research role and more in the context of establishing correlation with the IR machine than in a production role. The x-ray machine could, however, be used in that production manner.

7.0 SYSTEM DESIGN (IR)

The results of the IR tests described in Section 5 were sufficiently encouraging to us that efforts were made to pursue a design for an IR-based system. The advantage of the FTIR system over the original x-ray design was a much more rapid scanning (at the expense of depth penetration and spatial resolution), a much cheaper implementation, and the removal of safety and environmental concerns so prevalent with the use of x-ray based inspection equipment.

We have taken a tack similar to that employed in the x-ray system design. Namely, we have found a commercially available IR instrument and adapted it for use on this program. The advantage of the selected instrument is its versatility: It can be adapted for a variety of different experiments, should we wish to run them during the Phase II calibration phase.

We've chosen a Michelson interferometer design that utilizes a single moving part, a reciprocating mirror. There are no slits, no gratings and no conventional chopper wheel.

The head of this spectrometer will perform identically to the production system design. The difference between this prototype and the production system of Phase III is in the mechanical handling equipment for the textiles. (Since this is to be a prototype, the method for manipulation will be designed during Phase II, and provided during Phase III.)

7.1 IR system configuration

The IR system configuration is shown in Figure 36. This system is based on the same instrument with which all the mid-IR band measurements (discussed in Section 5) were made, the Digilab Model FTS-15/90 FTIR.

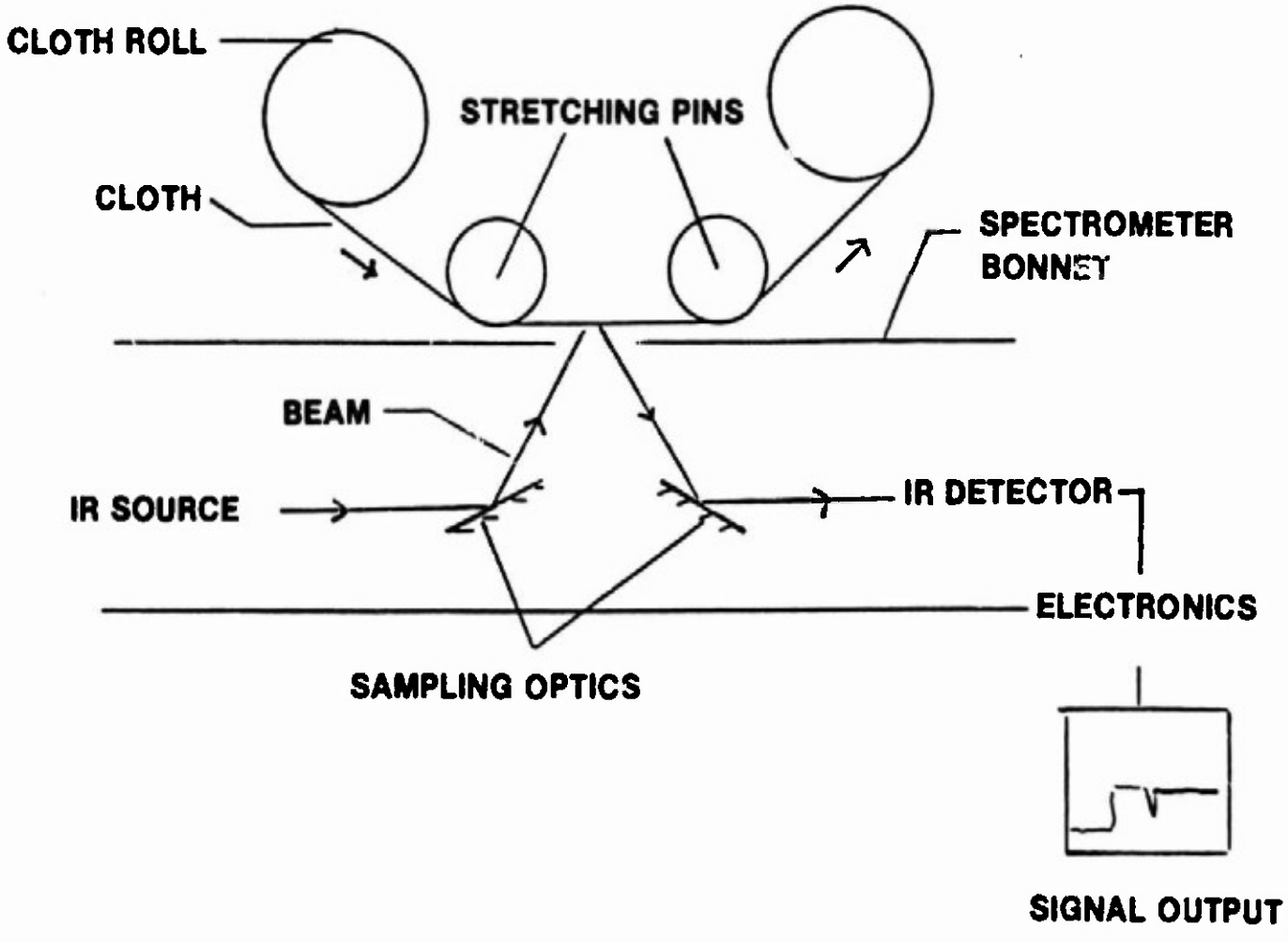

Figures 36. IR system configuration, showing mechanical approach for locating and testing arbitrary position on textile.

The spectrometer is shown with a roll of textile material, which is being sampled. These are currently shown only in schematic form. Figure 37 shows an orthogonal view.

The results of the experiment indicated that either D-R or R-A measurements yielded data indicative of the amount of the quinolinolate at or near the surface of the cloth. A problem in the sampling during the experiment was in the nonflatness of the sample in the wheel arrangement. We believe that this nonflatness was responsible for the relatively long-term drift observed in that experiment. For this reason, the textile is shown as being held taut by spring-loaded stretching pins. This will guarantee a flat surface (to the scale required by this apparatus) and yield a more uniform measurement.

The spectrometer consists of an IR light source, in this case an IR ceramic glowbar element. Light from the source is collimated, passed through the interferometer and modulated. The modulated beam is directed to the "sampling compartment". Ordinarily, this is a closed box in a laboratory spectrometer where one places a sample which is to be analyzed. In this case, however, the sample compartment is an area adjacent to the spectrometer body where the IR beam contacts the stretched cloth. The reason that a sample compartment is necessary is that water vapor will completely absorb signals in the band of interest, or at the very least, yield misleading results. In the sample compartment shown here, we simply purge the area with dry air or dry nitrogen so that the water vapor factor disappears.

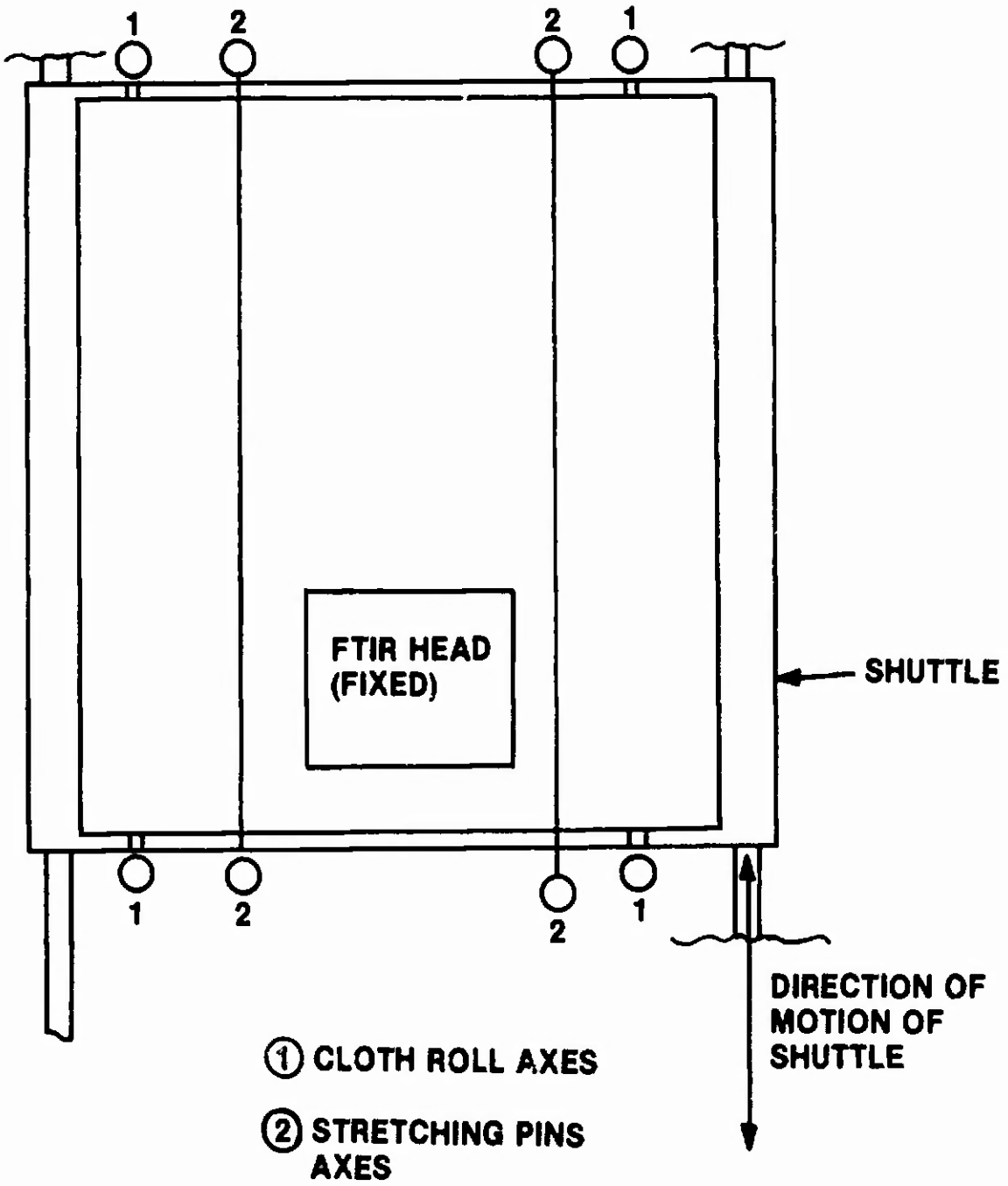

Figure 37. IR system configuration, orthogonal view.

The sample compartment has a set of spherical optics for focussing the collimated beam onto the sample. The description of the optical path to this point is exactly half-way to the end. The optics on the way out are identical (by symmetry) to the ingoing optical train: The spherical optics collect the reflected (or scattered) signal, the sample beam and the reference beam are recombined and sent to the detector. In this case, the detector is a cooled mercury-cadmium-telluride detector.

(In our experiment, the beam size is 6 mm; this was achieved by use of a 3 power condensing lens, set in front of the 18 mm source aperture.)

In this prototype system we will move the sample. While moving the spectrometer is attractive from a mechanical handling perspective, the optics in the spectrometer are very sensitive to even the slightest of vibrations. For this reason, we keep the spectrometer steady and move the cloth.

Performance expectations

We expect that a running average on the cloth can be taken at a factor of about 100 times faster than the sample was made. Thus, measurements can be made in 1 second or less (0.25 seconds) per spot. This implies either an averaging over a moving spot, e.g., a streak on the cloth, or a start-stop motion for the cloth.

We expect that the level of precision of quinolinolate present would be ascertained to 10% or so by this measurement.

Calibration

Like the x-ray approaches, a very careful cross-calibration is required between known samples and the ranges for acceptable treated-cloth performance. Of course, this will require repeated samplings between the x-ray and IR machines.

During the course of this calibration, we will be able to provide to the Army the tools for understanding the processing of these penetrating agents. A ratio of x-ray-to-IR results will yield a figure that is a measure of penetration of the applied agent.

Interface

The interface is determined by the existing Digilab interface. This includes a complete turnkey system that incorporates an internal minicomputer and preprogrammed sequences. Digilab also supports high-level scientific languages such as Fortran and Pascal. Primary operation is via standard keyboard and CRT combination.

Data can be stored in raw and in processed form on magnetic tape. Individual spectra can be plotted on hardcopy. Magnetic media are particularly important for archiving, should any further analysis be required.

The test specimen interface is a simple mechanical driven stage, situated so that different regions of the specimen can be interrogated as a function of time. This arrangement will yield sampling sufficient to determine whether various arrangements of the large-scale test specimen machinery will work.

8.0 ULTRASONIC INVESTIGATIONS AND THE UT SYSTEM

As discussed previously, an ultrasonic (UT) inspection measures a materials property that can be interpreted as depth of penetration of the fungicide into the sample. Moreover, if this is done at a number of different UT frequencies, it may be possible to obtain an inferred profile of concentration of the copper-8-quinolinolate through the fabric.

UT examinations are typically very fast, a millisecond usually being more than sufficient for a single frequency. UT instrumentation is usually very rugged and very inexpensive compared to either x-ray or infrared equipment.

8.1 Rationale for UT examination

While the x-ray and IR investigations have given great cause for optimism, there is one rare situation which they may not detect. This case concerns supplier malfeasance, where the purveyor of the fungicide-impregnated cloth has added copper salts so that the x-ray examination would yield the right amount of copper and has also sprayed just enough copper-8-quinolinolate on the outside layers of the fabric to pass the IR tests. This single situation could leave the interior of the fabric unprotected by the quinolinolate, and still pass the combined x-ray and IR tests. (See Section 9, Summary of Results and Conclusions, where all the different possibilities are addressed.)

Two hints lead us to believe that treated and untreated samples would have different UT signatures: The first is the fact that treated and untreated samples feel different to the touch, the copper-8-quinolinolate sections feeling much stiffer/less soft. The second hint was the broadening of the 1573 cm^{-1} quinolinolate absorption peaks in the IR measurements as seen in the cotton duck samples compared with the neat samples. This broadening is usually interpreted as a chemical cross-linking. Thus, it seemed reasonable that the acoustic signatures of treated and untreated samples would be different. Moreover, if quantitative measures of these acoustic signatures were significantly and

consistently different, then analysis of the actual data would yield the fractional amount of textile that has been penetrated by the fungicide.

8.2 UT experiment

A number of test specimens were cut from cotton duck, both untreated and treated with copper 8-quinolinolate. These were examined with a breadboard ultrasonic system incorporating an Ultran transmitting and receiving transducer Model WC37-1.0 operating at 1 megahertz in the pulse transmission mode. The experimental configuration is shown in Figure 38.

Mechanical pressure was applied from transmitter to receiver across each test specimen until no further increase in acoustic transmission was observed. No coupling agent was employed between the transducer and the sample — the coupling was "dry". The fixture allowed separate adjustments for holding and pressure application, so that independent alignment and pressure adjustments were possible.

8.3 UT results and discussion

Individual test pieces from each of seven different sample pieces were cut and measured for transit time onset (essentially a measure of sound speed) time-position of the peak (dispersion of the pulse) and, most importantly, transmission of the signal. There was little difference in transit time onset or in time position of the peak. The transmission measurements, however, differed significantly.

The transmission results for each of these pieces is shown in Figure 39. There was a clear difference between all the different sample pieces. In particular, the untreated segments (bleached and unbleached) had significantly less transmission than the fungicide-treated samples.

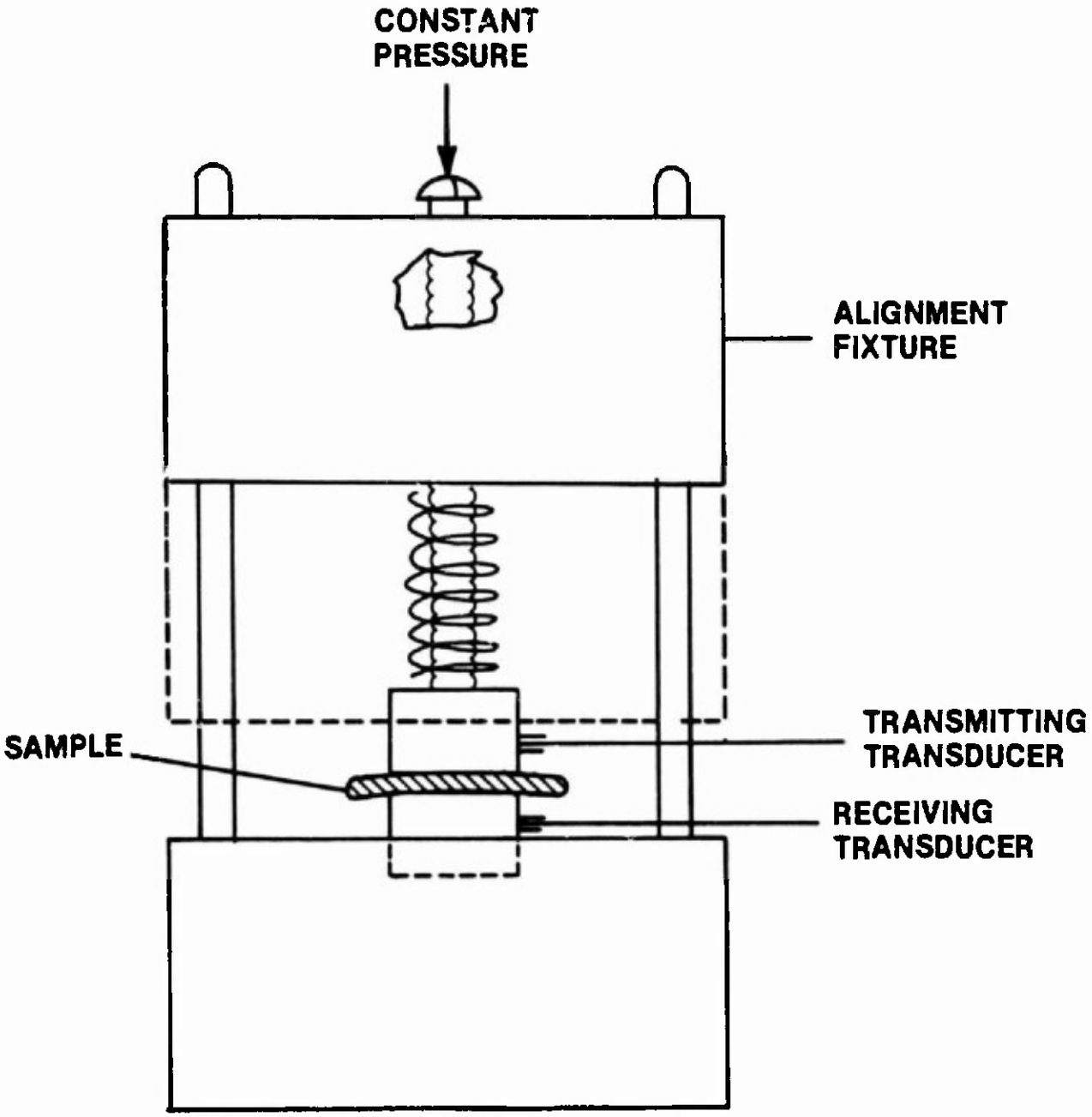

Figure 38. Ultrasonic experimental arrangement. The alignment and pressure functions are accomplished separately. Pressure was increased until no further increase in transmission was noted. All measurements were made at 1 MHz.

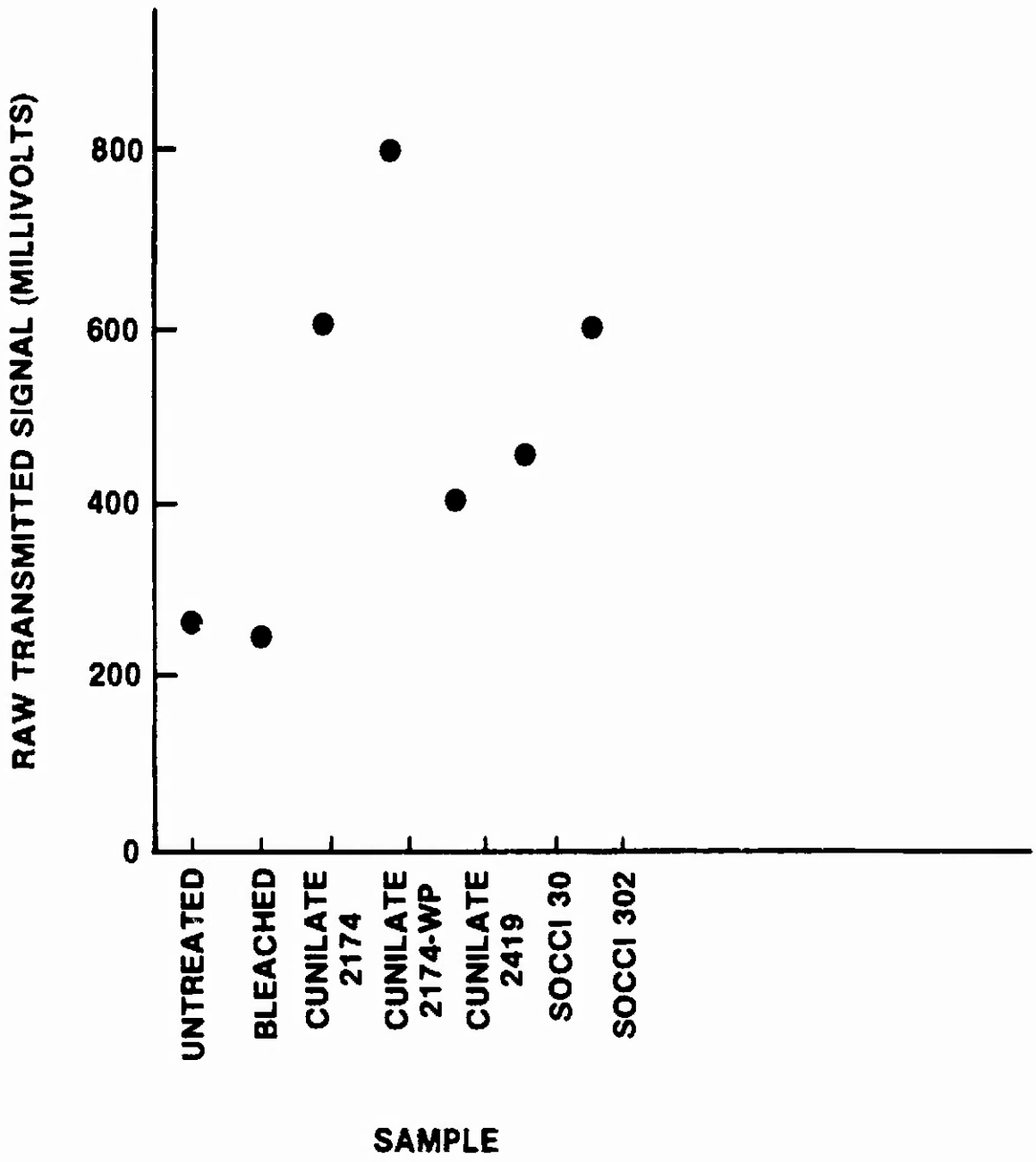

Figure 39. Transmission signal of each of the test specimens taken from different processes. The accuracy of the measurement is about equal to the dot size, +/- 10 millivolts. The fact that there is a wide distribution between different types of specimens indicates that a partial treatment will be easily detected, as long as the distribution within a type is narrow. (See Figure 40 for distributions within a population.)

In order to verify that the observations were not simple flukes, 10 specimens, each of the unbleached and Cunilate 2174 samples were also examined to confirm the consistency of the difference. These results are illustrated in Figure 40.

It is very clear that the differences are real and consistent. Thus, if a specimen measurement were between these two groups, we would know penetration to be incomplete. The quantitative degree of incomplete penetration is yet to be determined, but it is clear that the UT transmission mode is a sensitive correlator of the process (by virtue of the large dispersion between samples from different processes and the narrow dispersion between samples from the same process) and, hence, the penetration.

8.4 UT system configuration

Ultrasonic transducers are manufactured in a variety of different shapes and configurations. In particular, UT transducers are available in the form of constant pressure rollers. Thus, the transducer assembly can be configured to yield constant readings on 1 millisecond or finer temporal resolution scales. If the material speed is 30 yards/minute (46 cm/second), then the spatial resolution of this measurement is about equal to the size of the transducer head plus 0.2 inches (0.5 cm). If the speed is 120 yards/minute (1.8 m/second), the spatial resolution is the transducer head size plus 0.7 inches (1.8 cm). To first order, then, the spatial resolution is about an inch (2.54 cm). Indeed, finer temporal measurements can be made, in which case the spatial resolution is correspondingly finer. (The spatial resolution can be made finer than the transducer head size if deconvolution techniques are employed.) The system configuration concept for rolling UT transducers is shown in Figure 41.

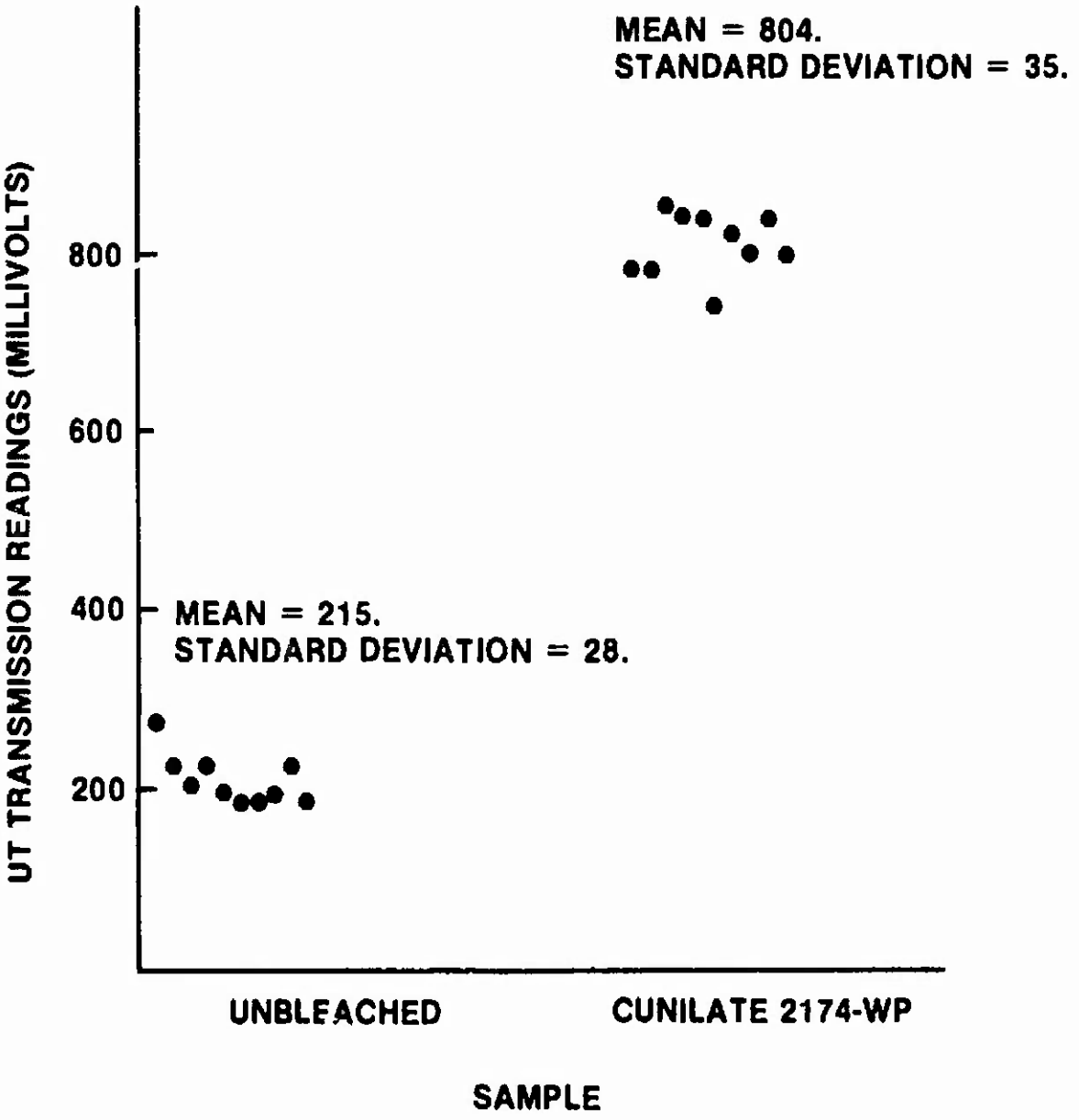

Figure 40. Ultrasonic transmission measurements of many test specimens within two sample populations (one unbleached cotton duck sample for control and one Cunilate 2174-WP). The separation of the two populations is obvious. Statistical data for means and standard deviations of the two sample distributions are shown. For optimized UT transducer alignment, the statistical spread within each population will probably decrease even further. Incomplete penetration of the fungicide treatment process would undoubtedly produce a reading between the two distributions.

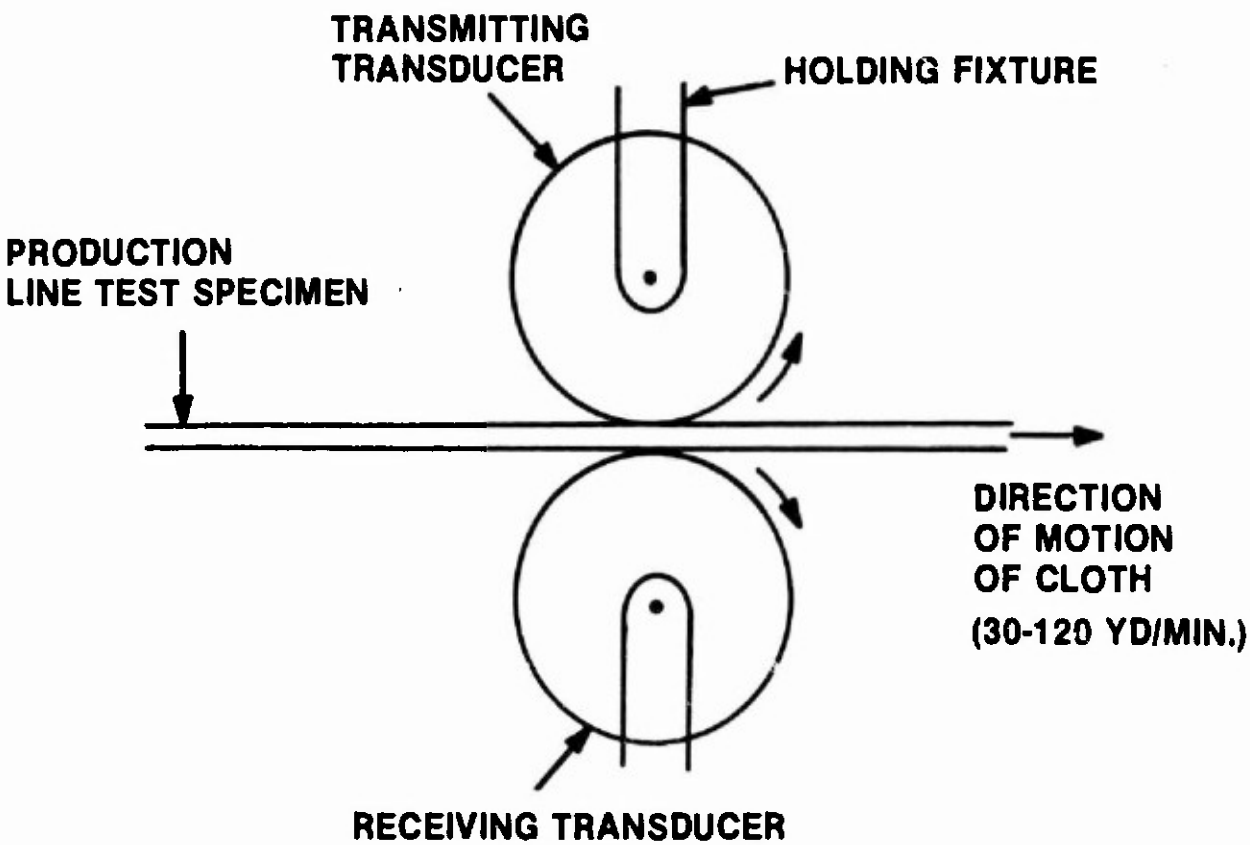

Figure 41. System configuration concept for rolling UT transducers. The measurement can be made in a time of 1 millisecond during which time the cloth has moved 0.7 inches or 1.8 cm (1.8 m/second). The spatial resolution is thus limited by the speed of the cloth. The rollers keep constant pressure on the fabric. For this type of roller and fixture arrangement, the alignment will stay constant as long as the pressure is constant.

UT systems are currently available from a variety of manufacturers with standard readout and waveform recognition systems. OEM costs for even the most sophisticated systems are in the $10-20K range. The handling equipment is to be handled in a manner similar to that for the x-ray and IR subsystems, namely teaming with a Phase III partner from the textile machinery manufacturing industry.

9.0 SUMMARY OF RESULTS AND CONCLUSIONS

The measurement of textile treatment uniformity and penetration is a problem that has existed since the earliest fungicide treatments were specified by the Army. It is clear from these studies that no one inspection technique will solve all problems. Table 3 shows all possible situations and shows how the three-prong approach resolves all of them.

TABLE 3. Possible Cu-8-Quinolinolate Situations/Resolution by Inspection

SITUATION	FLUORESCENCE X-RAY (COPPER)	DUAL-ENERGY X-RAY (COPPER)	FTIR (QUIN)	UT (TRANS-MISSION)
1.0 NO EXTRA COPPER				
1.1 COMPLETELY PENETRATING CU-8-QUINOLINOLATE				
1.1.1 SUFFICIENT CU-8-Q	OK	OK	OK	OK
1.1.2 INSUFFICIENT CU-8-Q	LOW	LOW	LOW	LOW
1.2 INCOMPLETE PENETRATION OF CU-8-Q				
1.2.1 SUFFICIENT CU-8-Q ON SURFACE OF DUCK	LOW	LOW	OK	LOW
1.2.2 INSUFFICIENT CU-8-Q ON SURFACE OF DUCK	LOW	LOW	LOW	LOW
2.0 EXTRA COPPER ADDED				
2.1 CU-8-Q COMPLETELY PENETRATING				
2.1.1 SUFFICIENT CU-8-Q	HIGH	HIGH	OK	OK
2.1.2 INSUFFICIENT CU-8-Q	OK	OK	LOW	LOW
2.2 CU-8-Q INCOMPLETE PENETRATION				
2.2.1 SUFFICIENT CU-8-Q AT SURFACE	OK	OK	OK	LOW
2.2.2 INSUFFICIENT CU-8-Q AT SURFACE	OK	OK	LOW	LOW
3.0 NICKEL (OR OTHER HIGH-Z SALTS)	OK	BAD	—	—

This matrix of tests can distinguish between all possible situations, whether due to carelessness or sloppy work habits or actual and purposeful cheating by the vendor. Indeed, it would take a well-informed and technically astute vendor to arrange that the different applications should just balance, a situation just possible without the use of the ultrasonic

testing component. The UT test effectively precludes this situation from going undetected.

The different approaches can all be used in a production context, with fabric speeds running between 30-120 yard/minute (0.46 - 1.8 m/second), although the sampling schemes and spatial resolution available will be technology specific.

Fluorescent x-ray technique -- Fluorescent x-ray inspection will yield the total amount of copper and other high-Z components present in the sample. Data acquisition time will be about 10 milliseconds per sample, with a spatial resolution of about an inch (2.54 cm). The drawback to this technique is that it is not extendible to thick materials, and that the fractional amount of copper present in a sample is made through indirect measure and careful calibration.

Dual energy x-ray technique -- Dual energy x-ray inspection will yield directly the total amount of high-Z (i.e., copper) material present and the fractional amount of high-Z material relative to total cellulose (i.e., base cotton fabric). Dual energy x-ray inspection can be performed at high spatial resolution, current capability being 0.010 inch square (0.25 mm square). The dual energy x-ray technique can present a detailed high-resolution high-Z map image of a sample treated with a copper-based fungicide or other agent (with $Z > 12$). For use with high spatial resolution imaging in Z, data acquisition time will be about 5 minutes for scan (research mode). For use with high speed production textile machinery, a single measurement can be accomplished in less than 0.02 seconds. For production machinery utilizing cloth speeds of 120

yards/minute (1.8 m/second), the implied spatial resolution is between 1 and 2 inches (2.5 and 5.1 cm) if the measurements are made while the cloth is moving.

Fourier transform infrared spectrometry -- FTIR methods uniquely find the quinolinolate portion of the compound and can measure the quantitative presence (to a precision of 10%) on the surface of the textile. The absorption feature at 1573 cm^{-1} can be tuned directly and unambiguously for the organic portion of the copper-8-quinolinolate. This method can be utilized in a production context, the sampling time being 0.25 seconds per sample. The implied spatial resolution in a production mode for continuous monitoring purposes is 4 inches (10 cm) or 18 inches (46 cm) at fabric speeds of 30 and 120 yards/minute (0.46 and 1.8 m/second) respectively.

Ultrasonic transmission -- The ultrasonic approach produces good correlation of known samples. Differences in transmission between different treatments were quite large, while separate specimens from identical treatments showed very small differences. UT promises rapid and inexpensive measurements over very large volumes of test material. A very large fraction (and perhaps 100%) of the total output of a large production run can be checked on-line. The spatial resolution is determined by the sampling rate of 1 millisecond (including all processing time, etc.). At a cloth production rate of 72 inches (1.8 m) per second, the implied spatial resolution is about 0.5 inches (1.3 cm) (including the effect of the transducer head size). The only drawback to the use of UT is that it produces an indirect measurement, rather than a specific sensitivity to the molecular structure or elemental composition of the fungicide. This is

also a strength: the technique is very valuable because the generality and nonspecificity of the approach makes it extendible to any other context where the materials properties are affected.

A combination of these inspection technologies is the most likely method of guaranteeing compliance under all situations in a production context. All technologies are useful in both research and production contexts. Production system designs are shown and discussed. A program plan for Phase II is shown in Appendix A. The key elements of the Phase II program are delivered hardware for each of the inspection approaches.

10.0 REFERENCES

1. Compton, A.H. and Allison, S.K., 1935, X-Rays in Theory and Experiment, 2nd edition, Van Nostrand, Princeton, NJ.

2. Judy, P.F., 1971, A dichromatic attenuation technique for the in vivo determination of bone mineral content, Ph.D. thesis, University of Wisconsin-Madison.

3. Nord, R.H., 1987, chapter 22 in Osteoporosis Update 1987, ed. by Harry Genant, pub. by Radiology Research and Education Foundation, 3rd & Parnassus, San Francisco.

4. Gilfrich, J.V. and Birks, L.S., 1968, Anal. Chem., 40, 1077.

5. Birks, L.S., 1959, X-Ray Spectrochemical Analysis, Interscience, New York, pp. 58-62.

6. Criss, J.W. and Birks, L.S., 1968, Anal. Chem., 40, 1080.

7. Griffiths, P.R. and de Haseth, J.A., 1986, Fourier Transform Infrared Spectrometery, vol. 83 of "Chemical Analysis," Wiley, New York.

8. Ferraro, J.R. and Basile, L.J., 1979, Fourier Transform Infrared Spectroscopy (Applications to Chemical Systems), vol. 2, Academic Press, New York.

9. Ferraro, J.R. and Basile, L.J., 1985, Fourier Transform Infrared Spectroscopy (Applications to Chemical Systems), vol. 4, Academic Press, New York.

10. Gagel, J. and Biemann, K., 1987, paper # b3.2, 6th International Conference on Fourier Transform Spectroscopy, Vienna.

11. Okhaku, R., 1971, Inorganic Chemistry, 10, 798.

12. Gagel, J. and Biemann, K., 1987b, Anal. Chem., 59, 1266.

APPENDIX A: PHASE II PROGRAM PLAN

The Phase II program plan is shown in Figure A-1. The plan consists of eighteen major tasks that are described below.

Task 1: Establish Performance Requirements

The x-ray and IR laboratory system performance requirements will be verified, based on the experimental data and analysis accomplished on the Phase I program. These performance requirements will be reviewed with the technical project officer (TPO) before proceeding with the system designs.

Task 1A: Determine Production Inspection Requirements

The production textile inspection system performance requirements will be generated and verified based on the performance requirements generated in Task 1 and on discussions with the TPO, and textile inspection specialists identified by the TPO. Results from the Phase I program will be taken into account.

Task 2: Design X-Ray System

The laboratory x-ray system as described in Section 6.0 will be designed in full detail to meet the performance requirements generated in task 1. This design will be reviewed with the TPO before proceeding with fabrication.

Task 3: Design IR System

The laboratory IR system as described in Section 7 will be designed to meet the performance requirements generated in Task 1. This design will be reviewed with the TPO before proceeding with fabrication.

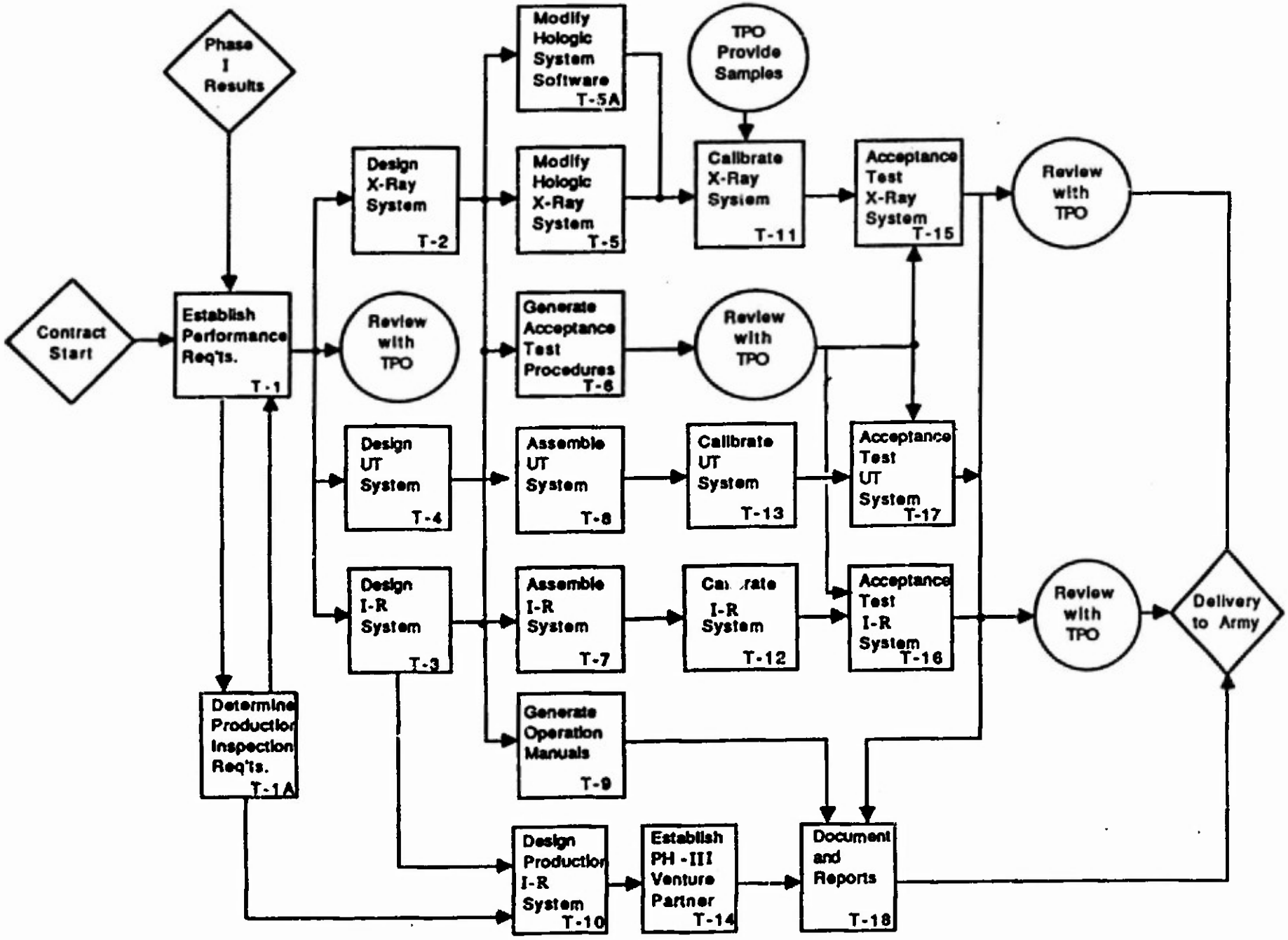

Figure A-1. Textile Inspection System Phase II Program Plan

Task 4: Design UT System

The ultrasonic system as described in Section 8 will be designed to meet the performance requirements generated in Task 1. This design will be reviewed with TPO before proceeding with fabrication.

Task 5: Modify Hologic Inspection System

A subcontract will be let to Hologic, Inc. of Waltham, MA to modify one of their standard medical x-ray systems in accordance with the design requirements generated in Task 2.

Task 5A: Modify Hologic System Software

As part of the subcontract let in Task 4, Hologic will modify their standard software to meet the performance requirements generated in Task 2.

Task 6: Generate Acceptance Test Procedure

The acceptance test procedures for both the x-ray and IR laboratory systems will be generated to demonstrate the performance requirements established in Task 1. These acceptance test procedures will be reviewed with the TPO before implementation.

Task 7: Assemble IR System

The laboratory IR system components will be procured and assembled at the principal investigator's facility in accordance with the design generated in Task 3.

Task 8: Assemble UT System

The ultrasonic system components will be procured and assembled at the principal investigator's facility in accordance with the design generated in Task 4.

Task 9: Generate Operation Manuals

Operations manuals will be written for both the x-ray and IR laboratory systems.

Task 10: Design Production IR System

A production IR system will be designed to meet the inspection requirements generated in Task 1A based on the laboratory system designed in Task 3. This task will intentionally overlap with Task 13 which brings a Phase III venture partner to assimilate his expertise into the design.

Task 11: Calibrate X-Ray System

The laboratory x-ray system will be calibrated at the Hologic facility under the direction of the principal investigator using calibrated textile samples provided by the TPO.

Task 12: Calibrate the IR System

The laboratory IR system will be calibrated at the principal investigator's facility using the textile samples provided in Task 11 above.

Task 13: Calibrate the UT System

The UT system will be calibrated at the principal investigator's facility using the textile samples provided in Task 11 above.

Task 14: Establish a Phase III Venture Partner

A manufacturer of textile machinery who is willing and who has the requisite experience will be identified. This manufacturer will produce the mechanical handling systems for the textile inspection systems in accordance with the design generated in Tasks 8 and 10. This task will be started early enough to involve this manufacturer in the design process in those tasks.

Task 15: Acceptance Test of X-Ray System

The laboratory x-ray system will be acceptance-tested at the Hologic facility using the acceptance test procedures generated in Task 6. The test results will be reviewed with the TPO prior to delivery of the system.

Task 16: Acceptance Test of IR System

The laboratory IR system will be acceptance-tested at the principal investigator's facility using the test procedures generated in Task 6. The test results will be reviewed with the TPO prior to delivery of the system.

Task 17: Acceptance Test of UT System

The ultrasonic system will be acceptance-tested at the principal investigator's facility using the test procedures generated in Task 6. The test results will be reviewed with the TPO prior to delivery of the system.

Task 18: Documentation and Reports

Quarterly technical progress reports and monthly financial reports will be provided as required by the contract. A final technical report, reporting on all the work done on the program, will be generated.

The scheduling of the tasks above is presented in the program master schedule, Figure A-2. There is sufficient contingency time in each task to complete this program comfortably in a 24 month period. This includes lead times of all hardware components.

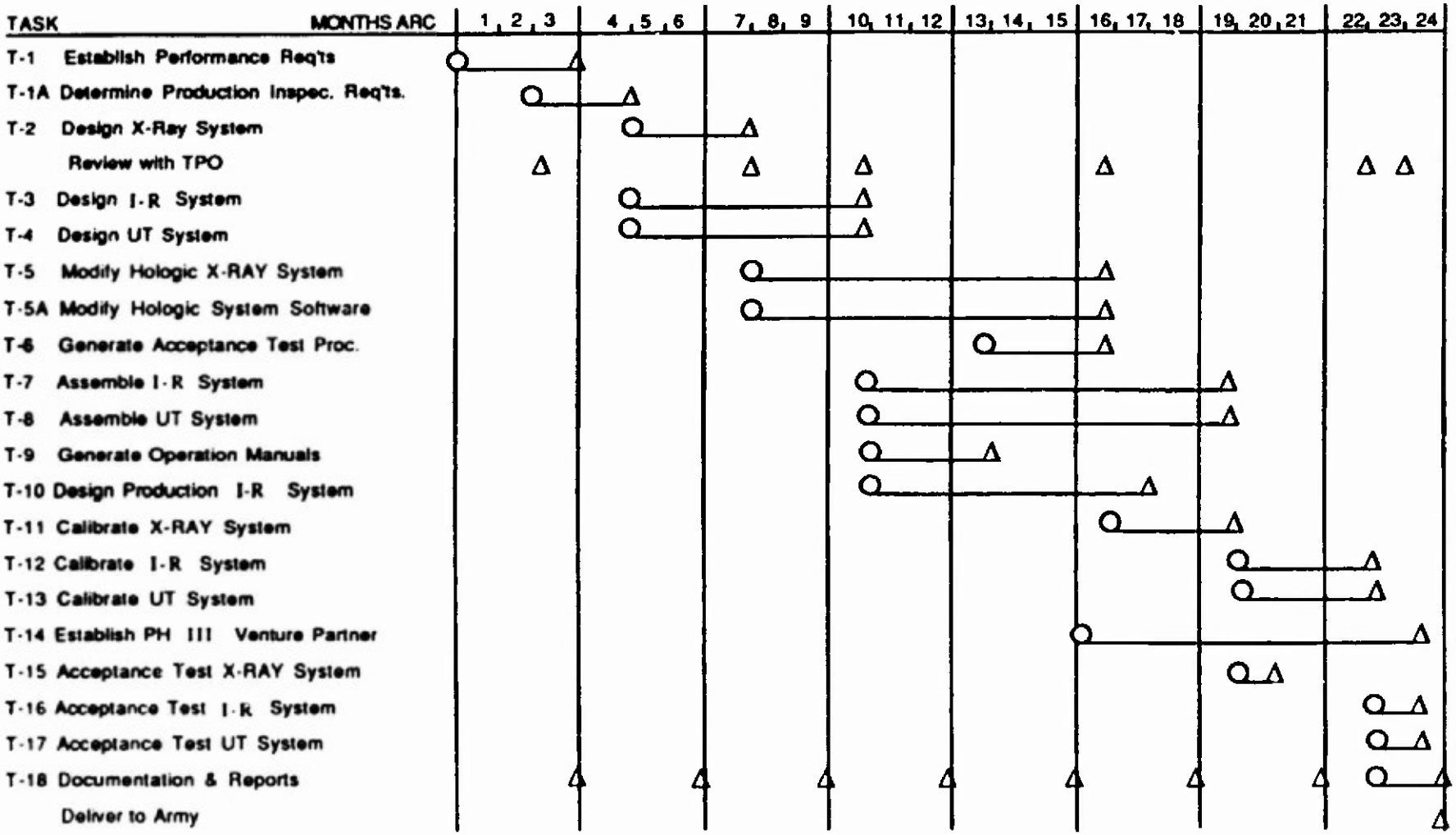

Figure A-2. Textile Inspection System Phase II Program Master Schedule.

APPENDIX B: SYSTEM PROGRAM SAFETY PLAN

B.1 Purpose

The purpose of the system program safety plan is to guarantee the radiation safety of personnel during the assembly, testing, installation, operation, and maintenance and repair of the equipment to be provided in Phase II of this program.

B.2 Overall description

The main components are all to be purchased from OEM vendors and modified and integrated into a prototype inspection system. The normal hazards of mechanical and electrical equipment apply, as well as the possibility of accidental irradiation of personnel due to x-ray generating equipment. It is the radiation hazard that we address in this plan.

B.3 Safety control and procedures

B.3.1 Radiation safety officer

In this case, Dr. Paul Burstein, the principal investigator, is also the radiation safety control officer. He has full responsibility for the safe operation of the equipment. Dr. Burstein has over 20 years of experience in the handling of radioactive sources and radiation generating equipment.

B.3.2 Radiation safety procedures

B.3.2.1 System design

Safety for radiation generating equipment is normally designed into the system from the onset. Thus, good design features include a safety interlock so that radiation generating equipment cannot be turned on unless all portals are closed. Radiation monitors may be included external to the x-ray inspection equipment so that an automatic alert of nearby personnel may be effected.

This system has no radioactive sources, only subsystems that contain x-ray generating equipment when energized. Thus, the normal precautions with regard to storing and tracking radioactive materials do not apply.

B.3.2.2 System assembly and test

During this phase of the program, many of the interlocks and other normal safeguards for use of the equipment in the standard inspection facility are not yet active. It is the responsibility of the safety officer or his designated representative to monitor the area for x-ray exposure of personnel every time a change is made to the x-ray generating equipment or its ancillary configuration (e.g., shielding).

B.3.2.3 System operation

During system operation, the acceptable levels of monitored radiation in areas accessible to personnel will be below the 0.2 mR/hour level. This is the acceptable BRH level for nonradiation workers, and well-below the level for radiation workers (2 mR/hour). We note that the Hologic system with its pencil beam approach already satisfies these requirements, and can operate in the open environment with no radiation danger to personnel. The effects of scatter due to the presence of the test specimen itself will be minuscule because the textile is itself so weak an absorber. We expect this scatter contribution to be negligible. It will, of course, be measured.

B.3.2.4 System maintenance and repair

System maintenance sometimes requires disabling the interlocks in order to test or repair a component. In these cases, only trained M&R personnel with proper radiation hazards training will be allowed to service the equipment. M&R personnel who disable radiation safety interlocks will

maintain active real-time radiation monitors at all times that the generating equipment is operating.

B.4 System hazard analysis

A brief hazard analysis will be presented to the project officer at the end of the radiation design tasks.

B.5 Safety reviews

Safety reviews will be conducted in concurrence with major program milestones, e.g., assembly, calibration, and installation.

B.6 System safety data

Data from all surveys, discrepancies and other items of interest for radiation health and monitoring purposes will be maintained in an active file. These data will be transmitted to the project officer with required progress reports.